Mechanically Stabilized Earth (MSE) Wall Backfill Water Infiltration

Ali Soleimanbeigi
William Likos
University of Wisconsin - Madison

Keli Bohrer
Greg Siemens
Royal Military College

WisDOT ID no. 0092-18-07

June 2021

RESEARCH & LIBRARY UNIT

WISCONSIN HIGHWAY RESEARCH PROGRAM

WISCONSIN DOT
PUTTING RESEARCH TO WORK

DISCLAIMER

This research was funded through the Wisconsin Highway Research Program by the Wisconsin Department of Transportation and the Federal Highway Administration under Project No. 0092-18-07. The contents of this report reflect the views of the authors who are responsible for the facts and accuracy of the data presented herein. The contents do not necessarily reflect the official views of the Wisconsin Department of Transportation or the Federal Highway Administration at the time of publication.

This document is disseminated under the sponsorship of the Department of Transportation in the interest of information exchange. The United States Government assumes no liability for its contents or use thereof. This report does not constitute a standard, specification or regulation.

The United States Government does not endorse products or manufacturers. Trade and manufacturers' names appear in this report only because they are considered essential to the object of the document.

TECHNICAL REPORT DOCUMENTATION PAGE

1. Report No. WHRP 0092-18-07	2. Government Accession No	3. Recipient's Catalog No
4. Title and Subtitle Mechanically Stabilized Earth (MSE) Wall Backfill Water Infiltration		5. Report Date June 21, 2021 6. Performing Organization Code
7. Authors Ali Soleimanbeigi, Keli Bohrer, William Likos, Greg Siemens		8. Performing Organization Report No.
9. Performing Organization Name and Address University of Wisconsin-Madison Royal Military College		10. Work Unit No. (TRAIS) 11. Contract or Grant No. WHRP 0092-18-07
12. Sponsoring Agency Name and Address Wisconsin Department of Transportation Research & Library Unit 4822 Madison Yards Way Madison, WI 53707		13. Type of Report and Period Covered Final Report 2018-2021 14. Sponsoring Agency Code
15. Supplementary Notes		

16. Abstract

The stability of Mechanically Stabilized Earth (MSE) walls may be compromised in undrained conditions such as during heavy rain, flooding, or rapid drawdown. For MSE walls potentially subject to inundation, such as those located adjacent to rivers, canals, detention basins or retention basins, understanding pore pressure evolution during infiltration and drainage of the backfill soils and the corresponding implications to wall stability is essential. In this research, a complimentary program of full-scale physical model tests and numerical computer simulations was conducted to quantify infiltration, drainage and corresponding stability of MSE walls subject to flooding and rapid drawdown. Two full-scale MSE walls were constructed at an indoor geostructure testing facility located at the Royal Military College of Canada. Relatively fine and relatively coarse sand, both falling withing grain-size design specifications, were used as backfill soils in the two tests. Instrumentation was installed to measure pore pressure distribution, moisture content distribution, strain in the reinforcement layers, connection loads, wall deflections, horizontal and vertical toe loads, and earth pressures during flooding and rapid drawdown. Numerical simulations were carried out using model geometry and material properties calibrated to match the full-scale physical test results. Stability analyses were conducted to evaluate stability of the MSE wall and calculate factors of safety during infiltration and drawdown. Parametric studies were conducted to examine how backfill hydraulic conductivity, flood height, and length of the backfill affect time to backfill saturation and wall stability during flooding and drawdown. A series of generalized charts are provided for estimating the extent and timing of infiltration or drainage from flooding/drawdown and corresponding impacts to wall stability.

17. Key Words MSE wall, infiltration, rapid drawdown, backfill	18. Distribution Statement No restriction. This document is available to the public through the National Technical Information Service 5285 Port Royal Road Springfield VA 22161

19. Security Classified.(of this report) Unclassified	20. Security Classif. (of this page) Unclassified	21. No. of Pages 109	22. Price N/A

Form DOT F 1700.7 (8-72) Reproduction of completed page authorized

Table of Contents

LIST OF TABLES

LIST OF FIGURES

CHAPTER 1 : INTRODUCTION

"Control of water infiltration and providing adequate drainage are critical to the performance of retaining walls and abutment walls. The ability of the wall backfill to drain water that infiltrates it from rain, snow melt, or ground water shall be considered in the design of the wall and its stability…" (WISDOT, 2013).

Background

The stability of Mechanically Stabilized Earth (MSE) walls may be compromised in undrained conditions such as during heavy rain, flooding, or rapid drawdown. Excess pore pressures in non-freely draining backfills may not dissipate quickly enough, and thus may reduce effective stresses in the backfill soil, which in turn may cause a reduction of shear strength at the soil-reinforcement interface (Bobet, 2002). Excess pore pressure also reduces the effective weight (buoyancy) of the reinforced soil zone and sliding resistance for external stability is decreased. Additional problems related to poor backfill drainage include increased potential for piping, internal erosion, external soil erosion from the toe, around the edges or at the top of the wall (Berg et al. 2009) and a potential destabilizing effect due to an increase in seepage forces. Koerner and Koerner (2012) analyzed causes of failure of 141 MSE walls (34 cases of excessive deformation and 107 cases of actual collapse) and found that 58% were caused by internal or external water and that the major design inadequacy was the lack of proper drainage within the reinforced soil zone.

For MSE retaining walls potentially subject to inundation, such as those located adjacent to rivers, canals, detention basins or retention basins, AASHTO specifies that a minimum hydrostatic pressure equal to 3 ft (1 m) should be applied at the high-water level for the design flood event (AASHTO section 11.10.10.3.) Effective unit weights shall be used in the calculations for internal and external stability beginning at levels just below the application of the differential hydrostatic pressure. Situations where the wall is influenced by tide or river fluctuations may require that the wall be designed for rapid drawdown conditions from the high-water level (HWL) (see Figure 1-1), which could result in differential hydrostatic pressures considerably greater than 3.0 feet. Corresponding destabilizing effects can be significant. Aubeny et al. (2014), for example, conducted numerical analysis to model rapid drawdown conditions for wall systems and found that rapid drawdown could reduce factor of safety by 24%. Laboratory experiments conducted by Bobet (2002) indicated that undrained

backfill conditions can reduce the pullout capacity of MSE wall reinforcements by as much as 50%.

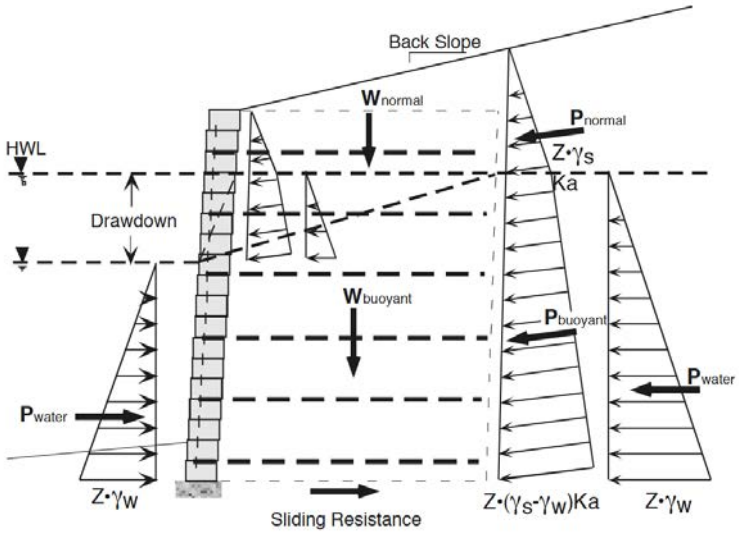

Figure 1-1. Rapid drawdown conditions for an MSE retaining wall (after Keystone, 2003)

Rapid drainage conditions may be expected when clean coarse-grained material (e.g., shot rock or open graded gravel) is used as backfill and/or any engineered drainage system behind the MSE wall is not clogged. Backfill material meeting the gradation requirements in the AASHTO LRFD Bridge Construction Specifications for MSE structure backfill, however, is not considered to be rapid draining. If the backfill material is not free draining, or if the drainage system is clogged, dissipation of pore water pressure during rapid drawdown or infiltration is delayed and can compromise wall stability by any of the mechanisms described above. Within the unsaturated zone above the wetting front in the backfill, negative pore water pressure or matric suction develops and can have a significant effect on the active earth pressure exerted by the backfill soil (e.g., Vahedifard et al. 2014). It is thus important to know the location of the wetting front during rapid drawdown or water infiltration into MSE structure backfill, how this location changes over time, and how corresponding excess pore pressures can reduce the internal and external stability of the wall. From a practical perspective, a readily implementable model is needed that can predict the interface between saturated and partially saturated soils (wetting front) and the corresponding impact to internal and external lateral earth pressures.

Research Approach

A combined physical and numerical modeling program was conducted to evaluate flooding and rapid drawdown processes in backfill materials for MSE walls and corresponding implications to wall stability. The laboratory testing program was designed to measure and monitor seepage, pore pressure evolution, soil-structure interaction forces, and deformations for two full-scale MSE walls subject to flooding and rapid drawdown. A unique aspect of this task has been collaboration with the Royal Military College of Canada (RMC) using the RMC Full-Scale Soil Structures Test Facility located within their Civil Engineering Department Structures Laboratory. A complementary numerical modeling effort was developed to quantify evolution of pore pressure and saturation (wetting front propagation) for generalized flooding and drawdown events. Corresponding internal and external MSE wall stability was assessed during transient flooding and rapid drawdown. Parametric studies were carried out to produce generalized design charts for a range of flood characteristics, wall geometry, and backfill properties.

Physical Modeling Program

Two full-scale MSE walls were constructed at the Royal Military College of Canada's (RMC) Full-Scale Soil Structures Test Facility, which is depicted in Figure 1-2. The Full-Scale Soil Structures Test Facility has been in operation for more than 3 decades. The facility has specialized in physical testing of full-scale MSE Walls since the late 1990's with partial funding received from the AASHTO MSE Pooled Fund, Washington State DOT, National Concrete Masonry Association, as well as other sponsors. The test facility allows soil retaining wall structures that are 3.6 m high by 3.4 m wide with backfill soil extending to a distance of 6 m from the front edge of the facility. The backfill soil and wall facing are seated on a rigid concrete foundation. The soil is laterally contained between two parallel reinforced concrete counterfort walls bolted to the structural laboratory floor. A series of hollow steel sections at the top of the facility confine a series of air bags that can be used to apply a uniform surcharge (up to 150 kPa) to the entire soil surface. The toe of full-scale wall models is located at the front of the test facility. The back of the soil mass is restrained by a series of rigid reinforced concrete bulkheads at the opposite end of the test facility. Plane-strain conditions are encouraged by covering the interior side-walls of the test facility with multiple layers of lubricated polyethylene sheeting.

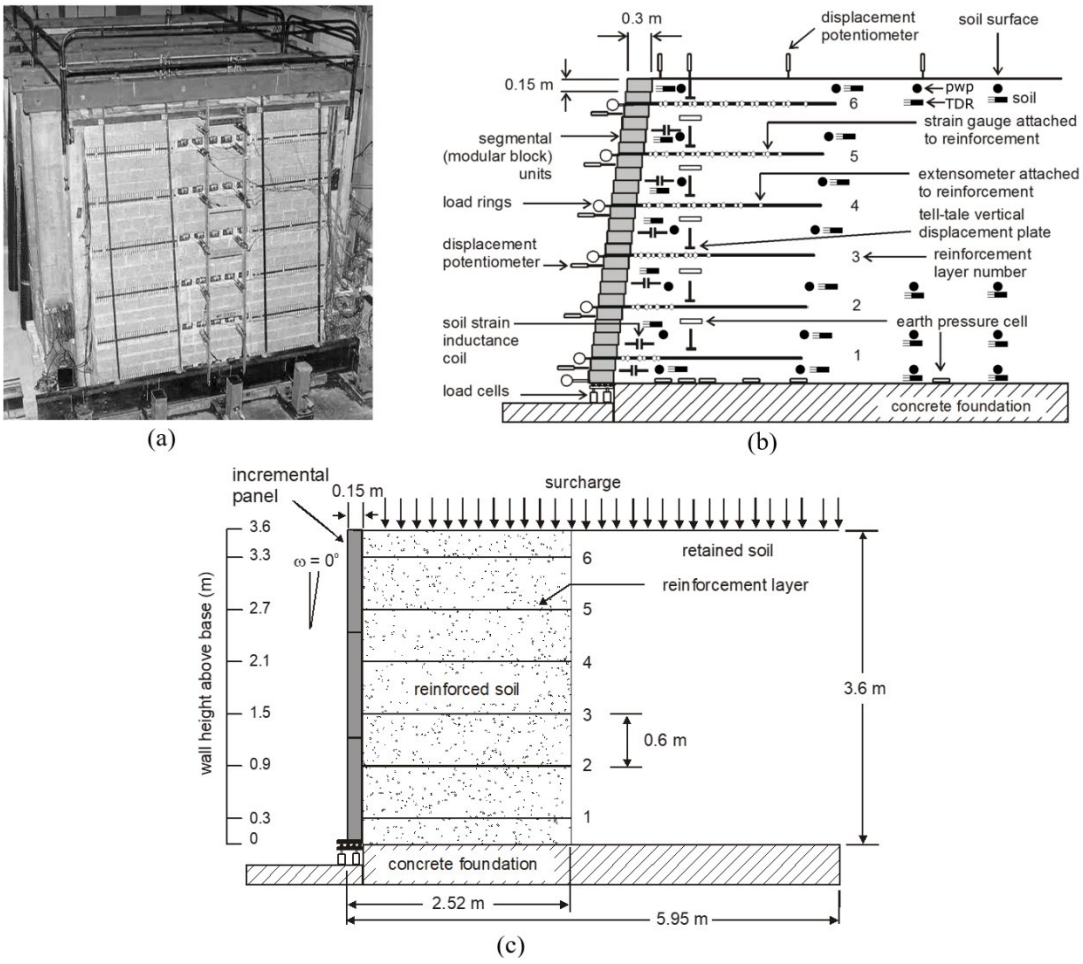

Figure 1-2. a) Photograph of RMC Full-Scale Soil Structures Test Facility; b) typical instrumentation layout for full-scale MSE wall tests; and c) full-scale MSE wall with precast concrete panels.

For this project, a small tank was constructed in front of the wall to accommodate temporary face flooding and drawdown testing. Experiments were conducted to measure the extent of water infiltration through the face of precast panel MSE walls when the bottom portion of the wall was temporarily inundated with standing water by filling the tank and corresponding infiltration through the facing panels into the backfill. Instrumentation (moisture, pore pressure) was placed to best capture the wetting front in this zone of the backfill. Drawdown tests were run by rapidly draining water from the external tank. Instrumentation was installed to allow measurement of:

1. Pore water pressure distribution (positive and negative using piezometers and tensiometers).

2. Moisture content distribution.
3. Strain in the reinforcement layers.
4. Connection loads between the facing and reinforcement layers.
5. Wall facing deflections.
6. Horizontal and vertical toe loads.
7. Earth pressures at the base of the soil mass and within the soil mass.

Numerical Modeling Program

A series of numerical models was developed using geometries selected to match the wall geometry of the full-scale physical tests, and calibrated using measurements from those tests. Seepage and stability analyses were conducted using SVFlux GT and SVSlope GT from the software package SVOffice Version 5.0. Seepage analyses were done for two scenarios: (i) infiltration of the MSE wall backfill from flooding at the face of the wall, and (ii) rapid drawdown. Measured water levels at the wall front and the two standpipe piezometer locations were used to calibrate the numerical model. Simulations were then conducted to replicate the physical model tests using fine and coarse sands as backfill, respectively. Stability analyses were conducted to evaluate stability of the MSE wall and calculate the factor of safety against sliding failure in limit equilibrium condition using the GLE (Fredlund) method. Parametric studies were conducted using the calibrated numerical models to examine how backfill hydraulic conductivity, flood height, and length of the backfill affect the backfill saturation time and wall stability during flooding and drawdown.

Organization of the Report

This report is organized into six chapters. Chapter 1 (Introduction) introduces the motivation for the research, summarizes key background concepts, and summarizes the basic research approach. Chapter 2 (Literature Review) summarizes key elements of MSE wall design and performance, with emphasis on flooding and rapid drawdown phenomena. Chapter 3 (Laboratory Full-Scale Tests) summarizes construction processes, instrumentation, and test processes for two full-scale physical model tests conducted at the Royal Military College of Canada. Chapter 4 (Full-Scale Test Results and Analysis) summarizes results and analysis from the physical modeling program. Chapter 5 (Numerical Analysis) summarizes the numerical modeling program, parametric studies, and recommended design charts. Finally, Chapter 6 (Conclusions and Recommendations) offers a series of conclusions and recommendations for implementing the results of the research.

CHAPTER 2 : LITERATURE REVIEW

MSE Walls

Mechanically Stabilized Earth (MSE) walls are retaining walls with face angles from 70^{o} to 90^{o}. MSE walls are internally stabilized and comprise three main components: facing, internal reinforcement (e.g. geosynthetics or metallic components) and selected backfill. Coarse, free-draining material is generally chosen for backfill in order to ensure high drainage capacity as well as structural integrity of the wall (Berg et al. 2009). The interaction between reinforcement and backfill allows MSE walls to sustain significant loading and deformation, and to behave like a flexible unit (Rathje et al. 2006; Berg et al 2009). A general schematic model of an MSE wall is shown in Figure 2-1.

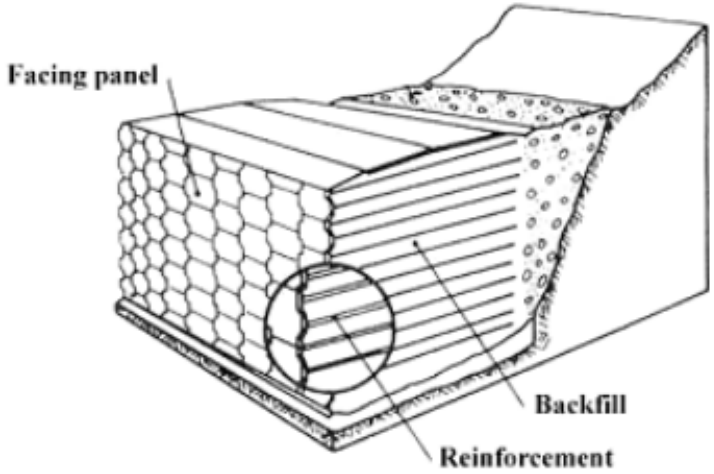

Figure 2-1. Schematic view of a MSE wall cross-section (FHWA 2009).

MSE walls offer economic and technical advantages over conventional types of retaining walls (e.g. Gravity, Semi-Gravity, Cantilever and Counterfort), including less site preparation requirements, reduction of right-of-way acquisition and stability for wall-heights over 30 m. Geosynthetic reinforced MSE walls are the least expensive choice for most wall heights (Koerner et al. 2000). MSE walls eliminate the need for deep foundations and are flexible and are thus capable to tolerate deformations due to poor subsoil conditions. In addition, MSE walls are more resistant to seismic loading and can tolerate much larger settlements than conventional retaining walls (Koerner 2000; Elias et al. 2001; Berg et al. 2009).

The most critical components of a MSE wall are the selected backfill and reinforcements. The facing component is important for aesthetical purposes, but contributes

little to the overall stability of the MSE wall system. The components of the MSE walls are discussed below:

Selected Backfill

Backfill materials can be natural or recycled materials that meet design criteria established by regulatory agencies (e.g. AASHTO, FHWA, state DOTs, etc.). The backfill used in MSE walls consists of coarse-grained material with low fines content (less than 15% passing sieve #200) (AASHTO 2010; Anderson et al. 2012).

The selection of backfill material considers the long-term performance of the wall system. The material shall offer good drainage, and thus the hydraulic conductivity of a selected material must be high enough to allow water to percolate freely through the backfill. Excessive amounts of fines can reduce the hydraulic conductivity of a given coarse material, thus contributing to long-term performance issues of the wall (Elias et al. 2001; Rathje et al 2006). Based on the AASHTO T-27 criteria discussed by Berg et al. (2009), to obtain reasonable drainage, the fines content of the selected material for reinforced fill shall have no more than 15% fines (as determined from passing No. 200 sieve) and 60% fine sand size particles (as determined from particles passing No. 40 sieve). The plasticity index of the material shall be less than 6.

The potential corrosion of metal reinforcements can be enhanced if water is retained by poorly draining backfill. For this reason, the use of material with high water absorption potential such as clay and silt is not recommended as backfill (Elias et al. 2001; Berg et al. 2009). Corrosion is a major concern when the MSE wall system utilizes metal reinforcements because it can result in sudden failure of the wall system (Berg et al. 2009; Anderson et al. 2012).

The mechanical stability of the wall depends, in part, on the mechanical properties of the backfill. The material should yield adequate angle of internal friction allowing high shear strength against horizontal pressures imposed by the soil mass (Elias et al. 2001; Rathje et al. 2006; Berg et al. 2009). The selected backfill should also develop sufficient interface friction with the reinforcement. Well-graded and less angular materials yield higher values of dry unit weight during compaction (Berg et al 2009). Materials compacted at low dry unit weight and low water content can experience significant settlement upon wetting (Basma et al. 1992; Rathje et al. 2006; Berg et al. 2009).

Reinforcements

The function of reinforcements is to provide shear strength to the backfill against the lateral earth pressure. Reinforcements used in MSE walls can be classified as extensible and inextensible (Koerner 2005; Das 2008). Inextensible reinforcements show deformation at failure much less than the deformability of the soil. Steel strips and bar mats are examples of inextensible reinforcement. Extensible reinforcements, on the other hand, show deformation at failure equal to, or greater than the deformability of the soil. Geotextiles, geogrids and woven steel wire mesh are extensible reinforcements (Koerner 2005; Das 2008; Berg et al. 2009).

Backfill Specifications

Specifications for backfill of MSE walls follow guidelines set by state and federal agencies. The WisDOT adopts the recommendations set forth by the FHWA and AASHTO except when provisions by the agency are made necessary. The following requirements presented here are consistent with current practice. The backfill material should be as free as possible of organic and other deleterious materials (Berg et al. 2009; AASHTO 2010; Anderson et al. 2012; WisDOT 2015). Table 2-1 summarizes a range of values for gradation, plasticity index and soundness (Holtz et al. 1998; Berg et al. 2009; AASHTO 2010). MSE walls require high quality wall fill for durability, good drainage, constructability, and good soil reinforcement interaction which can be obtained from well graded, granular materials. Many MSE systems depend on friction between the reinforcing elements and the soil. In such cases, a material with high friction characteristics is specified and required. Some systems rely on passive pressure on reinforcing elements, and, in those cases, the quality of reinforced wall fill is still critical. These performance requirements generally eliminate soils with high clay contents.

Unstable broadly graded soils (i.e., Cu > 20 with concave upward grain size distributions) and gap-graded soils should be avoided (Berg 2009). These soils tend to pipe and erode internally, creating problems with both loss of materials and clogging of drainage systems. In addition to the specifications and recommendations regarding grain size distribution, Koerner (2005) suggests a specific backfill gradation for maximizing drainage while minimizing installation damage in geotextiles and geogrids. These values are shown in Table 2-2. Additionally, the backfill material must meet the electrochemical criteria by the WisDOT as presented in Table 2-3 (WisDOT 2015).

Table 2-1. MSE wall selected granular reinforced fill requirements (after Berg et al. 2009; AASHTO 2010).

Gradation: (AASHTO T-27)	**U.S. Sieve Size**	**Percent Passing** [a]
	102 mm (4 in.) [a,b]	100
	No. 40 (0.425 mm)	0-60
	No. 200 (0.075mm)	0-15
Plasticity Index: (AASHTO T-90)	PI $\leq$ 6	
Soundness: (AASHTO T-104)	The materials shall be substantially free of shale or other soft, poor durability particles. The material shall have a magnesium sulfate soundness loss of less than 30% after four cycles (or a sodium sulfate value less than 15 % after five cycles).	

Notes:
(a) To apply default F* values, Cu should be greater than, or equal to 4.
(b) As a result of recent research on construction survivability of geosynthetics and epoxy coated reinforcements, it is recommended that the maximum particle size for these materials be reduced to (19 mm) for geosynthetics, and epoxy and PVC coated steel reinforcements unless construction damage assessment tests are or have been performed on the reinforcement combination with the specific or similarly graded large size granular fill. Prequalification tests on reinforcements using standard agency fill materials should be considered.

Table 2-2. Recommended Soil Backfill Gradation for Geotextile and Geogrid Reinforcement Applications (Walls and Slopes) (After Koerner 2005).

Sieve Size (No.)	Particle Size (mm)	Percent Passing
4	4.76	100
10	2.0	90 - 100
40	0.42	0 - 60
100	0.15	0 - 5
200	0.074	0

Table 2-3. Electrochemical Property Criteria for Reinforced Fill in MSE Walls (WisDOT 2015).

Reinforcement Material	Property	Criteria
Metallic	Resistivity	> 3000 ohm cm/H
Metallic	Chlorides	< 100 ppm
Metallic	Sulfates	< 200 ppm
Metallic / Geosynthetic	pH	3.5 < pH < 9
Metallic / Geosynthetic	pH	4.5 < pH < 10

The recommended maximum effective friction angle (ϕ') assumed for design of reinforced backfill fill is 34^o (Berg et al 2009 and AASTHO 2010), and 30^o (WisDOT 2015)

in the absence of specific data. For desired friction angles higher than 30^{o}, direct shear tests (AASTO T-236) shall be performed on the portion of material finer than the No. 10 sieve (WisDOT 2015). If the measured friction angle exceeds 40^{o}, then the design angle of friction should not exceed 40^{o} (Article 11.10.6.2, AASHTO 2010). Cohesion is considered to be 0.0 kN/m^3 for all cases (Berg et al. 2009). The WisDOT recommends a minimum unit weight of 18.9 kN/m^3 and cohesion of 0.0 kN/m^3 (WisDOT 2015).

Failure Modes

The modes of failure of MSE walls are divided into excessive deformation and collapse. Of 141 reported case history failures, *internal instability*; e.g., wide spacing, short lengths and low shear strength soil, accounts for 37 cases (26%), *external instability;* e.g., poor foundations, sloping exit angles, excessive surcharge loads, seismicity and low global shear strength accounts for 23 cases (16%); *internal water*; e.g., leaking drainage systems, broken water mains, and infiltrating water, accounts for 51 cases (36%); and *external water*; e.g., from the retained zone, tension cracks and elevated water level, accounts for 30 cases (22%) (Koerner and Koerner 2012).

The primary causes of MSE wall failures are reported to be inadequate or improper design and/or construction. The *major design inadequacy* appears to be the lack of proper drainage procedures. The *major construction inadequacy* is the use of fine-grained silt or clay backfill soils and inadequate placement and compaction. Corresponding poor drainage leads to hydraulic pressures mobilized behind or within the reinforced soil zone, and requires the use of back and base drains to dissipate the pressures and remove the water at the front of the wall (Koerner and Koerner 2012). Figure 2-2 shows different failure modes for illustration.

The stability of Mechanically Stabilized Earth (MSE) walls may be compromised in undrained conditions such as during heavy rain, flooding, or a rapid drawdown event. Excess pore pressures in non-freely draining backfills may not dissipate quickly enough, and thus may reduce effective stresses in the backfill soil, which in turn may cause a reduction of shear strength at soil-soil or soil-reinforcement interfaces (Bobet, 2002). Excess pore pressure also reduces the effective weight (buoyancy) of the reinforced soil zone and sliding resistance for external stability is decreased. Koerner and Koerner (2012) analyzed causes of failure of 141 MSE walls (34 cases of excessive deformation and 107 cases of actual collapse) and found that 58% were caused by internal or external water and that the major design inadequacy was the lack of proper drainage within the reinforced soil zone.

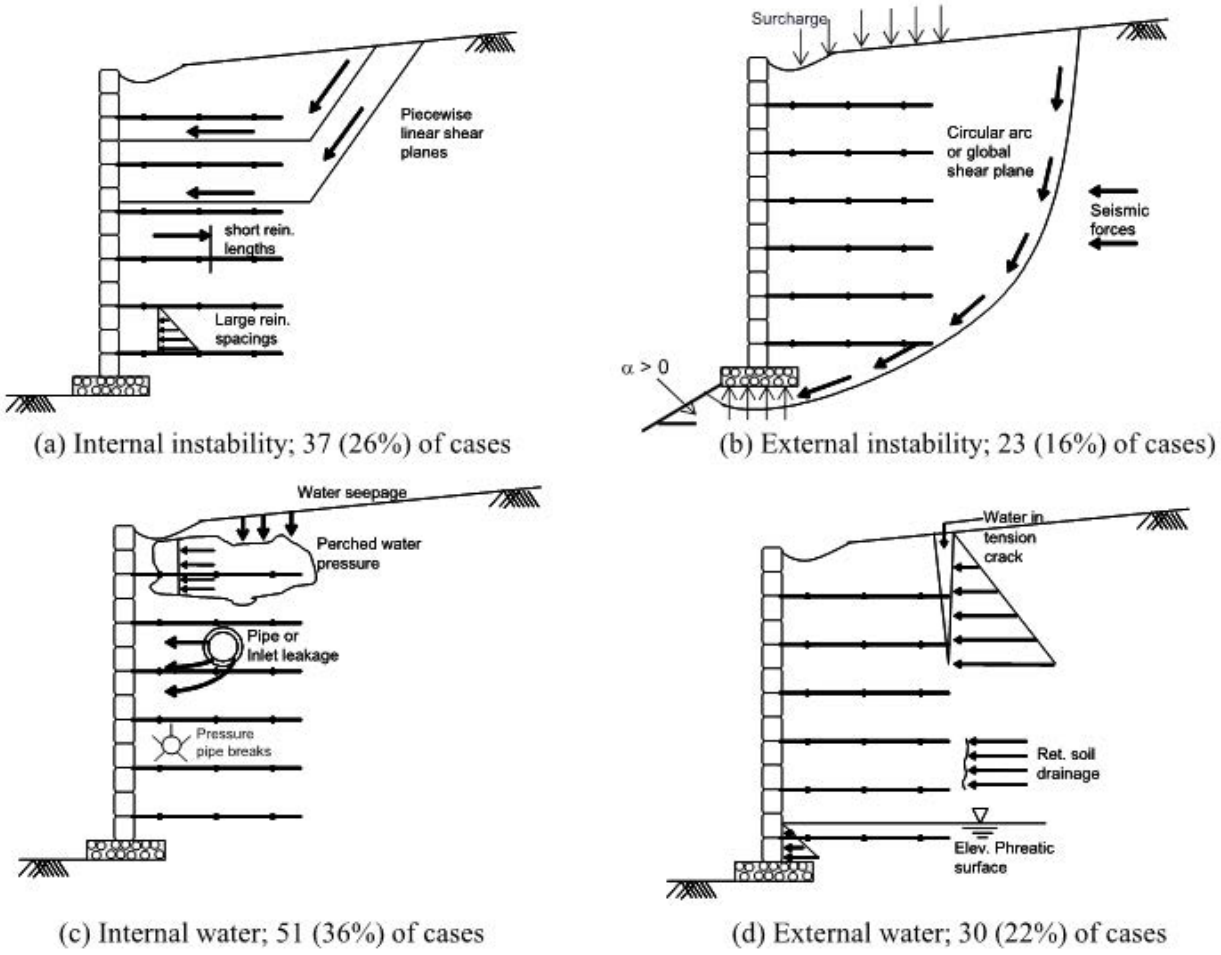

Figure 2-2. MSE wall failure mechanisms (after Koerner and Koerner 2012).

Rapid Drawdown

For MSE retaining walls potentially subject to inundation at the wall face, such as those located adjacent to rivers, canals, detention basins or retention basins, AASHTO specifies that a minimum hydrostatic pressure equal to 3 ft (1 m) should be applied at the high-water level for the design flood event (AASHTO section 11.10.10.3.). Situations where the wall is influenced by tide or river fluctuations may require that the wall be designed for rapid drawdown conditions from the high-water level, which could result in differential hydrostatic pressures considerably greater than 3.0 ft (1 m). As an alternative to designing for rapid drawdown conditions, No. 57 coarse aggregate, as specified in AASHTO M 43, could be provided as reinforced backfill for the full reinforced zone of the wall and to the maximum height of submergence of the wall. A geotextile filter should be provided at the interface of the No. 57 coarse aggregate and reinforced backfill above it, at the interface of the retained backfill

behind it, and at the interface of the coarse gravel and subgrade beneath it, unless the coarse aggregate meets the soil filtration criteria for the adjacent soils. Adjoining sections of geotextile filter/separator shall be overlapped by a minimum of 1 ft (0.3 m).

Figure 2-1 shows an example detail. Corresponding destabilizing effects due to undrained conditions from rapid drawdown can be significant. For example, Aubeny et al. (2014) conducted stability analysis on an MSE wall subjected to rapid drawdown. The granular reinforced soil and the retained soil had friction angles of 34^o and 30^o; respectively. The rapid drawdown reduced the slope stability factor of safety by 22 to 33% depending on the amount of drawdown.

Bobet (2002) investigated the pullout capacity of geogrid reinforcement in MSE walls under drained and undrained conditions for different types of soils. The results showed that undrained conditions significantly reduce the pullout capacity, by as much as 50%. This is caused by the generation of excess pore pressures in the soil under rapid loading which decrease the effective stress at the soil-reinforcement interface. The magnitude of the pullout reduction is related to the permeability of the soil since for large permeabilities the dissipation of excess pore pressures is very rapid and no sustained reduction in pullout capacity is produced; in contrast for low permeabilities the dissipation of excess pore pressures is slower than the rate of pullout and thus a reduction may occur.

Within the unsaturated zone above the wetting front in the backfill, negative pore water pressure or matric suction develops and can have a significant effect on the active earth pressure exerted by the backfill soil (e.g., Vahedifard et al. 2014). It is thus important to know the location of the wetting front during rapid drawdown or water infiltration into MSE structure backfill, how this location changes over time, and how the corresponding excess pore pressures can reduce the internal and external stability of the MSE wall. Understanding the evolution of free water surface in a MSE wall backfill during flooding and rapid drawdown events and variation of stability factor of safety during these conditions warrants a research that evaluates these phenomena through physical and numerical modeling.

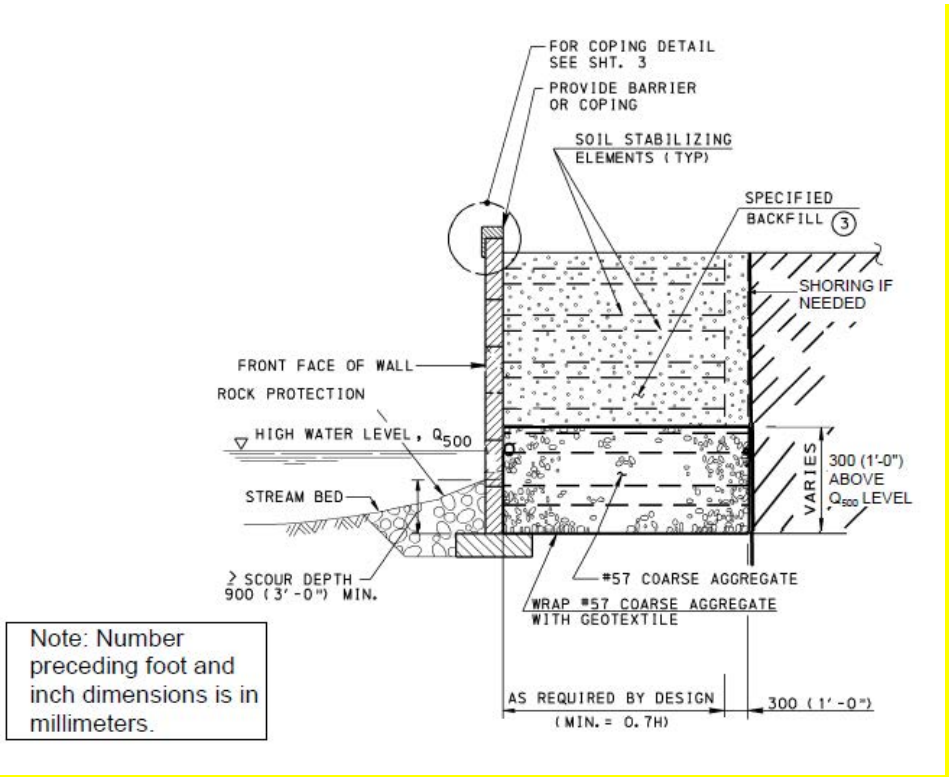

Figure 2-3. Example detail for wall that may experience inundation.

CHAPTER 3 : LABORATORY FULL-SCALE MSE WALL PHYSICAL MODELS

This chapter describes the testing methodology and materials to evaluate and monitor construction and infiltration into the MSE structure backfill, water table evolution, and drainage capacity of the backfill for full-scale MSE walls. Two walls with different soil backfill were constructed and tested. The purpose of this task is to perform a detailed analysis of the infiltration, drainage and the internal and external lateral ground pressures that develop within the walls of the MSE under conditions that would be expected in the field.

This task was accomplished using the Retaining Wall Test Facility of the Royal Military College of Canada (RMC), which has more than 30 years of experience with more than 15 tested walls. The facility (Figure 3-1), as well as wall components, instrumentation, data acquisition, and construction equipment, were available for this project. This also follows on the experimental philosophy at RMC of varying one variable including wall facing type, facing batter, reinforcement type and properties, reinforcement vertical spacing, and backfill soil. Important research has been carried out at RMC, which contributed to the advance of understanding the behavior of MSE walls (e.g. Bathurst 2014, Bathurst et al. 2005, 2006, Miyata and Bathurst 2007, Walters et al. 2009, Bathurst et al. 2000).

The Retaining Wall Test Facility consists of three main components, soil, facing and reinforcement. The choice of these materials followed technical recommendations and utilized reinforcement and facing common in North America. The main difference between the two walls was the backfill material, which follows the AASHTO (2010) and Berg et al (2009) recommendations but differ in soil grain-size distribution and permeability.

After construction, the MSE wall was subjected to flood events, as well as 1 m drawdown events (according to AASHTO 11.10.10.3) in order to assess how the moisture regime develops within the MSE backfill material and retained soil. In order to perform the flooding and rapid drawdown test, a small tank was developed in front of the wall face that could simulate a flood as well as drain water during the rapid drawdown test. Temporal measurements of moisture distribution allow evaluation of the wetting front location (the line between saturated and partially saturated soil) throughout the tests. Internal and external instrumentation allowed simultaneous monitoring of MSE wall performance throughout flood and rapid drawdown events.

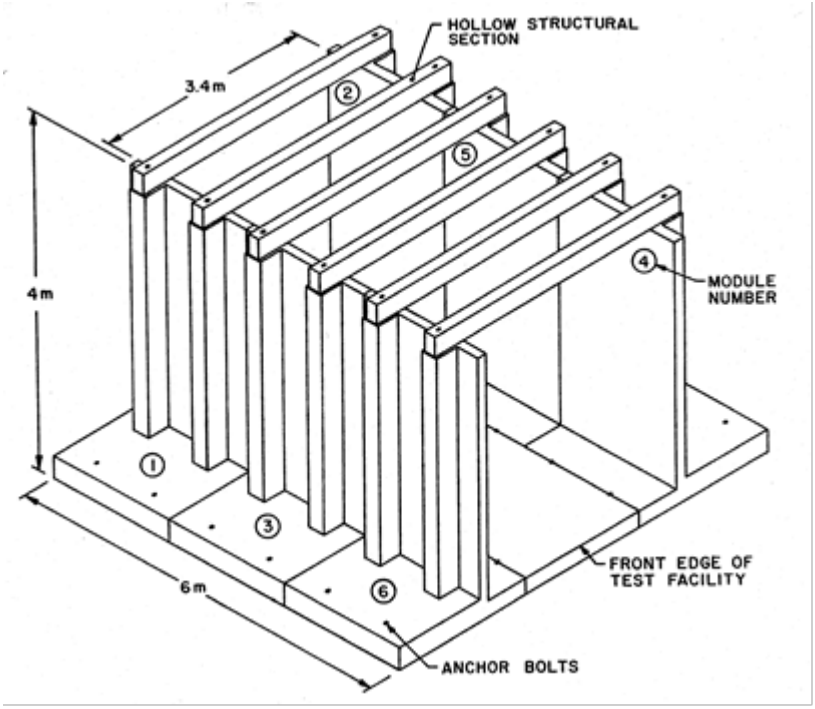

Figure 3-1. Retaining Wall Test Facility (Bathurst et al. 2000).

Each wall was monitored using more than 200 instruments during construction, testing, and excavation. The instrumentation is presented in this chapter.

Materials

Backfill Soil

According to AASHTO (2010) and Berg et al (2009), the backfill material must contain less than 15% fines (sieve No. 200) and a plasticity index (PI) of less than 6%. Following the recommendations, the first wall was constructed using a poorly graded sand whereas the second wall used a poorly graded sand with gravel. Soil testing for both materials occurred following the standards summarized in Table 3.1.

Table 3-1. Laboratory test standards and methods.

Purpose	Test	Standard/Reference
Soil classification test	Grain size analysis test	ASTM D6913-04
	Unified soil classification system	ASTM D2487-06
Compaction test	Standard Proctor test	ASTM D698-12e1
Permeability test	Permeability of Granular Soil (Constant Head)	ASTM D2434-19
Soil friction angle	Direct Shear Test of Soil	ASTM D3080M-11
Suction test	Soil water characteristic curves	ASTM D6836-16

To classify the backfill soil grain size analysis (Figure 3-2-a) was performed. From the grain size results, it was possible to classify the material following the USCS (Unified Soil Classification System) classification. The Standard Proctor Test was used to find the maximum dry density and optimum moisture content (Figure 3-2-b). A series of direct shear tests were also conducted on the material in accordance with ASTM D3080. From regression of peak shear strength values were determined for both walls. The permeability tests were conducted to determine the coefficient of permeability by a constant-head method (Figure 3-2-c).

Soil water characteristic curves (SWCC) for the backfill soil used in the analysis are shown in Chapter 4. SWCC were measured using the hanging column method for the sample compacted directly into a Buchner funnel as well as for the sample compacted into a confining ring placed in a Buchner funnel. Both samples were compacted to target values determined by Proctor compaction tests.

Table 3-2 summarizes the results for both soil used in Wall#1 and Wall#2, however, details about the results are presented in Chapter 4. The main aspect that differentiates one MSE wall from another in this study is the backfill material. Figure 3-3 shows the Grain Size Distribution for both backfill.

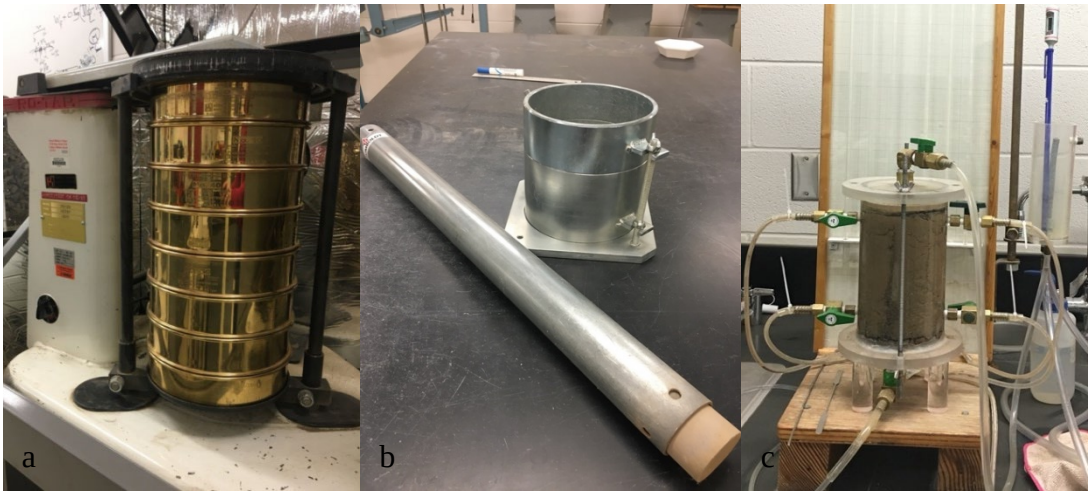

Figure 3-2. Laboratory tests (a) Grain size analysis; (b) Standard Proctor test; (c) Permeability test.

Table 3-2. Summary of soil results.

		Soil#1	**Soil#2**
Coefficient of **uniformity**		3.94	46.2
Coefficient of curvature		0.85	0.82
Maximum dry density (kN/m3)		17.78	21.93
Optimum moisture content (%)		8.8	7
Permeability (cm/s)		$7.4x10^{-4}$	$3.5x10^{-5}$
Soil friction angle	ϕ_{peak}	40.8	44.5
	$\phi_{cte\ volume}$	35.7	42.4
USCS classification		poorly graded sand	poorly graded sand with gravel

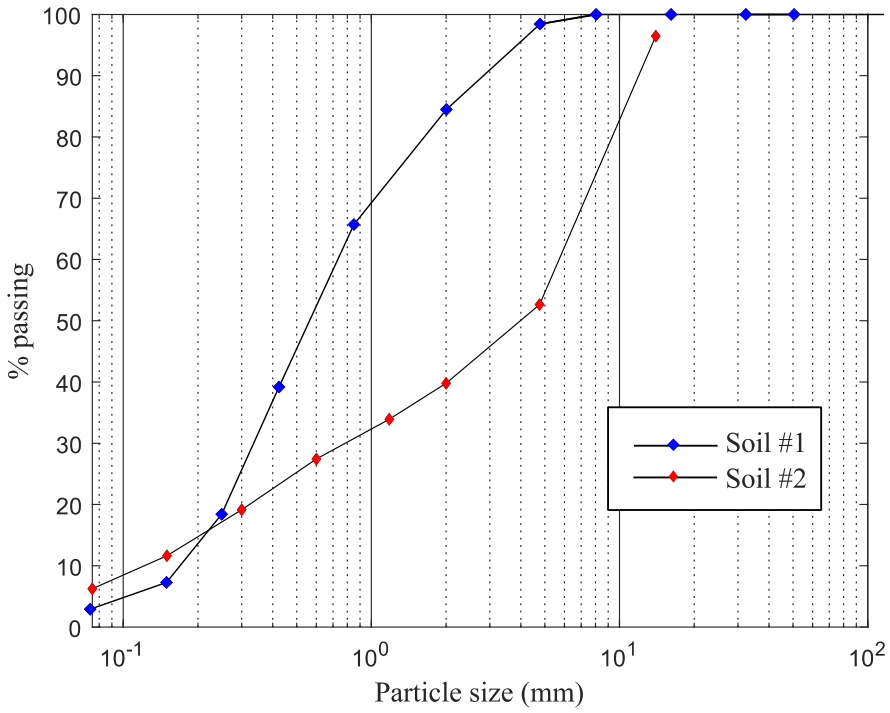

Figure 3-3. Grain Size Distribution - Soil#1 and Soil#2.

Reinforcement

The reinforcement for both Walls consists of steel strips that have been engineered to provide additional strength and stiffness to the compacted backfill, while having no potential for voids between the soil and reinforcement. High-Adherence (HA) Ribbed Reinforcing Strips are manufactured by Reinforced Earth Company of Reston, Virginia, and intended primarily for MSE applications.

The advantages of reinforcing steel strips are their high tensile strength and high pullout strength. High-grip reinforcing strips are hot-dip galvanized steel strips, ribbed perpendicular to the long shaft and a single screw hole at one end. The strips are structurally connected to the galvanized tie rods on opposite panels using a high strength nut/bolt/washer assembly. The dimensions of the steel strips used in the project were 50 mm in width, 4 mm thick strip, and 3.3 m in length. Details of the steel strip design can be seen in Figure 3-4. The allowable reinforcement tension used for design shall not exceed 448 MPa.

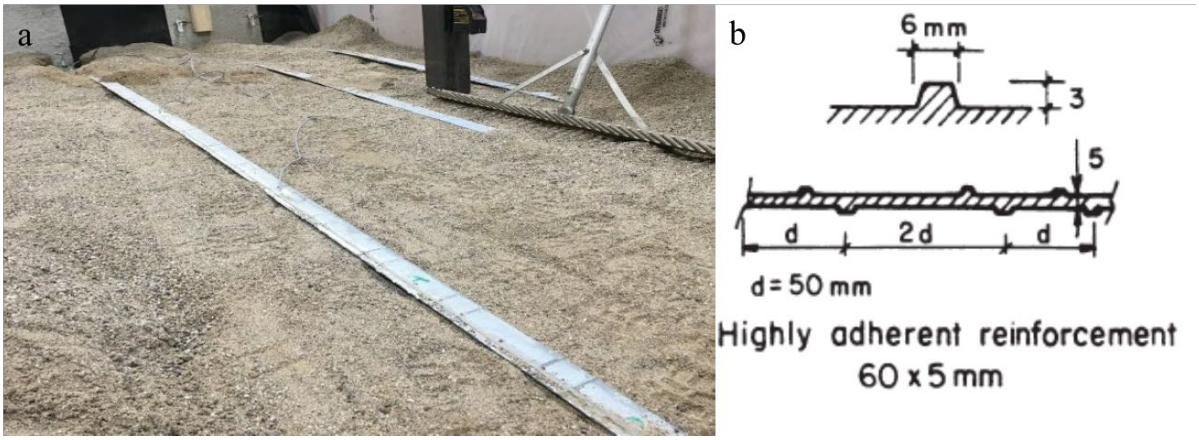

Figure 3-4. Steel strip (a) Located at first layer, (b) Detail of the friction elements (Fang,1990).

Facing

Facing elements were constructed with nine modular precast concrete panels. The panels are cruciform (1.5 m x 1.5 m) (or half cruciform for the lateral panels) and make up a puzzle. The panels typically have a structural thickness of 14 cm, not including aesthetic relief. The central panels weigh about 7.75 kN whereas the lateral panels weigh about 5.15 kN.

The joints between the panels are spaced using pad rubbers that do not allow one panel to touch the other (avoiding concrete breakage). These joints are covered by geotextiles on the back face to provide adequate drainage of the structure while preventing backfill loss (Figure 3-5). Details of the connections between the face panels and steel strips are shown in Figure 3-6.

Figure 3-5. View from inside of facility displaying geotextile used to cover gaps between adjacent panels.

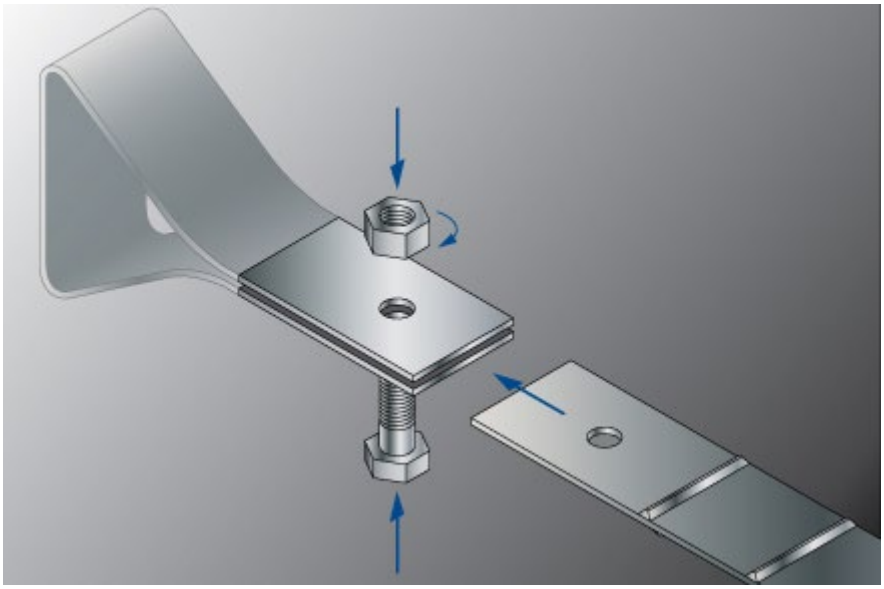

Figure 3-6. Detail of connection between facing and steel strip (Reinforced Earth, 2021).

Components of the Test Facility

General

The test facility components, instrumentation, data acquisition, construction equipment, and infiltration and drainage simulators are used for this project and are described in this chapter. Instrumentation allowed the measurement of the following:

- Moisture content distribution;
- Strain in the reinforcement layers;
- Connection loads between the facing column and the reinforcement layers;
- Wall facing deflections;
- Horizontal and vertical toe loads;
- Earth pressures at the base of the soil mass and within the soil mass;

The Full-Scale Test Facility

The Full-Scale RMC test facility is an indoor facility capable of reproducing retaining walls measuring 3.7 m high by 3.3 m wide and up to 6 m long (Bathurst et al. 2000). Located within the Structures Laboratory of the RMC Civil Engineering Department, the facility allows controlled environment testing and, for this project, a small tank to simulate a river flood was utilized. The backfill soil and wall facing are seated on a rigid concrete foundation. The soil is contained laterally between two parallel reinforced concrete counterfort walls bolted to the laboratory floor. At the rear of the test facility, a series of 330 mm high by 150 mm thick rigid concrete bulkhead panels are placed sequentially to contain the backfill as construction proceeds. In front of the facing, a structure with five vertical beams, plywood closure and enveloped with an impermeable membrane, allowed the construction of a small tank measuring 2 m in height by 3.3 m in width and 0.6 m in length to simulate flooding of the wall's front face.

Backfill Soil Compaction

The soil was placed and compacted in the wall following the same procedure for all layers. The soil was stored and moved through bags that provided ease of movement for this material with the operation of a crane in the laboratory. The backfill soil was compacted in 150 mm lifts, totaling 24 layers. Each layer was compacted using a hand tamping plate measuring 250 by 250 mm and weighting 5 kg (Figure 3-7-a) in the first meter from the wall facing and the remaining 5 meters were compacted by a lightweight jumping jack tamper compactor (Wacker model ES 45Y Figure 3--b) for the first wall and a vibratory plate (Figure 3-7-c) for the second wall. The first soil layer (15 cm) was compacted only with the hand tamping plate, as shown in Figure 3-7-a for both walls. The use of lighter compaction near the facing is consistent with field compaction procedures (Berg et al 2009) and reduces the effects of compaction on the wall face. To reach the optimum dry density, the manual compactor's

drop height was about 200 mm and four consecutive drops were performed at each location, this procedure was performed twice (totaling eight drops). On the other hand, the light vibratory compactor was passed twice to reach the desired density for the first wall. The compactor plate was passed four times to reach the target density.

Density and moisture content readings were obtained using a Troxler 3411-B nuclear densimeter surface moisture density gauge (Figure 3-8). For each layer, nine readings were taken at specified locations. The average measured values of moisture content and bulk unit weight were verified to be within 95% of dry density for each layer.

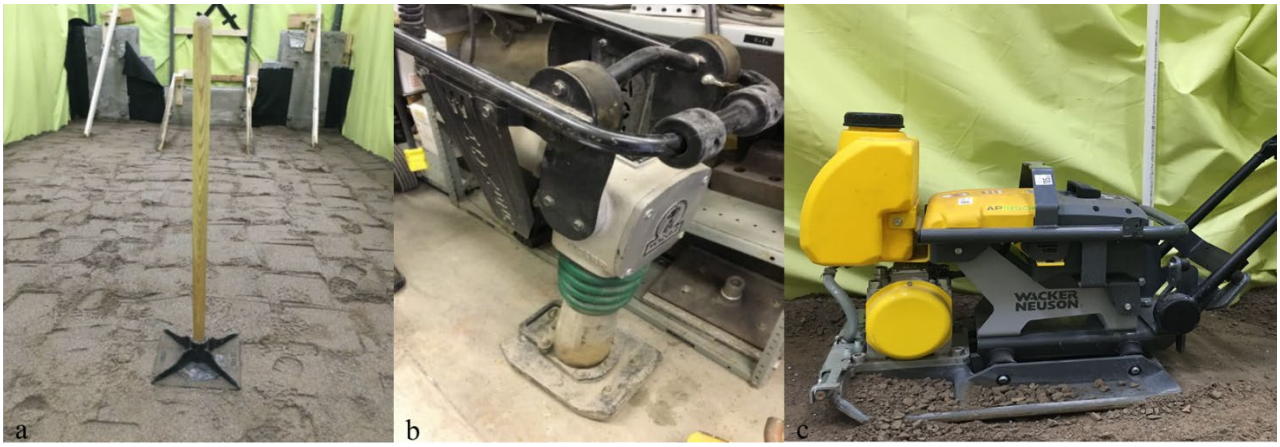

Figure 3-7. Compaction devices (a) hand tamping plate and (b) lightweight jumping jack tamper (c) vibratory plate.

Figure 3-8. Nuclear densometer – Troxler 3411_B.

Sidewall Friction

To decrease lateral friction and simulate plane strain conditions in the test facility, a lubricated polyethylene sheet system was developed by previous RMC researchers (e.g., Nelson 2005). The system is composted by a layer of Plexiglas sheet and three layers of polyethylene sheet with grease between the layers. The sheets have been properly stretched to prevent wrinkles. Between this system and the backfill soil an impermeable membrane is placed that served as a barrier to infiltration water during the flooding and rapid drawdown tests.

The combination of the lateral plane strain system and the concentration of the instrumentation at the central part of the wall simulates field conditions in a well-controlled laboratory environment.

Data Acquisition System

The data monitoring and recording during all phases of the project were achieved using an Agilent 34980A data acquisition system combined with 34980A BenchLink Data Logger data acquisition software. A special data acquisition was used to collect the reading to the Moisture Content Sensors, CR1000 and TDR 100 Campbell Scientific were used to send the

electro waves responsible for generating the pulse to collect the moisture content. The software used for these CR1000 and TDR100 was PC200W Datalogger. A personal computer (PC) with i5-4590 CPU, 3.30GHz, 4 Core(s) processor and 8GB of RAM was connected to the Agilent and CR1000 units.

The Agilent 34980A system has a capacity to monitor 560 channels distributed in eight cards. Cards three to six were reserved for strain gauges, which used an advanced high precision reading system. Two channels were used for each strain gauge.

To connect the devices to the data acquisition system cards, distribution boards were used. They were able to distribute input voltages to the instruments. The input voltages for each set of instruments were continuously scanned by selected channels of the Agilent unit to check that there were no fluctuations in instrumentation excitation levels that could distort interpretation of data.

A comma delimited file is created for each construction and flooding event. All files were saved and then converted from DCV and Ohms to the engineering units (kN, mm, kPa, strain) using a MATLAB code.

Instrumentation

A total of 230 instruments were used for the first wall and 234 instruments for the second wall to record the following measurements:

- Horizontal and vertical footing loads
- Horizontal wall facing deflections;
- Reinforcement layer strains;
- Vertical earth pressures at the base of the soil mass and within the soil mass;
- Connection loads between the facing column and the reinforcement layers;
- Moisture content on the backfill;
- Water level;
- Outward movement of the test facility sidewalls.

Figure 3-9 and Figure 3-10 show the schematical instrumentation for the first and second walls, respectively. Some modifications regarding the location of the measurement sensors can be seen for the second wall in relation to the first. This change of location, mainly of the moisture content sensors, occurred to improve the analysis of the water level during the /rapid drawdown tests. Table 3.3 summarizes the instrumentation type and quantity of instruments used in each of the walls.

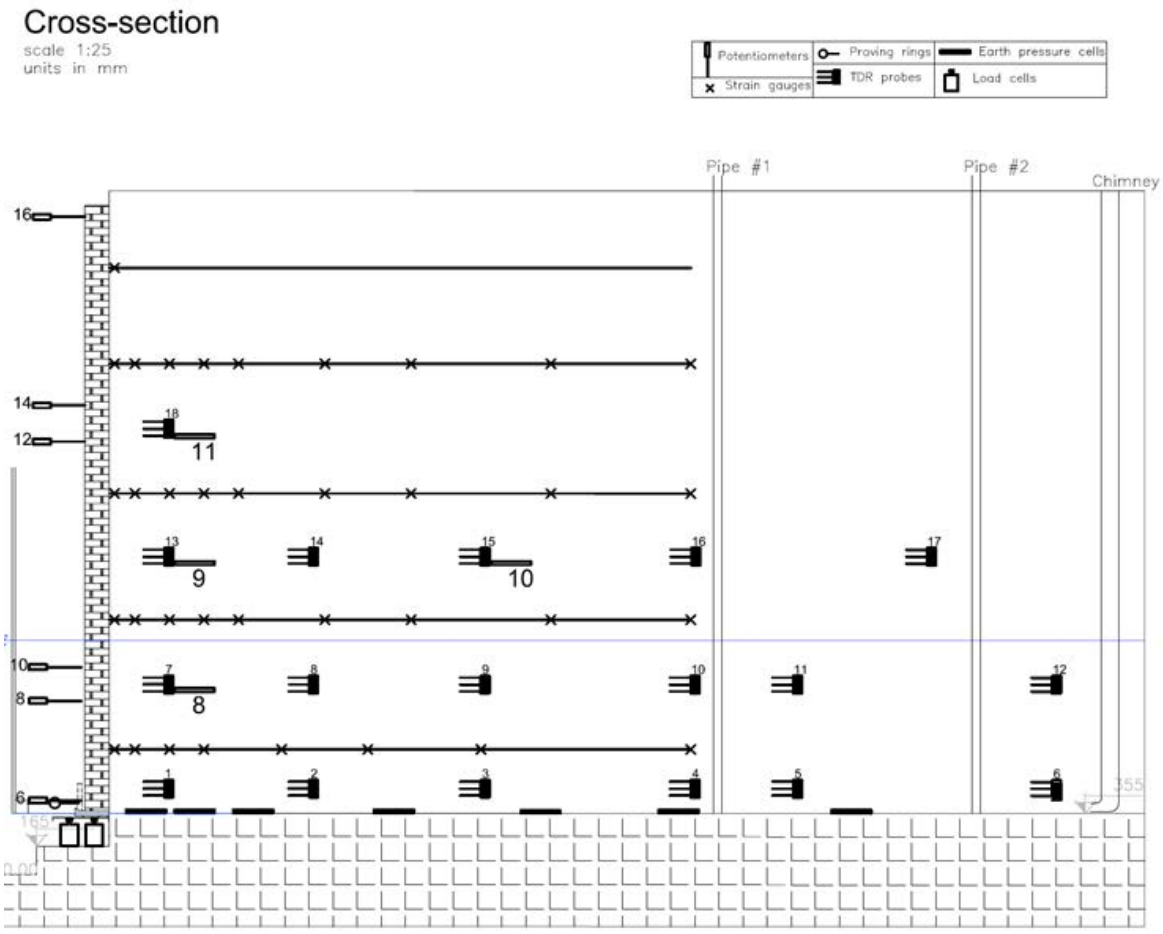

Figure 3-9. Wall #1 cross-section displaying instrumentation location.

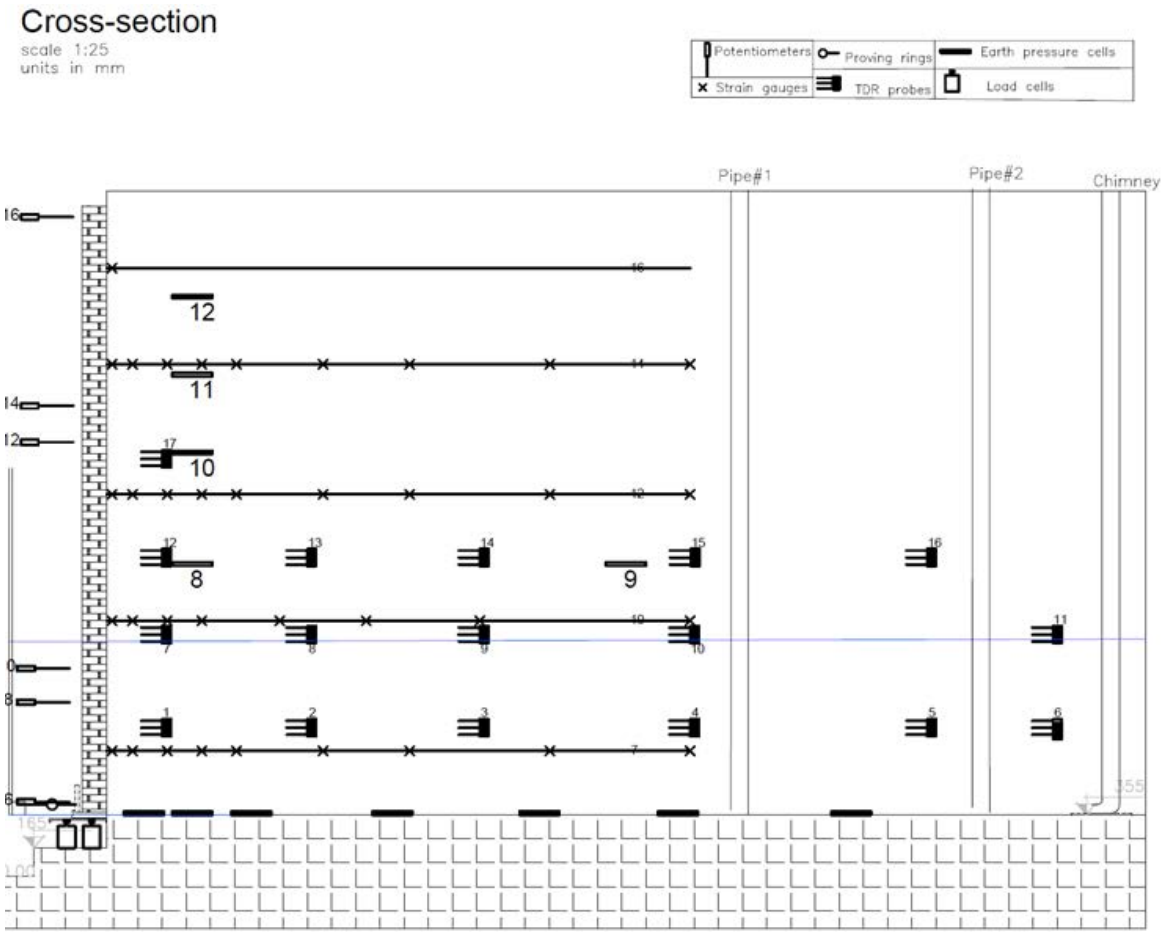

Figure 3-10. Wall #2 cross-section displaying instrumentation location.

Table 3-3. Instrumentation summary

	Instrument	Purpose	Number of instruments in Wall 1	Number of instruments in Wall 2	Manufacturer
Facing	Potentiometer (LVDTs)	Horizontal movement of facing	10	10	Penny and Giles
		Footing movement	6	6	Penny and Giles
	Toe load rings	Horizontal load at footing	6	6	Homemade
	Toe load cell	Vertical load at footing	18	18	Intertechnology Inc / Hoskin Scientific / homemade
Soil	Earth pressure cells	Soil pressure	12	12	Geokon EP4500
	Standpipes - piezometer	Water level	2	2	homemade
	TDR probes	Moisture content	18	18	Campbell Scientific
Reinforcement	Strain Gauges	Local strain in reinforcement	131	133	Showa Measuring Instruments
	Connections	Local strain in panel	22	22	Showa Measuring Instruments
Test Facility	Cable potentiometers (LVDTs)	Movement of sidewall	1	3	Penny and Giles
	Thermocouple	Temperature	4	4	Omega
Total			230	234	

a) Facing Deflections

Potentiometers were used to measure the horizontal movement of each panel face. Penny and Giles rectilinear potentiometers with 200 mm spring were installed on the central column of each wall. Each potentiometer was calibrated using calibrated stainless steel reference blocks and a 10-volt DC power source. The potentiometers were connected to the Agilent data acquisition system.

For each panel, four potentiometers were installed, measuring the movement of the four corners of each central panel. The potentiometers were installed on a lightweight steel and

timber frame and connected to the panels with fishing line. The horizontal movement at each reinforcement layer was taken as the average displacement recorded by the potentiometer pair.

In addition, six 200 mm stroke linear voltage displacement transducers (LVDT) were placed at the toe of the wall. Two LVDT was located at each of the Center, North and South sections of the wall to record the horizontal movement of the facing at the toe.

b) Reinforcement Strains

Reinforcement strains were measured locally using strain gauges bonded to the steel strips. All strain gauges were mounted in the longitudinal direction in order to capture strain associated with the outward movement of the wall face and development of potential failure planes through the reinforced soil zone. Strains in each reinforcement layer were measured successively to develop a strain distribution over the length of the reinforcement layer for any stage of the testing program. The strain gauges were N11-FA-5-120-11 type manufactured by Showa Measuring Instruments Company of Japan. The gauges have a 5.0 mm gauge length and a relative resistance of 120 ohms. The gage factor used was 2.12. Each strain gauge was then covered by a silicon sealant for protection. Strain gauges were mounted in pairs (above and below of each steel strip) and pairs placed at identical distances from the wall facing to provide redundancy and back-up in case of gauge failure. The strain gauges were connected to the D/A using the 4-wire ohm function in order to measure uniform single-axial strains.

c) Vertical Earth Pressure

To record the vertical earth pressures along the base of the wall and within the backfill ground, Geokon EP4500 earth pressure cells (EPC) were used.

The EPCs are made up of two circular stainless-steel plates with a diameter of 230 mm welded together at their edges and filled with an incompressible glycol solution. A semiconductor strain gauge pressure transducer located in a narrow tube protruding from the plates that measures the internal fluid pressure. The Geokon EPCs were powered by a 10-volt DC source and are capable of measuring pressure in a range from 0 to 450 kPa.

Each pressure cell was leveled in Plaster of Paris to anchor it to the floor of the facility. Earth pressure cells were calibrated in-situ for each wall using the self-weight of the soil above the cell for a height of 1 m and the voltage response from the Geokon cells.

Seven EPCs were located on the ground of the facility and five were located mid-height between each reinforcement layer.

d) Connection Loads

Strain gauges were installed in the clamps that connect the steel strip to the facing of the wall in order to measure the connection loads. These strain gauges are located on both sides of the clamps (above and below) on the panel and were calibrated prior to installation. A structure that is capable of applying a tension load to the connection was assembled. A tension captured by a load cell and the strain captured on the pair of strain gauges were related. The strain gauges were N11-FA-5-120-11 type manufactured by Showa Measuring Instruments Company of Japan.

e) Horizontal Toe Loads

Horizontal toe loads that were transferred from the facing column to the toe were measured using a series of six load rings anchored between a rigid beam bolted to the laboratory floor and the first row of facing panels. The vertical and horizontal loads acting at the toe were decoupled using a series of roller bearings at the base of the facing column. The aluminum load rings measured the load at the connection by means of four strain gauges attached in a Wheatstone bridge circuit. These rings were calibrated prior to installation. The first row of panels was seated on a steel plate which was placed on six rows of steel roller bearings to ensure that the load rings registered only the horizontal component of the force transferred to the toe. The load rings had the load capacity of 22 kN each. They were powered by a 5 VDC power supply.

f) Vertical Toe Loads

A series of 18 load cells divided in north, south and center plates were placed to collect the total load on the toe of the facing. The vertical load was measured by two columns of load cells supporting the roller bearing system placed at the first row of facing panels. Three types of load cells with four different capacities were used, one being a Canister type load cell models C62H1K-10P3 (4.5 kN capacity) and C62H-3K-10P3 (13.5 kN capacity) manufactured by Intertechnology Inc., the other being a disk compression load cell (manufactured by Hoskin Scientific) which have 22 kN capacity. A third type was a homemade load cell that has four strain gauges bonded on a steel disk when the compression is applied on the disk. The difference between the resistance in each strain gauge can be relate to the applied load, using the calibration.

g) Volumetric Water Content

To measure soil volumetric water content, CS645 type probes were installed in the backfill. The CS645 probes, manufactured by Campbell Scientific, are used in Time Domain Reflectometer (TDR) based systems that generate a short rise time electromagnetic pulse that is applied to a coax system that includes a TDR probe for soil water measurements. This probe consists of three pointed rods and a low loss cable with each rod measuring 7.5 cm. The CS645 acts as a waveguide. The impedance along the rods varies with the dielectric permittivity of the surrounding soil. As soil dielectric permittivity depends on the amount of water present, the soil volumetric water content can be calculated from the reflected measurements. In total, 18 TDR probes were distributed in the backfill to measure the volumetric water content distribution.

h) Water level sensors

Three different points were chosen to read the water level using open pipe piezometers. The first point chosen was the tank in front of the facing and the other two near the back of the backfill, one located at 3.5 meter from the back of facing and the other located at 5 meters from the back of facing. Water level indicators consist of a probe, a cable with laser marked graduations and a cable reel. When the probe comes into contact with the water surface, the LED lights up and a sound is emitted. The water table level at the tip of the piezometer is calculated by subtracting the depth of water from the total length of the piezometer.

Test Procedures

In general, the two walls in this study were planned to be built similarly to the previous walls of the RMC program. A small tank was constructed in front of the facing wall to contain the water reservoir during infiltration. The two walls were identical, except for the backfill soil. Each wall measures 3.55 m high, 3.3 m long and the backfill extends over 6 m behind the front facing. Each wall was constructed with five layers of steel strips reinforcement and a vertical concrete panel facing. The backfill soil was placed in 24 compacted lifts of 150 mm thickness.

Flooding and rapid drawdown tests were performed four times for the first wall and nine times for the second wall. Each test for the first wall took about seven days to be completed (one day for flooding and six days for the rapid drawdown), for the second wall the test took three days to be completed (11 hours for flooding and two days for the rapid drawdown). The flooding test was considered finalized when the backfill soil fully drained as indicated by the TDRs.

Preparation of RMC Test Facility and Instrument Calibration

Prior to the construction of the walls, the test facility was prepared and the instrumentation inspected and calibrated. The facility sidewalls were first prepared as discussed above. Geokon earth pressure cells were then installed on the facility floor, leveled, and then cured in Plaster-of-Paris. Each pressure cell was tested prior to any soil being placed in the facility. All other instruments were calibrated, inspected and tested before and/or during their installation.

An impermeable membrane measuring 8.5 by 12.5 meters Type 45 Safety Green Fabric with two drains on the horizontal surface was installed to enclose the water from the infiltration.

Construction

The total construction time for the first wall was 3,900 hours and for the second wall was 1,500 hours. The general procedure for construction was as follows:

- Tank in front of facing - A small wooden structure was constructed, enveloped with an impermeable membrane on the front of the face to simulate the flood of a river. This structure was built to keep water at 1-meter level as it seeped through the facing panels and into the backfill.
- Support for facing panels - To measure movement at the toe of the wall, a structure was developed. Load cells were placed on the laboratory floor and leveled. Above these load cells were placed metal plates. To allow horizontal displacement of the facing panels, rollers were placed. And at the base of the face panels, another metal plate with 10 mm thickness was installed which was level with the wall floor.
- Placement of the facing panels - Precast concrete panels were placed vertically with the aid of a crane. The center bottom panel was installed first and then the laterals. For erection, panels were handled by means of lifting devices set into the upper edge of the panels. Panel joint openings were 3/4” +/- 1/4”. Small rubber pads were placed between the panels to prevent friction, align the concrete panels and control the gap thickness.
- Placement of the backfill soil - The backfill soil was stored into bags, which were moved from the floor of the laboratory into the test facility with the aid of a crane. The crane was used to move the soil into the test apparatus where it was spread by hand into approximately 200 mm lifts. Since the soil would often come out of the stockpile at a moisture content below the optimum 4%, water was added until it reached the optimum moisture content.

- Compaction - To reach the target density, it was determined that two passes per lift reached the bulk density using the electric jumping jack tamper (first wall), vibratory plate (second wall) and the manual compaction plate. Each lift was compacted to a final depth of approximately 150 mm using a hand tamping plate on the front 1 m and the vibratory compactors elsewhere.
- Soil bulk density and moisture content measurement - At each lift, nine points were selected to measure soil density and moisture content using a Troxler 3411-B nuclear densimeter. All points should have a density equal to or greater than 95% compaction based on Standard Proctor. If any of these readings were not within the specified range of density and moisture content, the soil lift was recompacted accordingly.
- Reinforcement placement and facing connection - The compacted soil level was 5 cm above of the tie strips connections (following manufacturer instructions). Each reinforcement strip was connected to the embedded panel tie strip by inserting the end of the reinforcing strip into the gap between the two exposed ends of the tie strip. Three holes were combined and a bolt was pushed through the holes from below, placing a washer on top, threading on a nut and tightening. The bolts were mounted through both flange of the coupling strip, perpendicular to the steel surfaces, and had full bolt head and washer/nut against the tie strip flanges.

Flooding and rapid drawdown test

Four tests were performed on the first wall and nine for the second wall. All tests followed the same procedures. First, the data acquisition started to run. Second, the tank located in front of the facing was filled until the water level reached 1 m, after that, the tap was controlled in order to maintain the tank water level at 1 m. All measurements were taken throughout the test. When the water level reached 1 m across the backfill, i.e., the same hydrostatic pressure (about 24 hours after the flood started for the first wall and 11 hours for the second wall), the drains were opened and the drainage process started. The readings indicated that after six days (for the first wall) the backfill soil was at the same hydraulic pressure as the start of the test and two days for the second wall.

Excavation

The excavation of the walls was carried out following the inverse procedures as defined for the construction. Each layer of soil was removed manually and transported out of the

structure. The density and moisture content readings were taken again at selected soil lifts for comparison. Care was taken to remove devices that were installed inside the backfill and to keep the waterproof membrane free of damaged.

CHAPTER 4 : FULL-SCALE TEST RESULTS AND ANALYSIS

This chapter presents the results that were collected during the construction and testing of the first and second wall. The results reported for the walls include soil results and instrumentation readings and flooding/rapid drawdown tests.

Wall 1

Backfill Soil

Using the Unified Soil Classification System, the backfill material was classified as a poorly graded sand. Figure 4-1 provides the particle size distribution. The grain-size distribution parameters were determined as coefficient of uniformity of Cu=3.94 and a coefficient of curvature of Cc=0.85. The sand has a specific gravity of soil solids, Gs, of 2.65 and a maximum and minimum void ratio of 0.72 and 0.42, respectively.

From Standard Proctor tests, an optimum moisture content (OMC) of 8.8% and maximum dry unit weight of 17.78 kN/m^3 were found (Figure 4-2). During the construction, the compaction target was greater than 95% of the maximum dry unit weight. The permeability of sand under constant head was 7.4x10^{-4} cm/s.

Shear strength envelopes from direct shear tests presented a peak friction angle and constant volume friction angle of the 41 degrees and 36 degrees, respectively.

An important aspect when analyzing soil suction is the soil water characteristic curve (SWCC) that correlates Volumetric Water Content and Suction, these results are presented in Figure 4-3.

Figure 4-4 shows the soil unit weight and moisture content readings for the sand taken during construction. The soil readings presented an average dry density of 17.4 kN/m3 with a standard deviation of 1.23 kN/m3 with a moisture content of 6.94% with a standard deviation of 1.1%. A parameter that was difficult to measure was the moisture content because of the high sand permeability. However, given the relative flatness of the compaction curve, it was possible to interpret that soil moisture was not a determining factor in achieving the target compaction. More details on compaction can be seen in Appendix B.

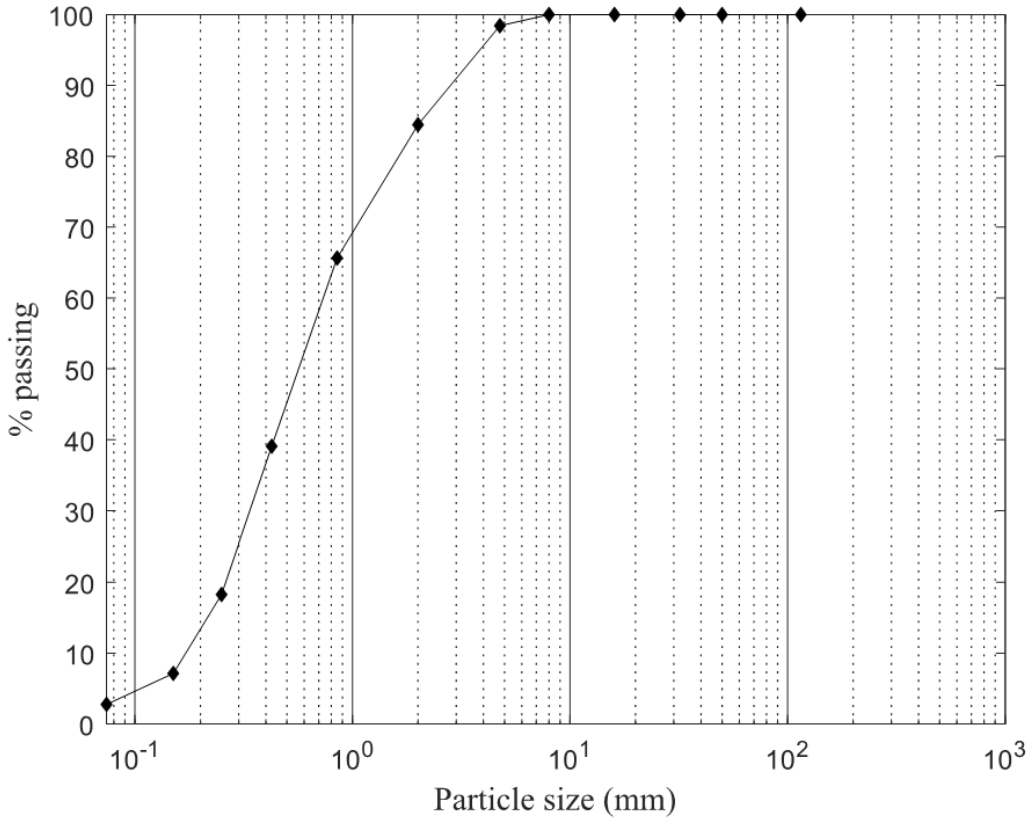

Figure 4-1. Wall #1 – Backfill soil grain-size distribution.

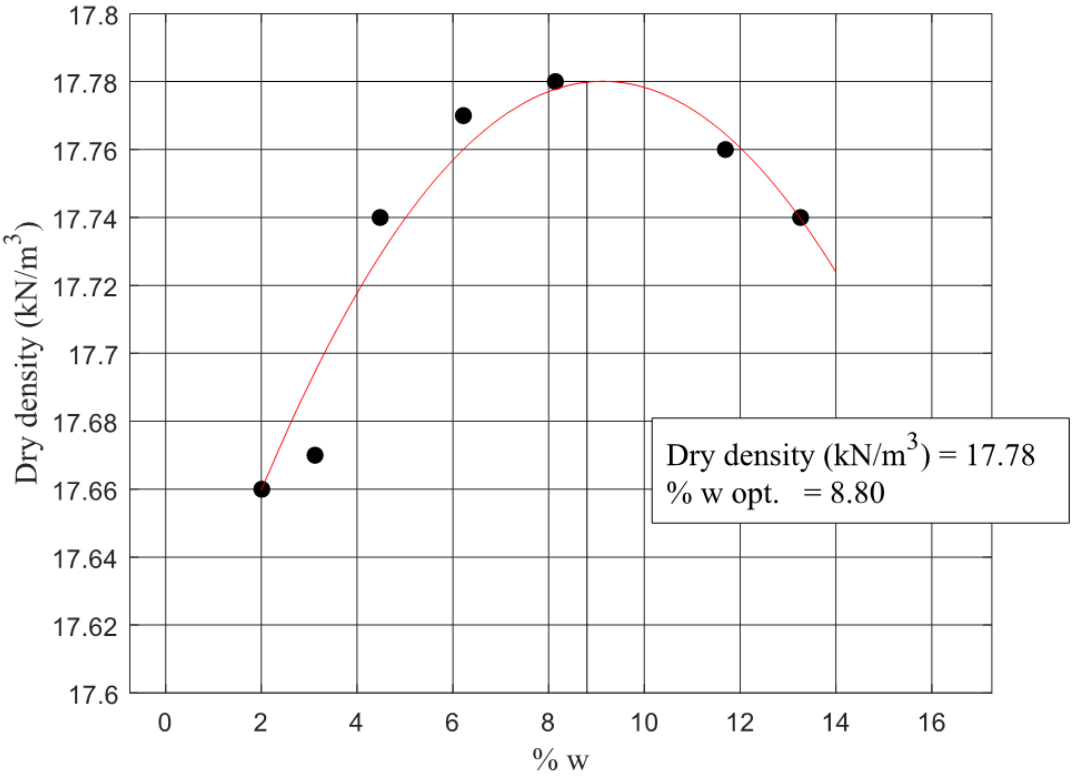

Figure 4-2. Wall #1 – Standard Proctor test results.

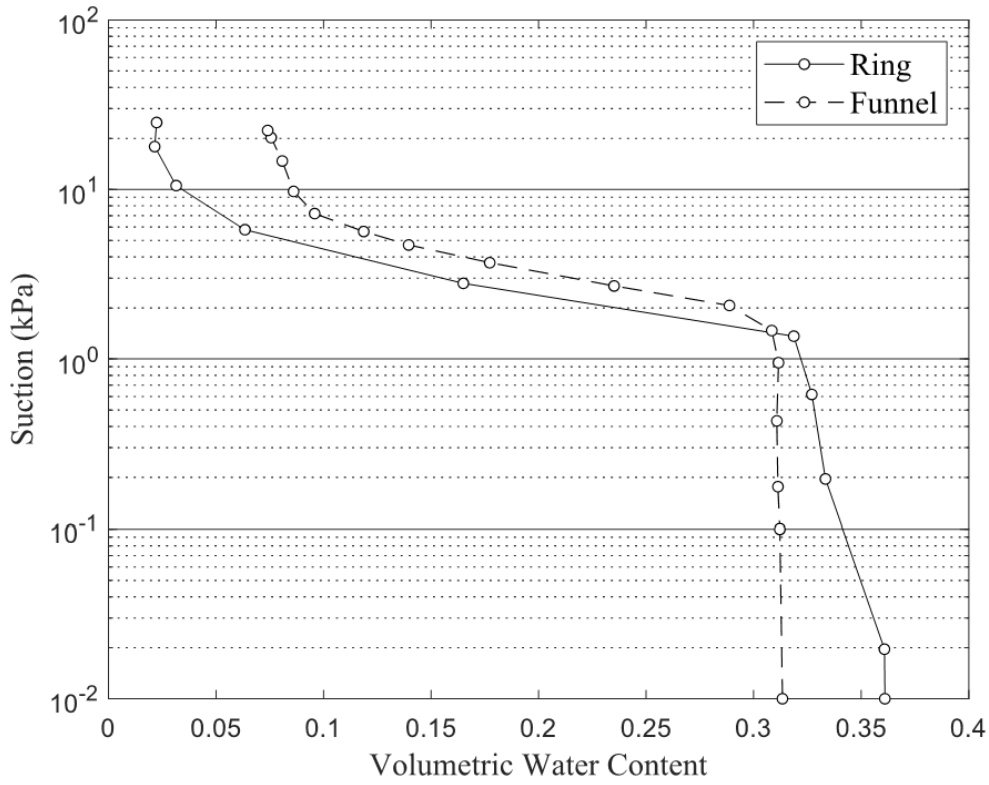

Figure 4-3. Wall #1 – Soil Water Characteristic Curve.

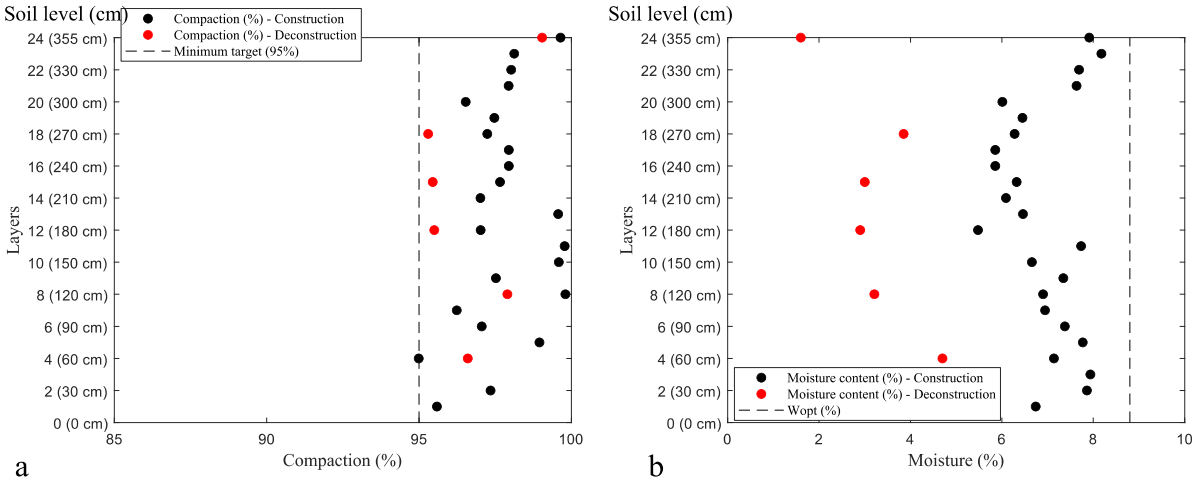

Figure 4-4. Wall #1 – Compaction readings from the densometer (a) Soil density readings and (b) moisture content.

Instrument measurements during construction

a) Facing Deflections

Displacement of the wall 1 panels was measured continuously during the construction period using potentiometer pairs recorded by the data acquisition system. These readings took place at the four corners of each central panels. For each level of the face, two instruments took readings and the result of each level was the average between the readings at the level.

Figure 4-5 shows the total displacement, considering the desired initial alignment of 90 degrees, of the 3 central panels. The results show a displacement of 8 mm at the top of the first panel at the moment when the floor level behind that panel was completed (moment immediately before the installation of the second panel). Outward displacement of 24 mm at the bottom of the second panel was recorded at the end of the construction of the second panel, and 34 mm at the top of the third panel at the end of the construction.

Figure 4-6 shows the average displacement measured by potentiometer pairs during the test. The maximum facing displacement measured with respect to the end of construction was approximately 19 mm, recorded at the bottom of the second panel (0.85 m). The difference between the potentiometer pairs presented a maximum value of 5 mm (12% of the total displacement) for the same level at the end of construction.

The total displacement of wall 1 was 34 mm at the top of the third panel. Variation in the panel movement is likely due, in part, to non-uniform bracing during the construction.

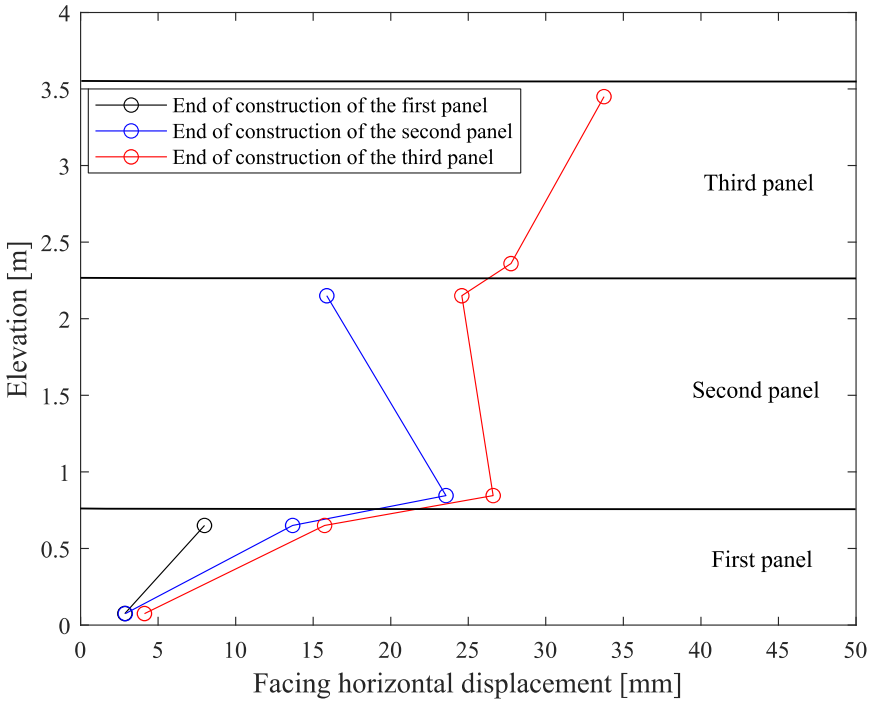

Figure 4-5. Wall #1 – Wall facing displacements.

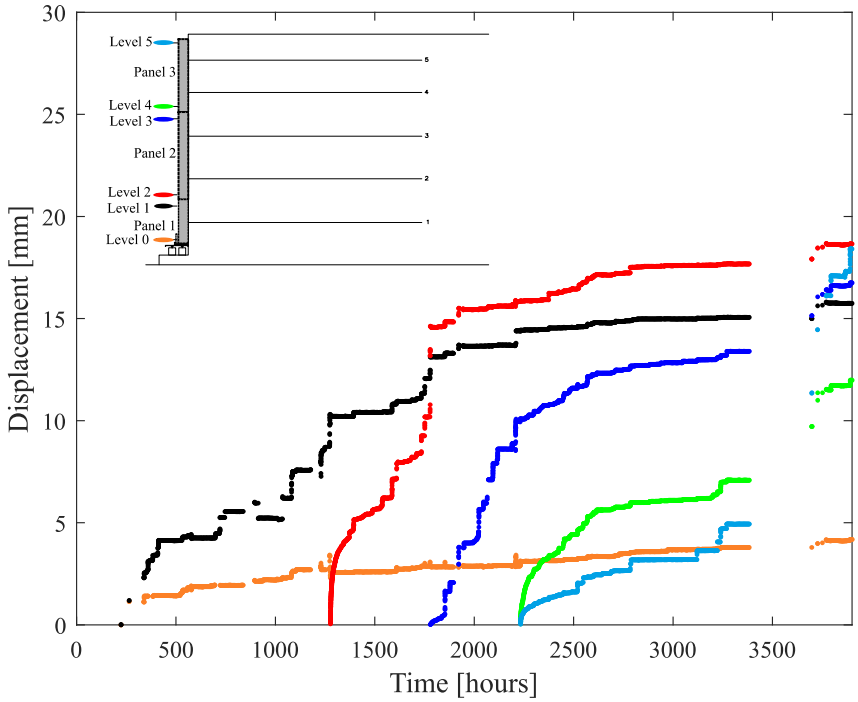

Figure 4-6. Wall #1 – Wall facing potentiometer measurements.

b) Reinforcement Strains

Pairs of strain gauges were installed on each reinforcement layer to measure strain distribution along the strip throughout the test. Eight (8) strain gauges were installed on each side of the strips, totaling 16 strain gauges per bar. The strain for each position was the average of the strain gauge pairs. Each pair of strain gauges was placed on separate longitudinal reinforcement strips but at equal distance from the wall facing. The maximum strain recorded by a strain gauge was approximately 600 με measured by the strain gauges in layer 2 at the end of construction (Figure 4-7). Figure 4-8 shows strain gauge versus time based on the average measurements from paired strain gauges during the construction period. An anomaly was observed in the sensor data located in the first reinforced layer at 2500 hours. This was due to an electrical failure on the board connecting these sensors, the issue was resolved quickly and did not generate issues for previous and subsequent data

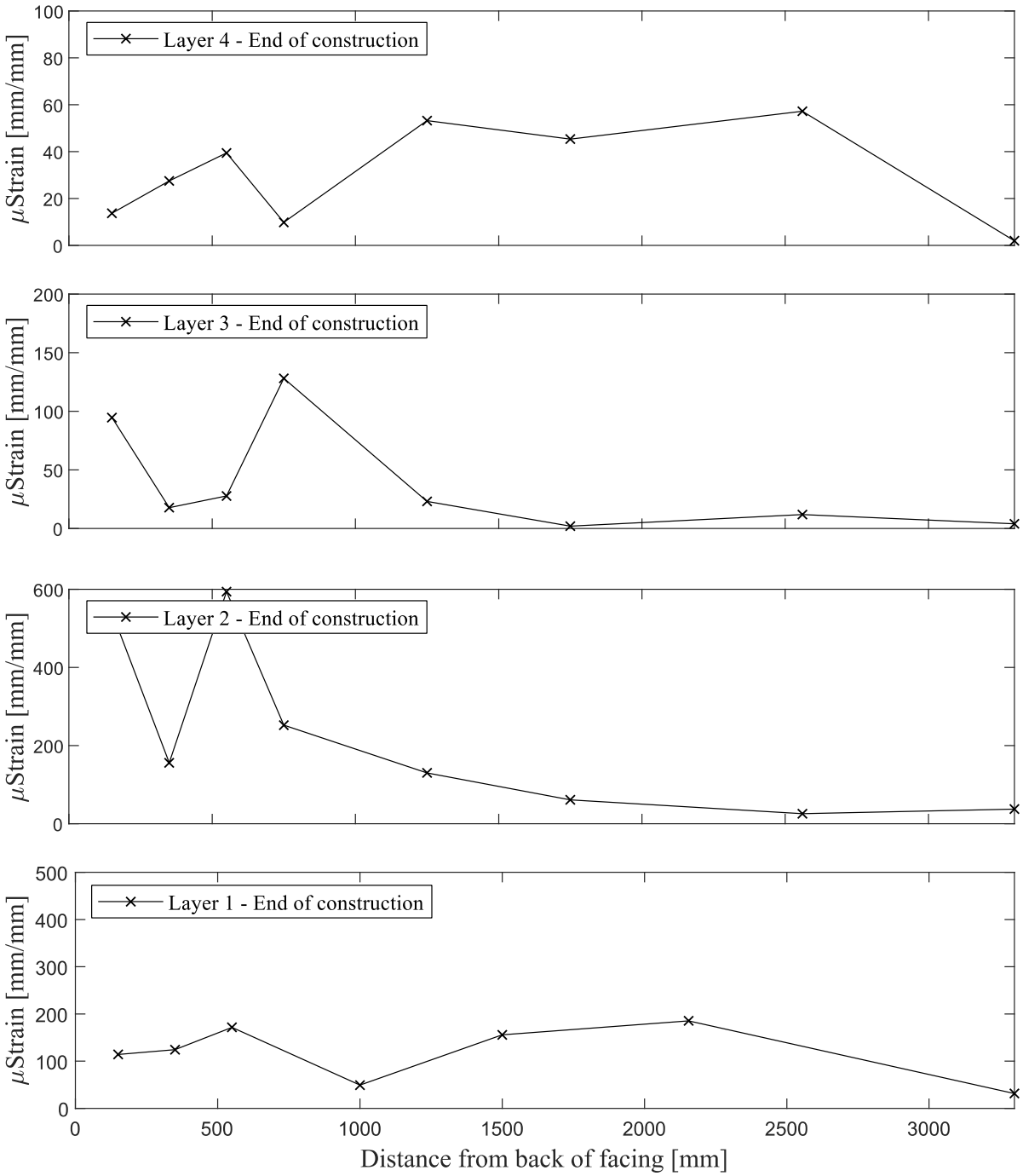

Figure 4-7. Wall #1 – Reinforcement strains at end of construction.

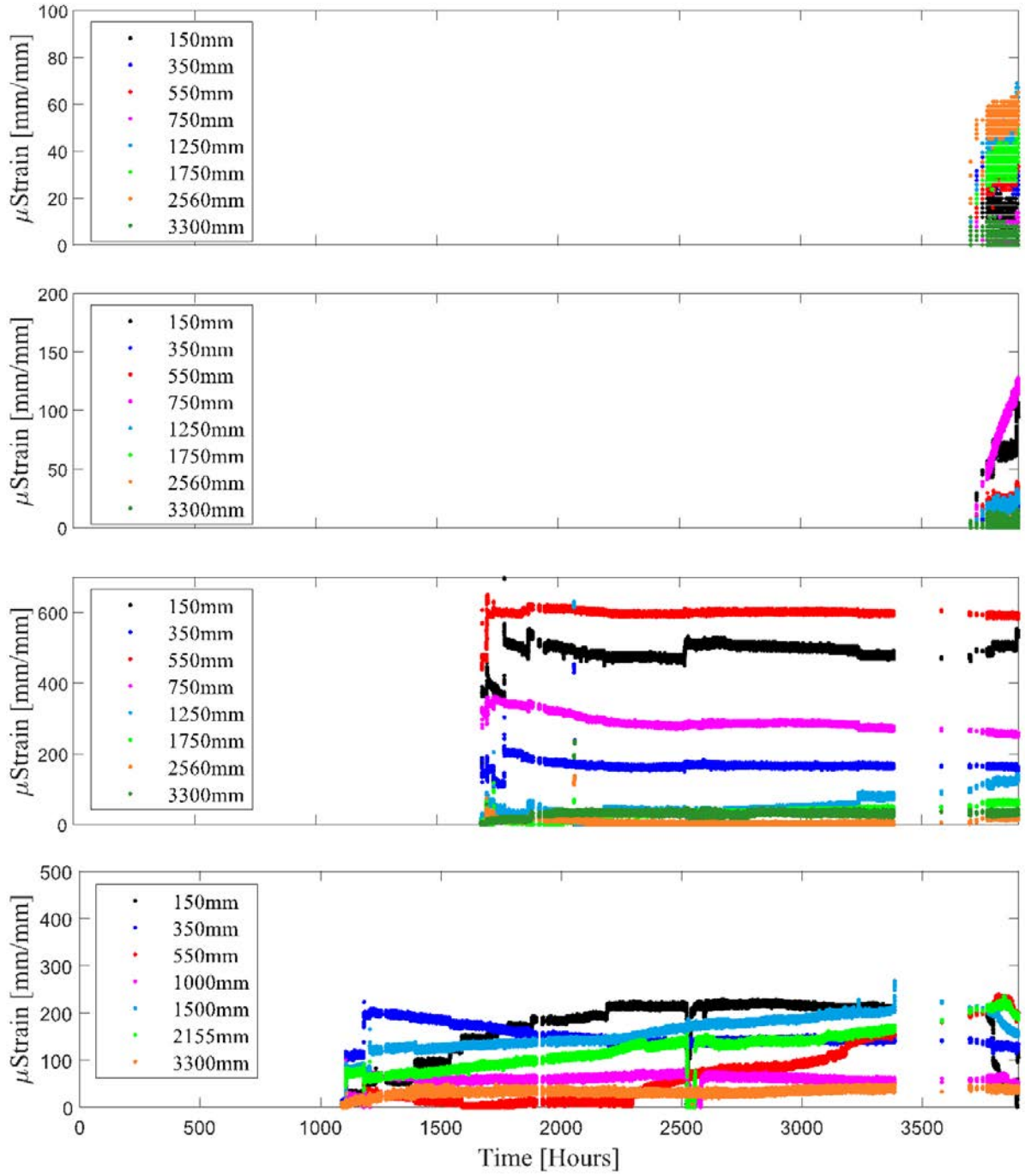

Figure 4-8. Wall #1 – Strain recorded by strain gauges versus time during the construction.

c) Vertical Earth Pressures

Earth pressure was measured using seven (7) earth pressure cells (EPC) located on the test facility's floor and 4 EPCs located within the backfill soil. The earth pressures measured by the seven pressure cells on the floor of the test facility are shown in Figure 4-9. At the end of construction, the earth pressure measurements varied between 42 and 170 kPa, which is representative of soil arching occurring within the reinforced zone. These values correspond

to 0.7 and 2.42, respectively, of the theoretical value of the earth pressure calculated for the column of soil (h) times bulk unit weight (γ). The bulk unit weight was calculated based on the results found in the average compaction of the readings taken during construction. The normalized curve is showed in Figure 4-10.

Figure 4-11 shows the pressure-time response for the EPC located in the reinforced soil zone immediately behind the facing for different levels. At the end of construction, the cell located at 75 cm, 145 cm and 240 cm from the ground measured about 58 kPa, 46 kPa and 12 kPa, respectively. These values are comparable to the theorical values.

Figure 4-12 shows the pressure versus time for two cells located at 1.45 m from the ground. The first cell is located at 80 cm from the back of the facing and the second one is located at 290 cm. Similar to the ground pressure cells located on the test floor, the cell located farthest from the facing (290 cm) showed a lower pressure value (16 kPa) compared to the cell located close to the facing (80 cm) (46 kPa).

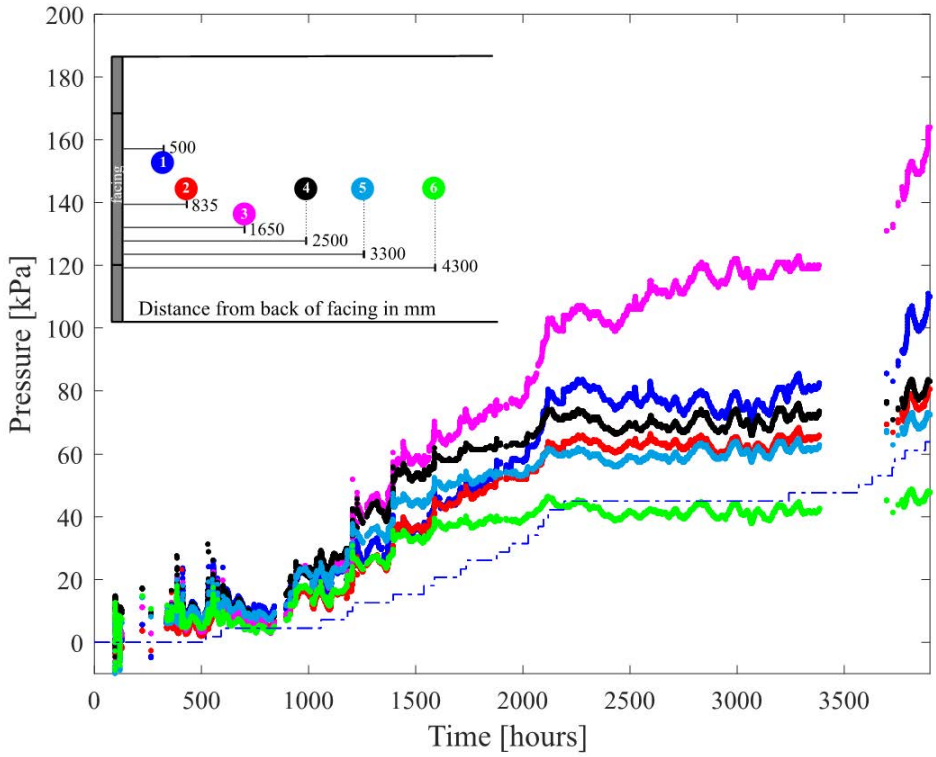

Figure 4-9. Wall #1 – Vertical pressures recorded at the base of test facility.

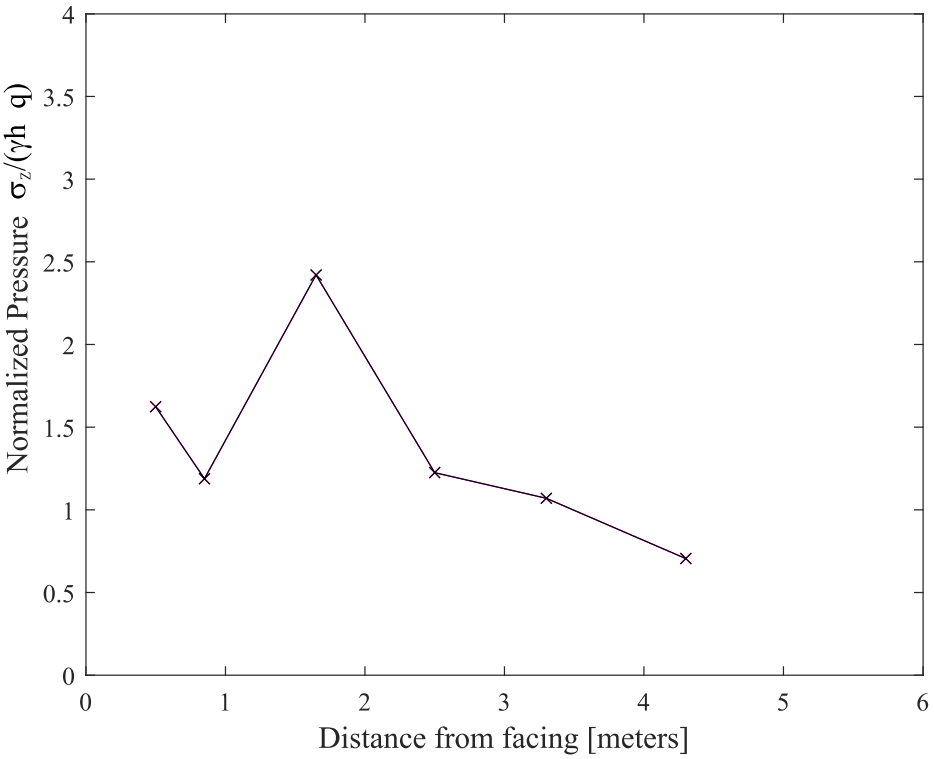

Figure 4-10. Wall #1 – Normalized vertical pressures recorded at the base of test facility.

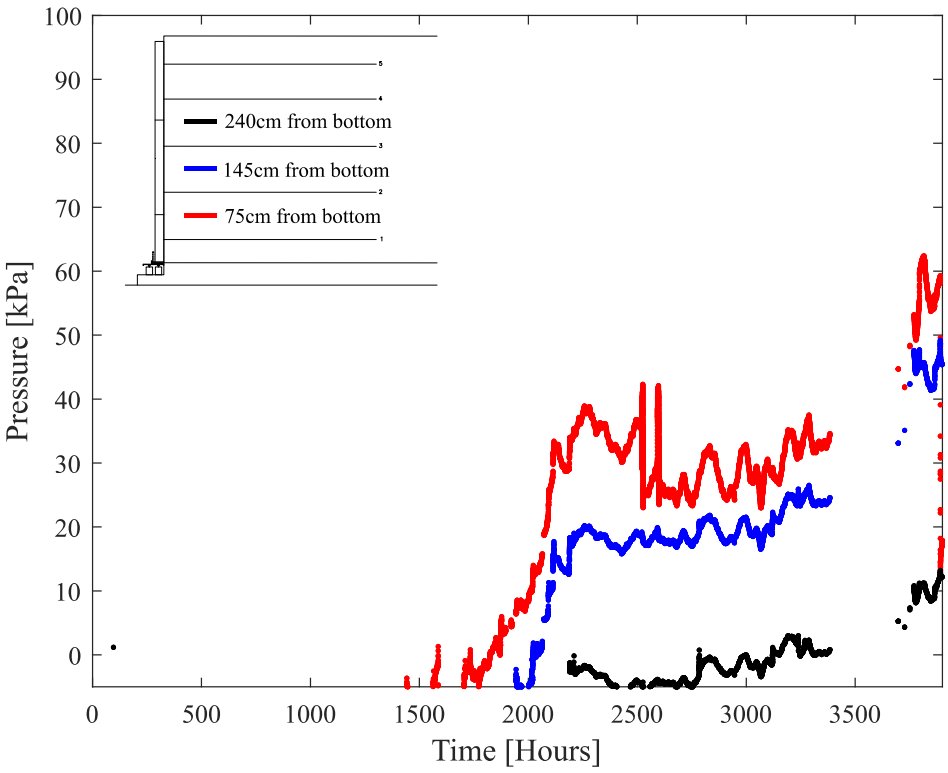

Figure 4-11. Wall #1 – Vertical earth pressures recorded immediately behind facing along profile.

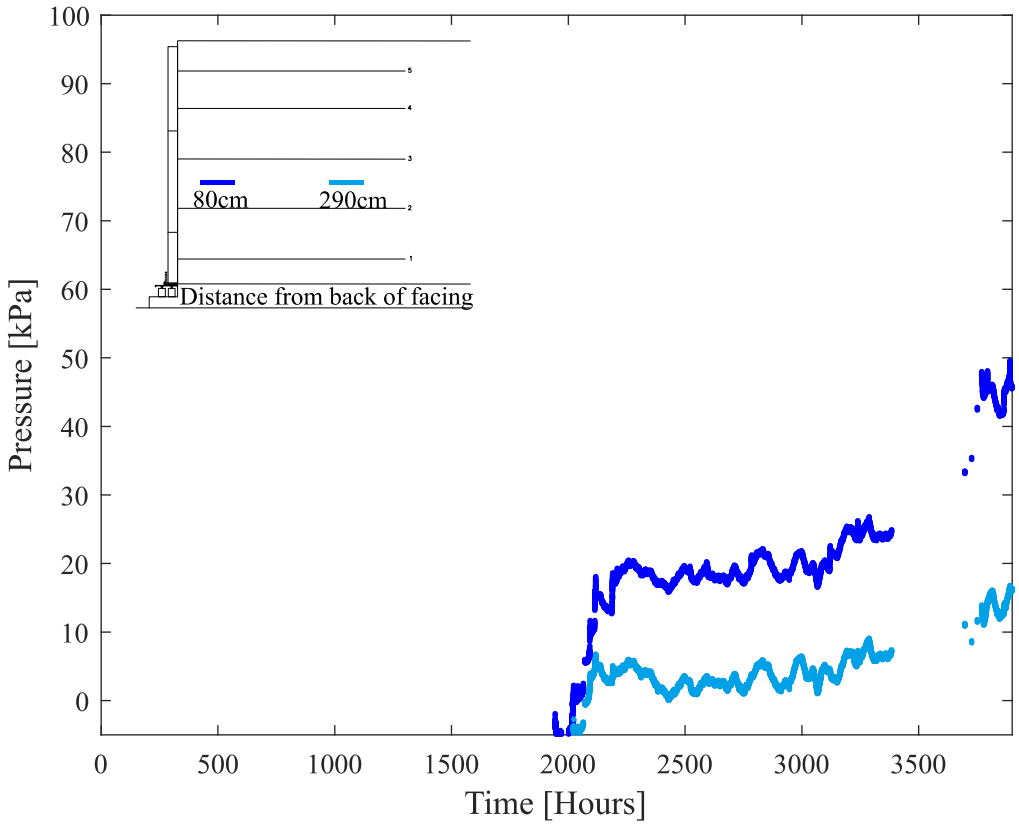

Figure 4-12. Wall #1 – Vertical pressures recorded at 1.45m elevation.

d) Connection Loads

Connection loads were measured at each reinforcement layer by two strain gauges in each clamp. The strain gauges were calibrated previously relating strain and load. The strain gauge located at the clamp of the first reinforced layer failed on the beginning of the test. Figure 4-13 shows the strain measured in each layer during the construction period. Layer 4 shows that the highest average load (4.5 kN) occurs at the end of the construction.

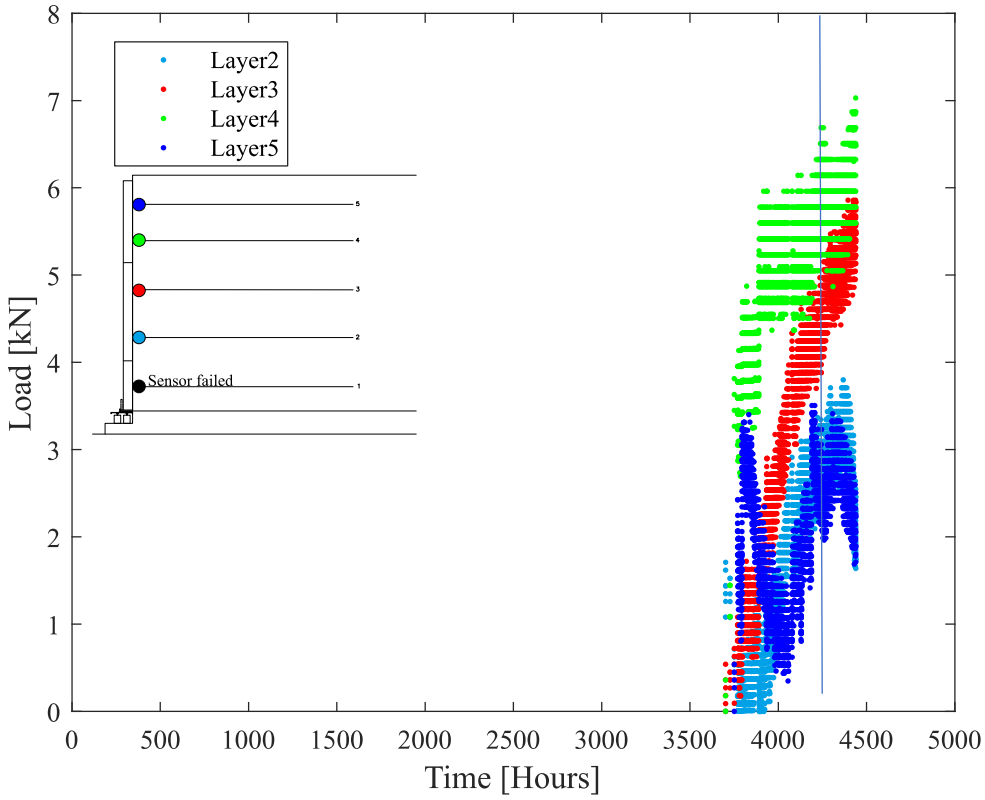

Figure 4-13. Wall #1 – Connection load vs time.

e) Vertical Footing Loads

Vertical loads at the footing were measured by eighteen (18) load cells. The load cells were divided into 3 different plates (North, Center and South). On each plate, the cells were distributed in 2 columns (toe and heel). Figure 4-14 shows the total vertical load measured by the 18 load cells on the toe and heel columns. The results show that the load was concentrated on the heel, directly below the panels.

Figure 4-15 shows the load distributed on each plate (North, South and Center) per meter. The load per meter of the wall measured under the center plate was approximately 12% greater than the load per meter on the north plate and 36% greater than the south plate.

Figure 4-16 shows the normalized curve of the vertical footing load. The total load was divided by the facing self-weight. At the end of the construction, the normalized load was 2.1 times greater than the load of the facing self-weight, which is reasonable based on previous measurements of full-scale walls and numerical models.

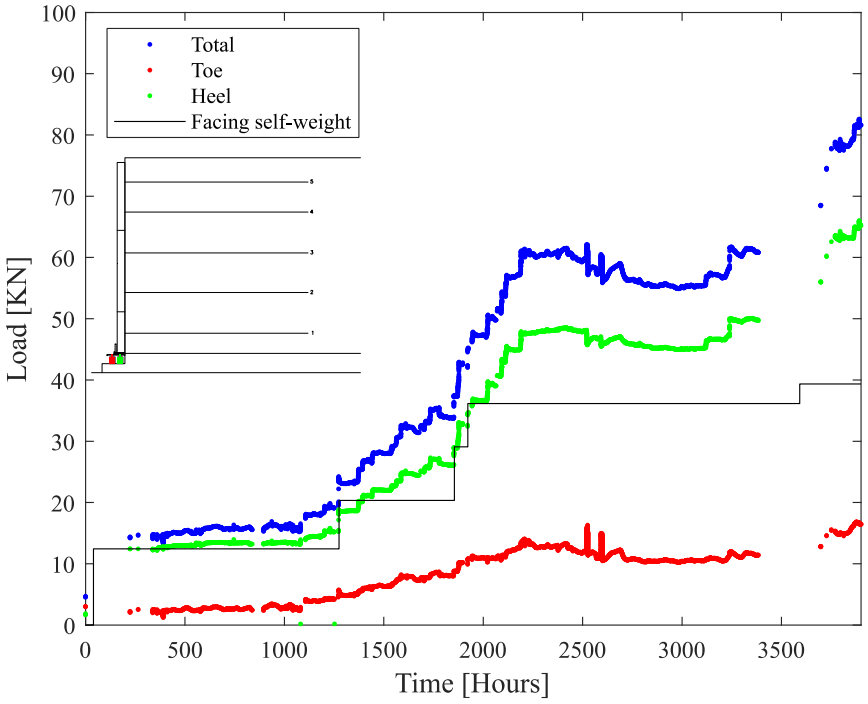

Figure 4-14. Wall #1 – Vertical footing loads vs time during construction.

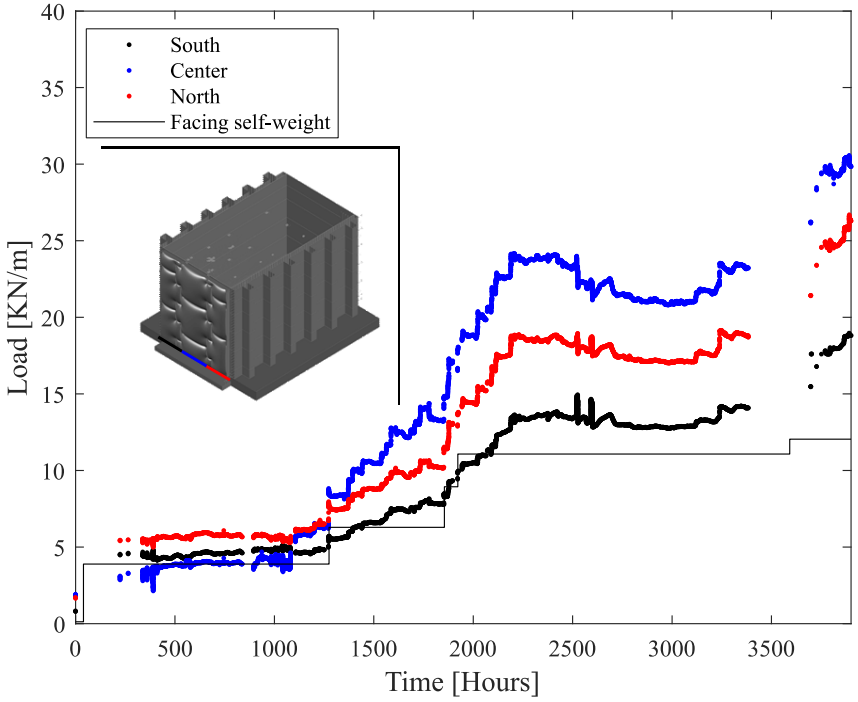

Figure 4-15. Wall #1 – Vertical footing loads per meter length of wall vs time.

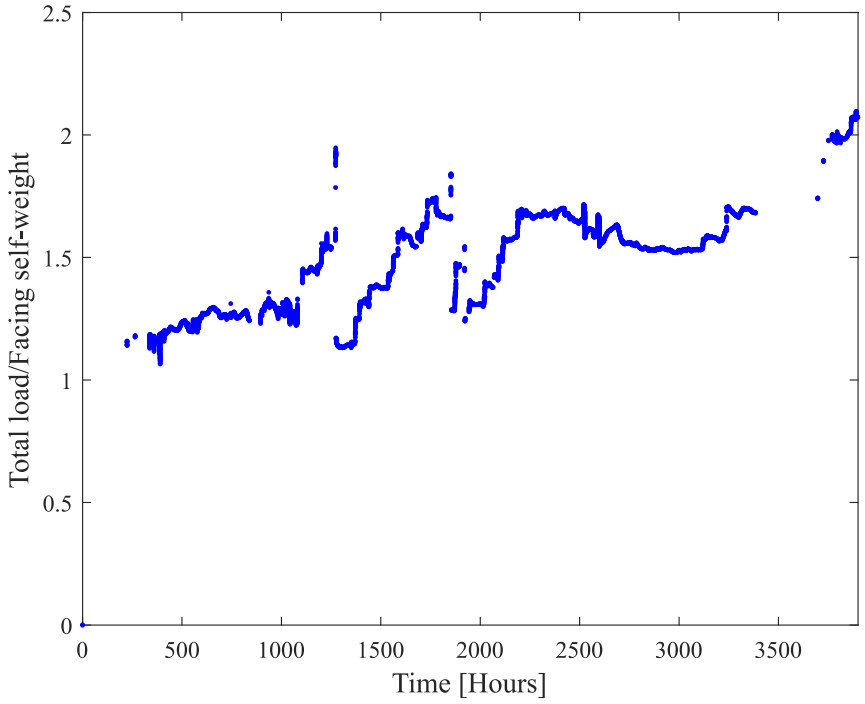

Figure 4-16. Wall #1 – Normalized vertical footing loads.

f) Horizontal Footing Loads

The horizontal footing load sensors located on the sides of the facing failed after 1200 hours of testing, and the sensors located in the center part failed after just over 1800 hours of testing. After the deconstruction of the wall, it was observed that the sensors failed due to a problem in the isolation (waterproof system) of the strain gauges that make up the sensor. Improvements were made to these sensors for wall 2.

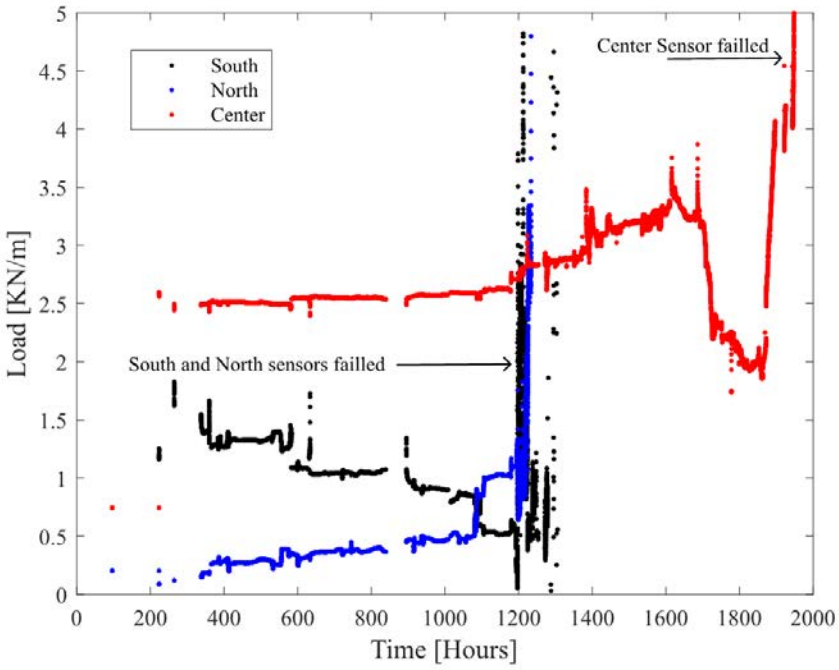

Figure 4-17. Wall #1 – Horizontal footing load per meter length of wall vs time.

Flooding and rapid drawdown test

a) Water level

During the flood test, water level readings were collected at three different locations within the facility. The first location is in the reservoir tank in front of the facing. The others 2 points are located within the backfill soil and the readings were taken through the 2 standpipes located at 3.5 m and 5 m from the back of facing panel. In total, 4 complete tests were performed. The four tests showed similar results and behavior.

Water percolation on the facing occurred through the 0.75 in. joints (according to AASHTO C11.10.4.1) located between the concrete panels. These joints were protected against material erosion through a geotextile filter that allowed the water flow. Figure 4-18 shows the results of the water level in the tank and in the 2 pipes versus time. The water level in the tank reached 1 m in height with 63 minutes from the beginning of the test. The flooding test was considered complete when all VWC sensors showed saturated readings and the water level on the pipes reached at 1 m, i.e., the same hydrostatic pressure.

Then, the rapid drawdown test was initiated when the drains located in the tank were opened and the water level in the tank began to decrease rapidly. The tank emptied in 18 minutes.

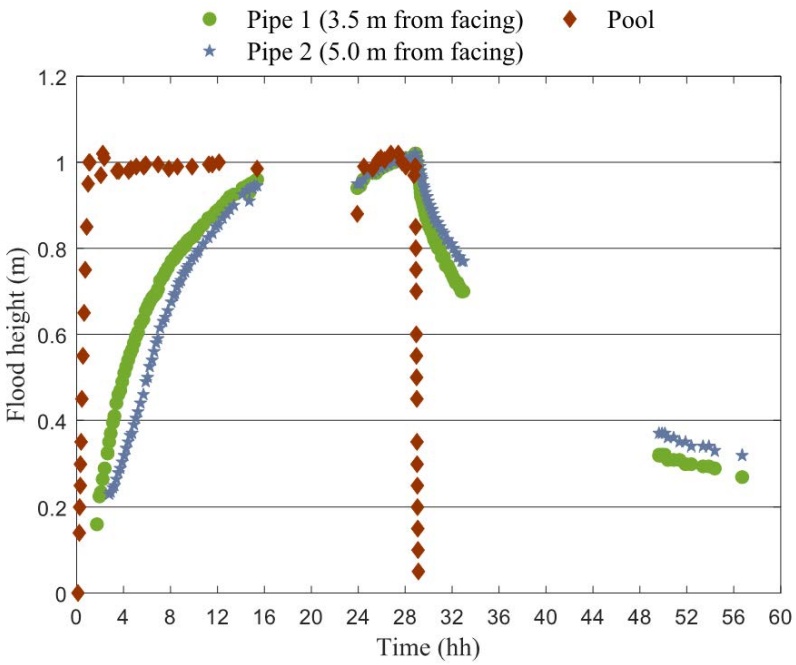

Figure 4-18. Wall #1 – Water level in reservoir and standpipes during a flooding and rapid drawdown event.

b) Volumetric Water content (VWC)

Figure 4-19 shows the volumetric water content on the first layer (15 cm from base of wall), the second layer (75 cm from base of wall) and the third layer (145 cm from base of wall) during the flood and drain test. VWC values of 0.35 indicate the soil is saturated. The first layer, with an elevation of 15 cm, remains saturated throughout the test. In the second layer, 75 cm of elevation, it is possible to check the change in VWC values and identify when the soil around the sensor was saturated. The third layer, being at an elevation higher than the water level, remains with low VWC levels throughout the test. Combining this VWC and water level data, it was possible to generate the wetting front curves (Figure 4.20) and the drying front curve (Figure 4.21). The results generated by the instruments located in the backfill soil and facing of wall 1 during the flood and rapid drawdown test are presented in Appendix A.

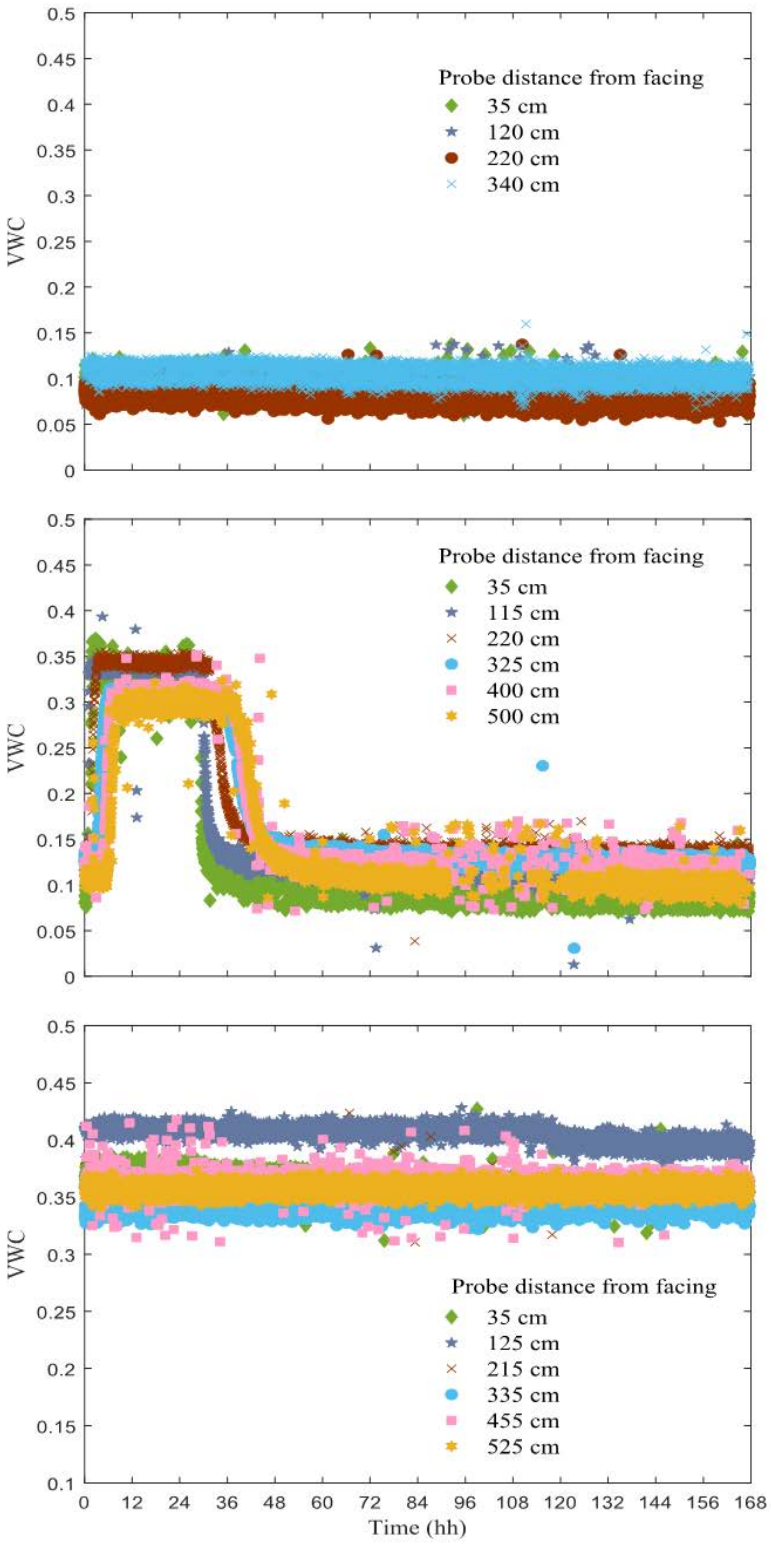

Figure 4-19. Wall #1 – Volumetric Water content (VWC) versus time for the flooding/rapid drawdown test.

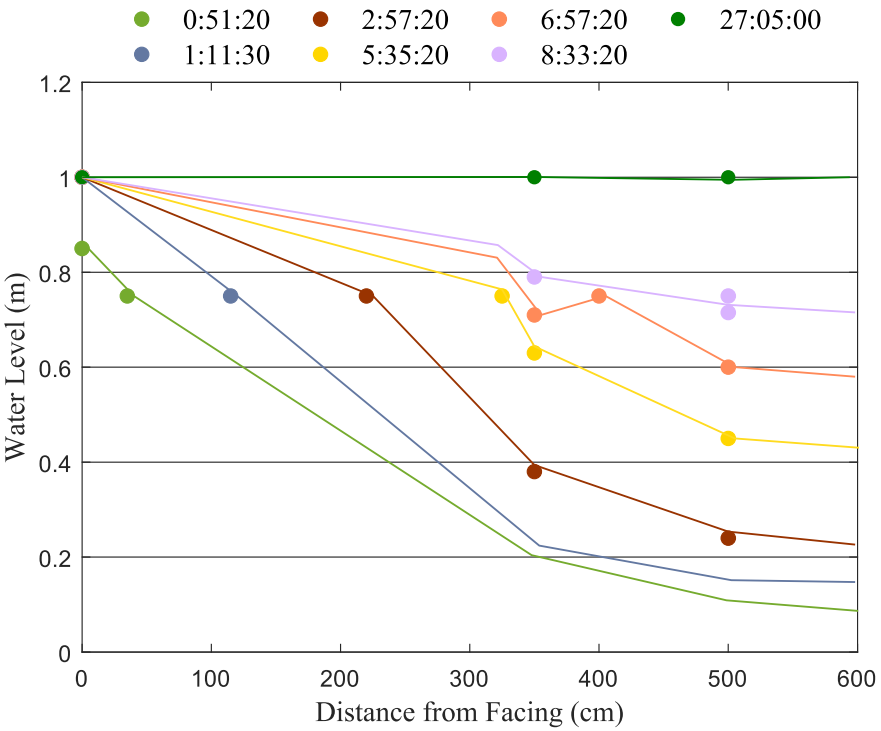

Figure 4-20. Wall #1 – Wetting front at discrete times during flooding.

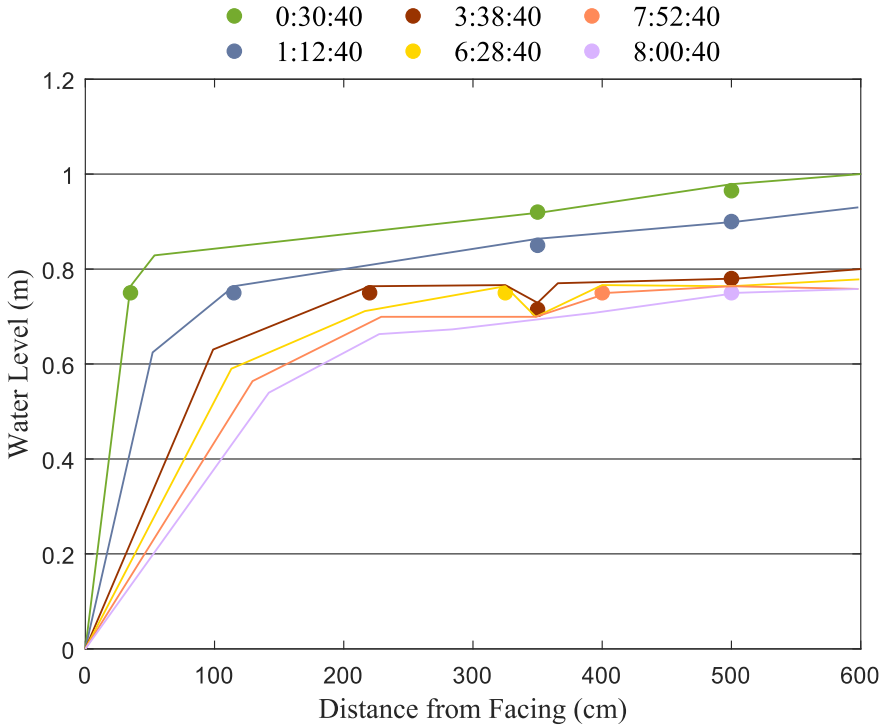

Figure 4-21. Wall #1 – Drying front at discrete times during rapid drawdown event.

Wall 2

Backfill Soil

The component that varied between the two walls was the backfill material. For the second wall, a material was chosen following the requirements of ASSHTO and FHWA for MSE walls and classified by the USCS as a poorly graded sand with gravel. The main difference between the soil of wall 1 and wall 2 was the grain-size distribution. Soil for Wall 2 included the presence of gravel as well as increased fines content.

Figure 4.22 shows the particle size distribution. From the grain size distribution, a coefficient of uniformity of 46.2 and a coefficient of curvature of 0.82 were assessed. Standard Proctor test results presented a maximum dry unit weight of 22.17 kN/m^3 and an optimum moisture content of 7% (Figure 4.23). The permeability of the sand with gravel under constant head was measured as $3.5x10^{-5}$ cm/s. The direct shear tests for wall 2 presented a peak friction angle of the 45 degrees and constant volume friction angle of the 42 degrees. The soil water characteristic curve (SWCC) are presented in Figure 4-24, these results correlate Volumetric Water Content and Suction. Construction of Wall 2 followed the same procedures as Wall 1 in terms of materials and controls. Figure 4.25 shows the compaction results from the wall 2. The soil readings presented an average bulk dry density of 21.08 kN/m^3 and moisture content average of 6.7%. The dry density readings of each layer showed values equal to or greater than 95% of the maximum dry unit weight value found through the Standard Proctor test. More details on compaction can be seen in Appendix B.

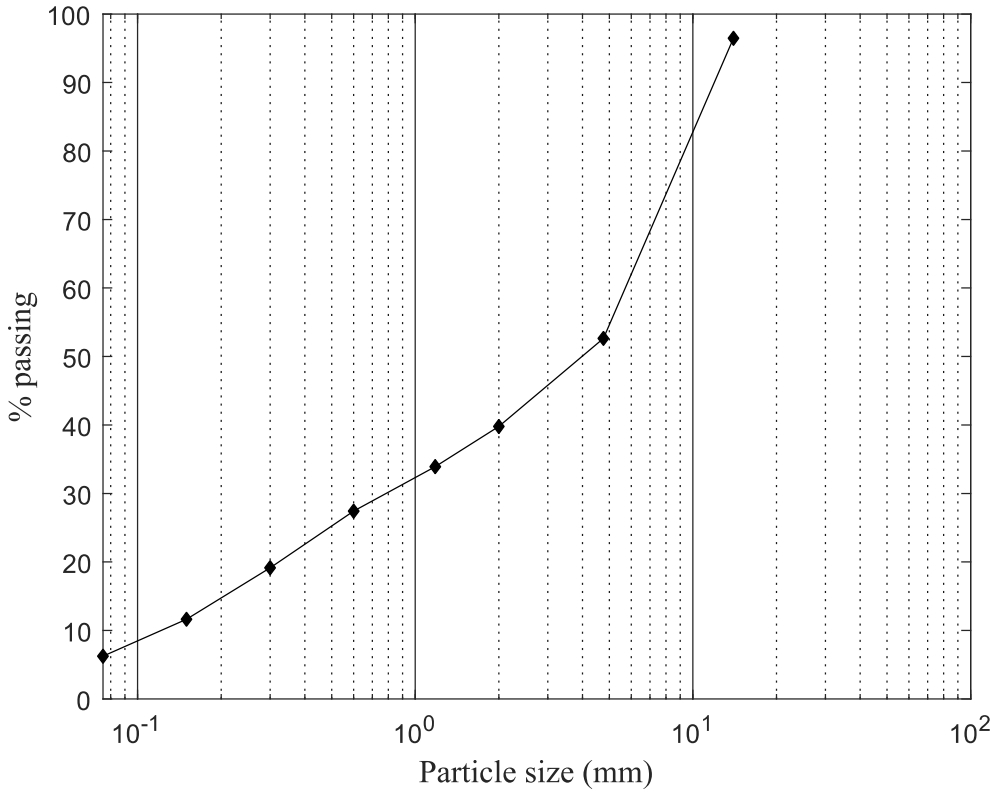

Figure 4-22. Wall #2 – Backfill soil grain-size distribution.

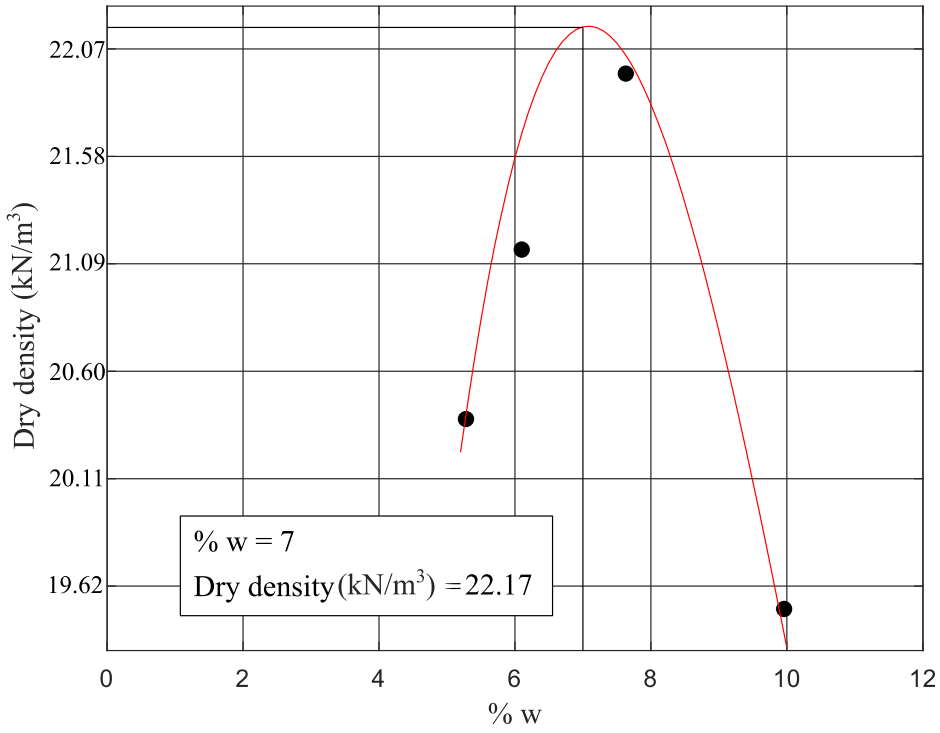

Figure 4-23. Wall #2 – Standard Proctor test results.

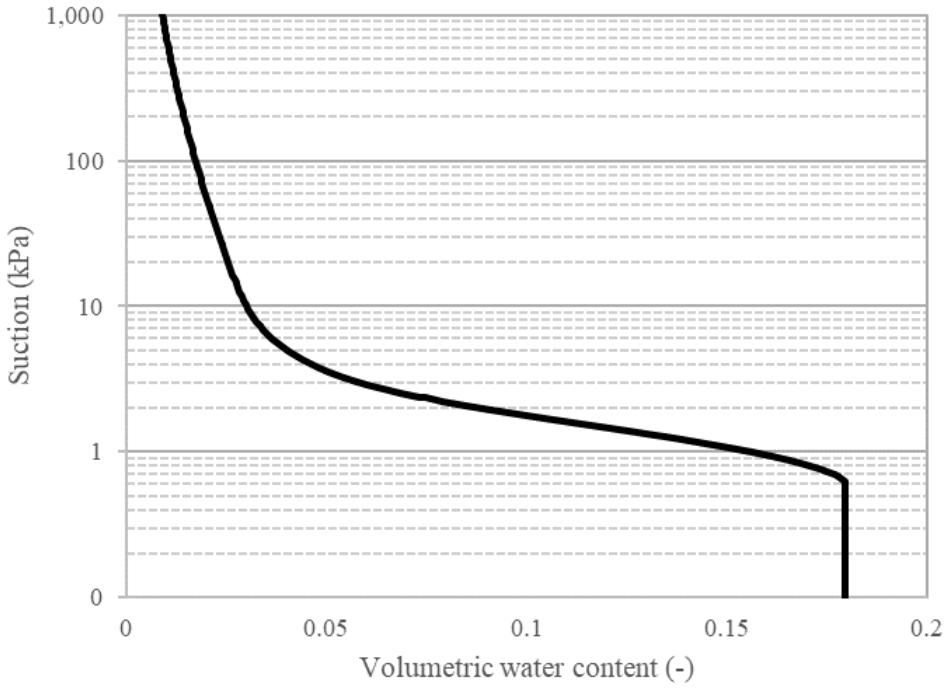

Figure 4-24. Wall #2 – Soil Water Characteristic Curve.

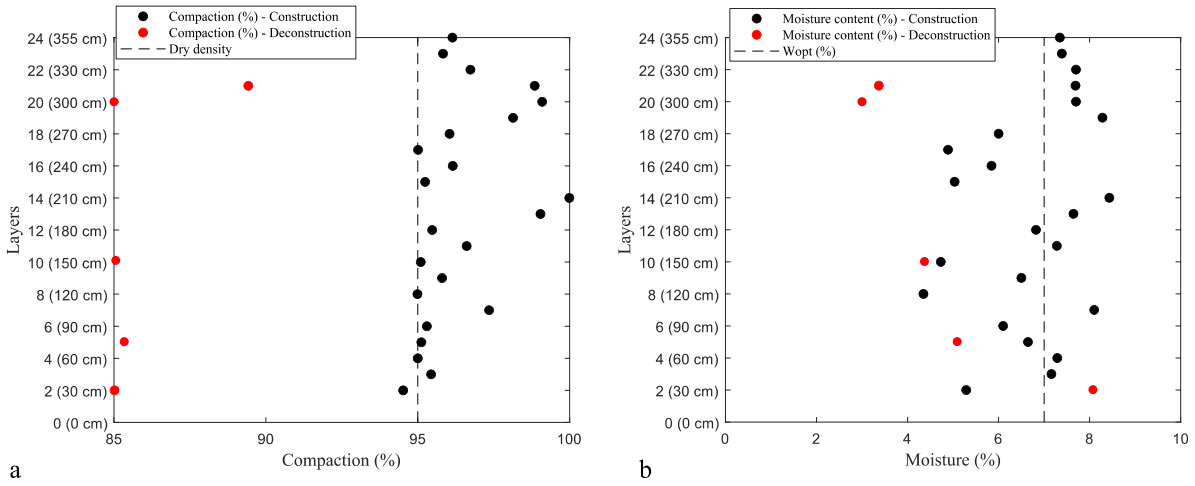

Figure 4-25. Wall #2 – Compaction readings from the densometer (a) Soil density readings and (b) moisture content.

Instrument measurements

a) Facing Deflections

As performed in wall 1, displacement of the wall 2 was measured using potentiometer pairs. The average of two instruments made the readings for each level of facing. Figure 4.26

shows the total displacement of the 3 central panels. For calculating the displacement of the second panel, for example, the displacement of the top of panel 1 (on the end of construction of panel 1) was added to the total displacement of panel 2, thus maintaining the initial reference of 90 degrees.

The maximum outward displacement occurred on the top of panel 3 (24 mm). This value is 0.66% of the overall wall height, which is reasonable for walls of this dimension.

Figure 4.27 shows plots of facing potentiometer pairs during the construction. The maximum facing displacement measured with respect to the end of construction was approximately 9 mm, recorded at the top of the second panel. The outward displacement shown in this plot, represents the displacement of each panel considering the installation point of each panel as zero.

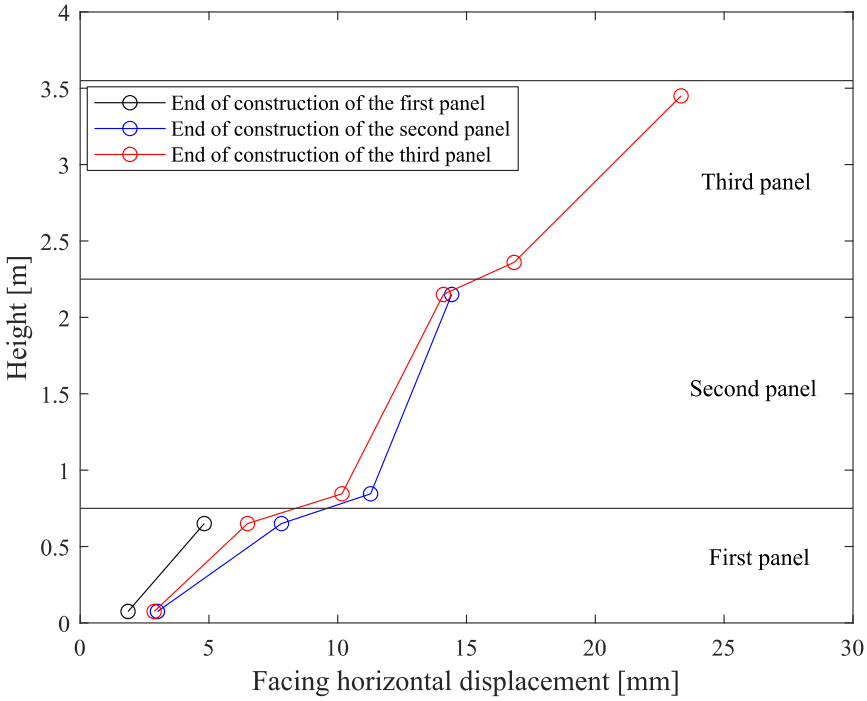

Figure 4-26. Wall #2 – Wall facing displacement.

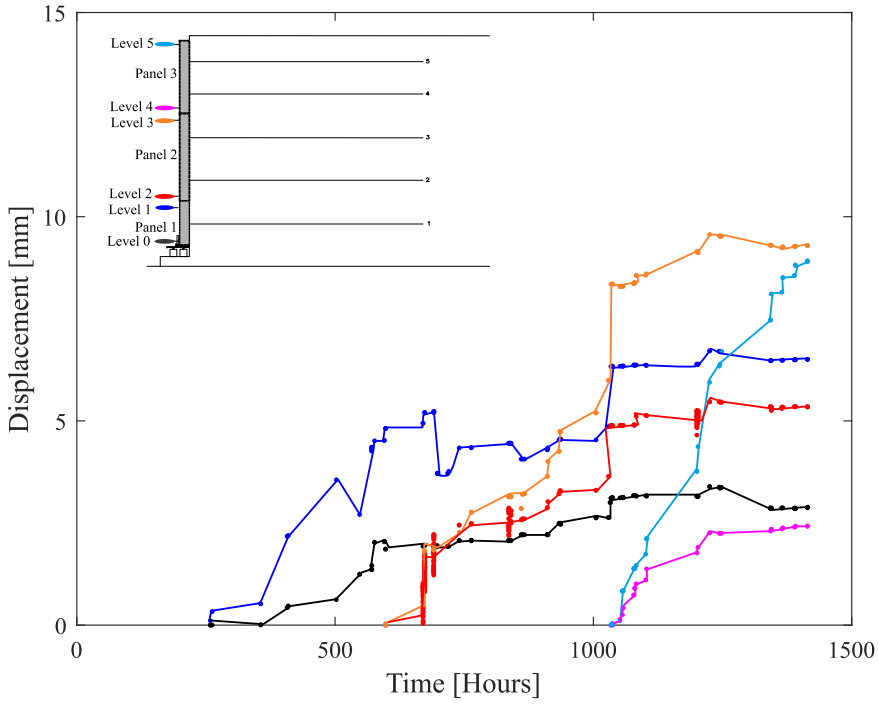

Figure 4-27. Wall #2 – Wall facing potentiometer measurements.

b) Reinforcement Strains

The reinforcement strips located in the central area of the backfill soil were instrumented with 16 strain gauges on each steel strip (8 pairs of strain gauge on each side of the strip).

Figure 4-28 shows the average strain in different locations of the reinforced steel strips at the end of construction. The maximum strain recorded by a strain gauge was approximately 250 με measured by the strain gauge in layer 1 at the end of construction. Figure 4.29 plots the strain variation of each pair of strain gauge during the construction period.

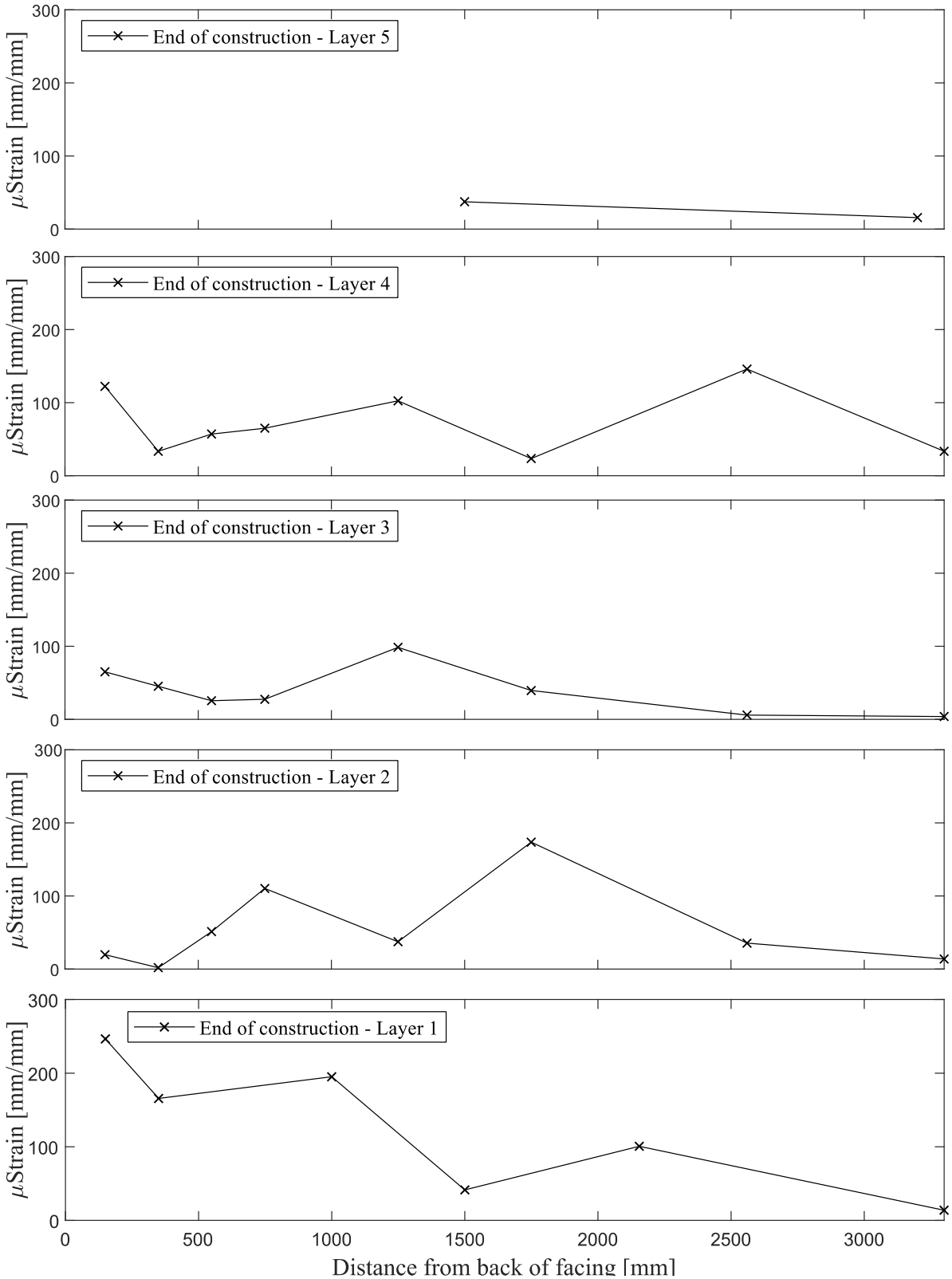

Figure 4-28. Wall #2 – Reinforcement strains at end of construction.

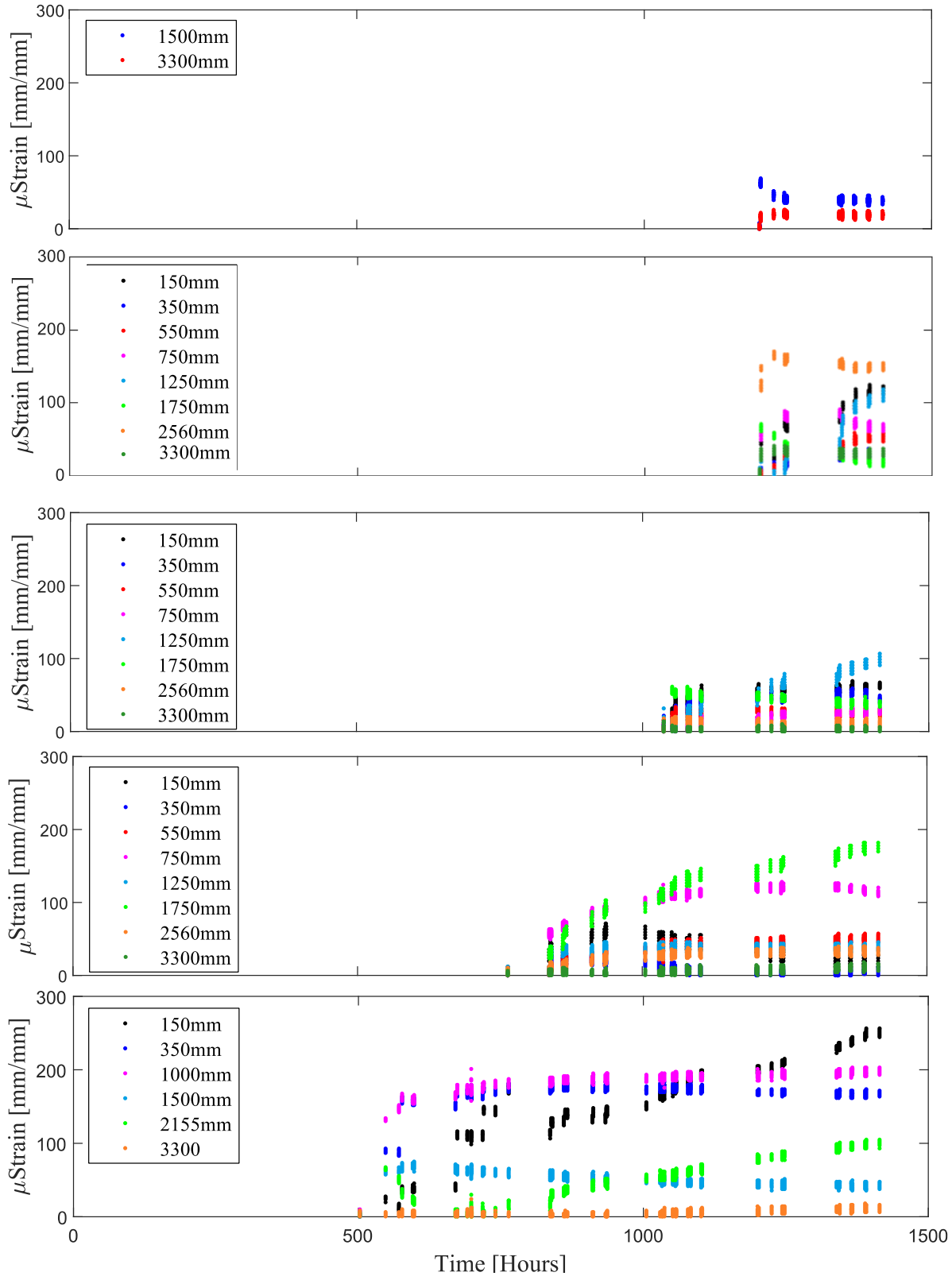

Figure 4-29. Wall #2 – Strain recorded by strain gauges versus time during the construction.

c) Vertical Earth Pressures

Seven earth pressure cells, located on the floor of the test facility, recorded the soil pressure during the construction period. The calibration for these earth pressure cells occurred in-situ, relating the voltage from the cells and the self-weight of the soil above the cells for 1 meter of soil.

Figure 4.30 shows the recorded earth pressure cells at the base of the test versus time for the period of construction. The maximum measurement at the end of construction was 76 kPa (96% of the soil self-weight), in a cell located at 1.65 meters from the back of facing and the minimum was 25 kPa (32% of the soil self-weight) recorded at 0.21 meters from the back of facing. The normalized curve for the end of construction is shown in Figure 4.31.

The EPCs located in the reinforced soil zone immediately behind the facing were located 1.45 m, 2.1 m, 2.55 m and 3 m above the base of the wall. Figure 4.32 shows the pressure-time response for these 4 EPCs. Figure 4.33 plots vertical pressure versus time for two cells located between 1.45 m and 3.00 m from the floor of the facility. The pressure-time response for these two cells were the same for the cell located at 50 cm and 300 cm from the back of facing. The results are consistent with the soil self-weight values at the level of 1.45 meters.

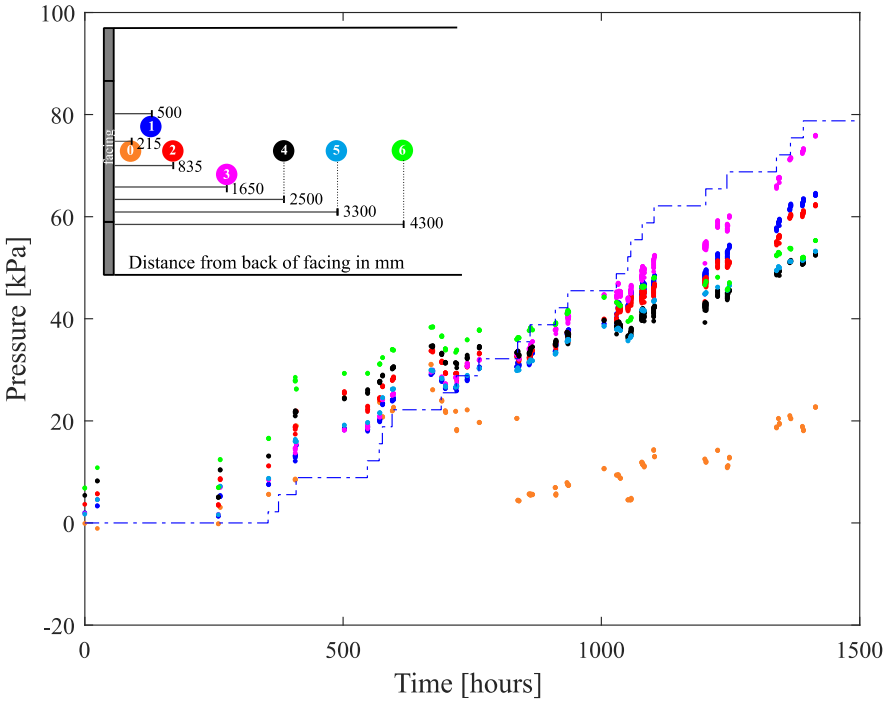

Figure 4-30. Wall #2 – Vertical pressures recorded at the base of test facility.

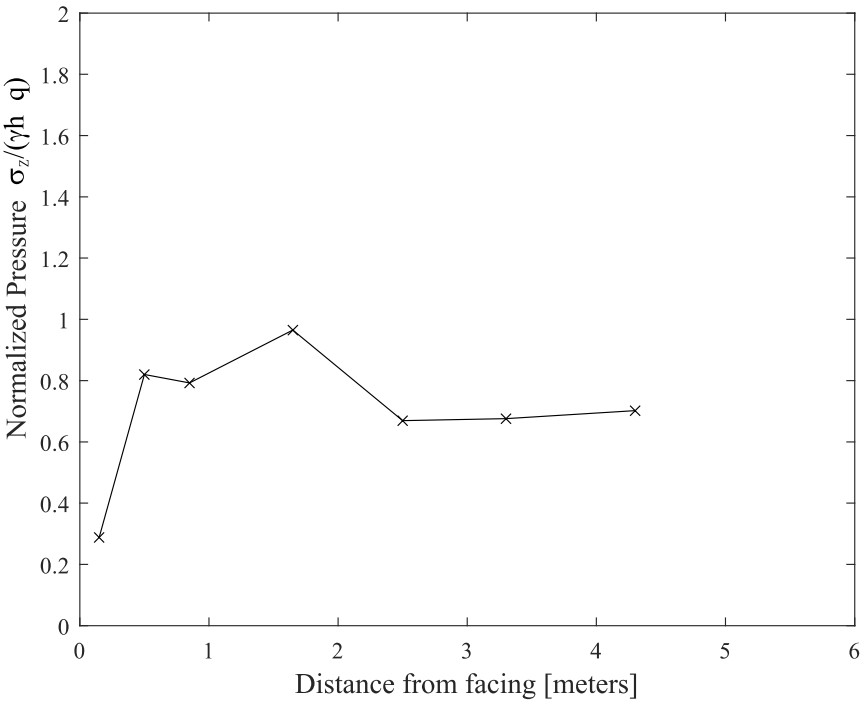

Figure 4-31. Wall #2 – Normalized vertical pressures recorded at the base of test facility.

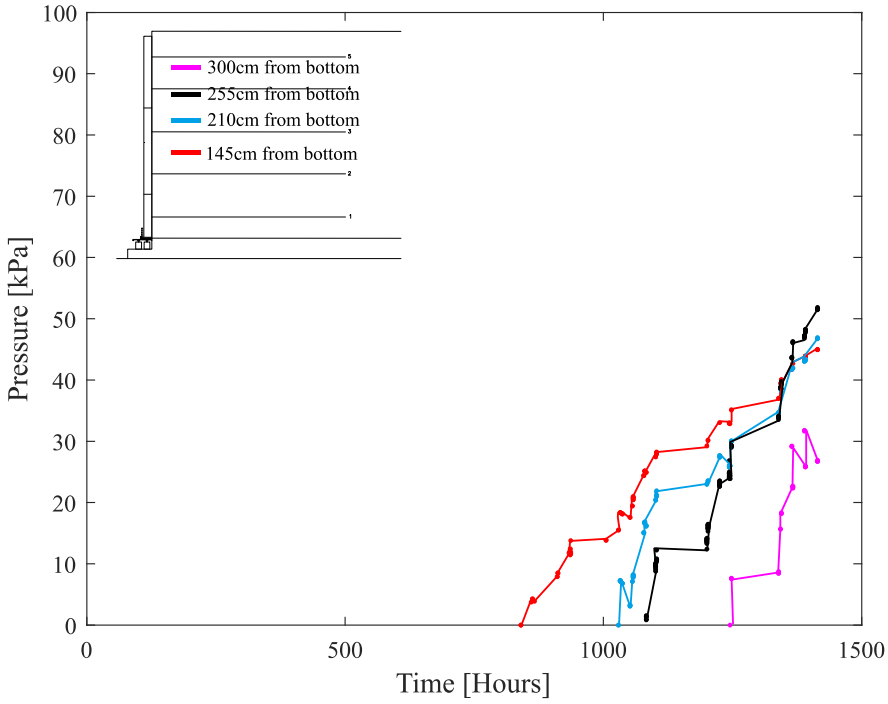

Figure 4-32. Wall #2 – Vertical earth pressures recorded immediately behind facing along profile.

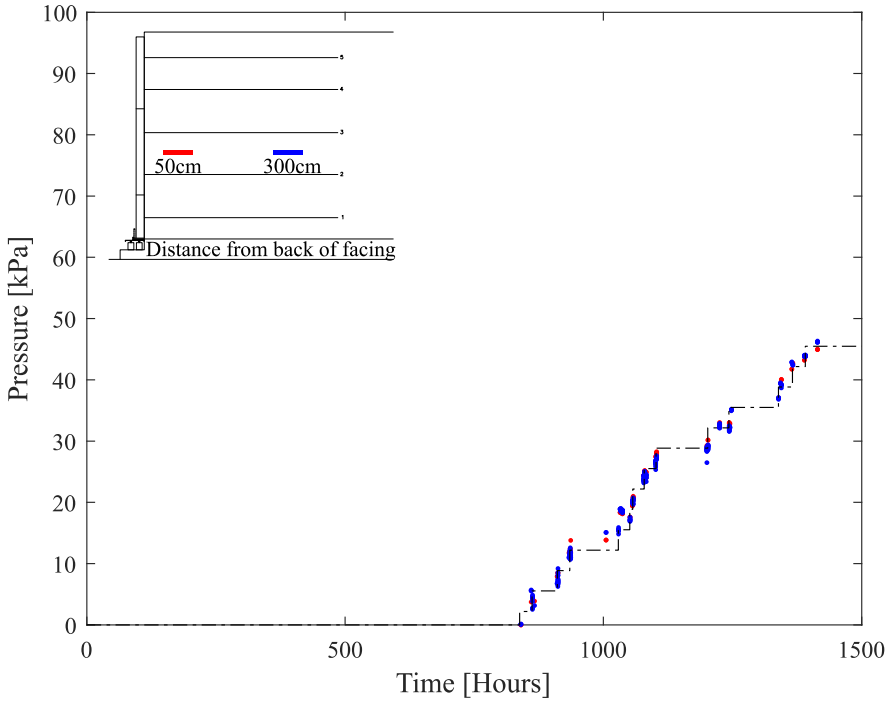

Figure 4-33. Wall #2 – Vertical pressures recorded at 1.45m elevation.

d) Connection Loads

Each reinforced layer recorded the load measured at the clamp between the concrete panel facing and the reinforced steel strips. On the clamp was installed a pair of calibrated strain gauges that related load and strain. Figure 4.34 shows the strain measured in each layer during the construction period. Layer 4, same layer as for wall 1, showed the highest load (12 kN) at the end of the construction.

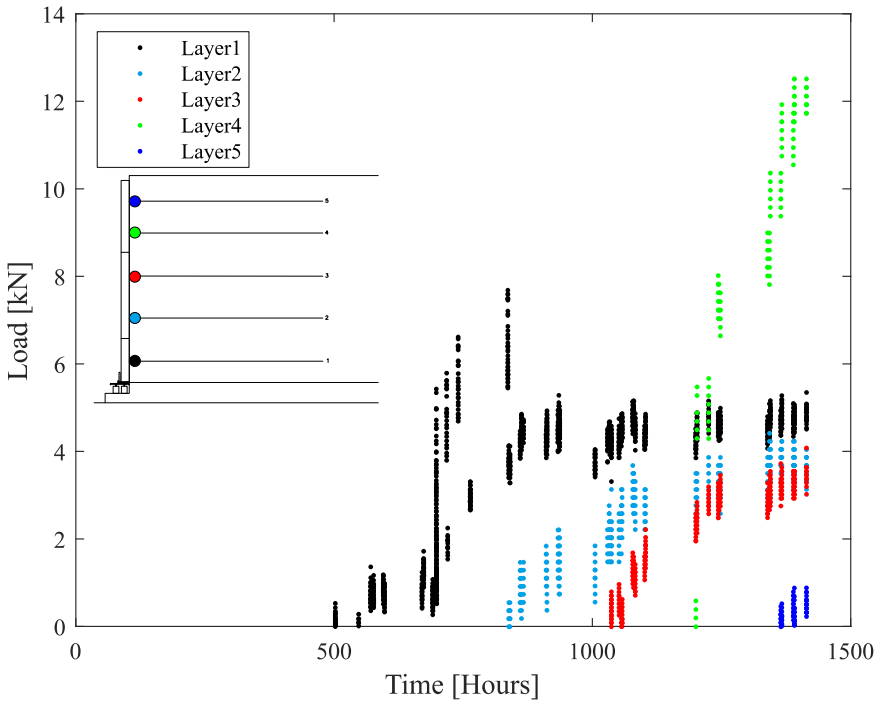

Figure 4-34. Wall #2 – Connection load vs time.

e) Vertical Footing Loads

The 18 vertical load cells were placed below the concrete panels facing. The cells were divided in three plates (north, south and center) and in each plate divided in 2 columns (toe and heel).

Figure 4.35 shows the results from the toe and heel for the period of construction. The heel column is the column that is located immediately below the panel facing and presents the greater value compared to the toe.

Figure 4.35 also shows the load distribution during the construction period. The load per meter of the wall measured under the south and north plates was approximately twice as greater than the load per meter on the center plate. At the end of the construction, the

normalized load presented a load approximately twice as great as the load of the facing self-weight.

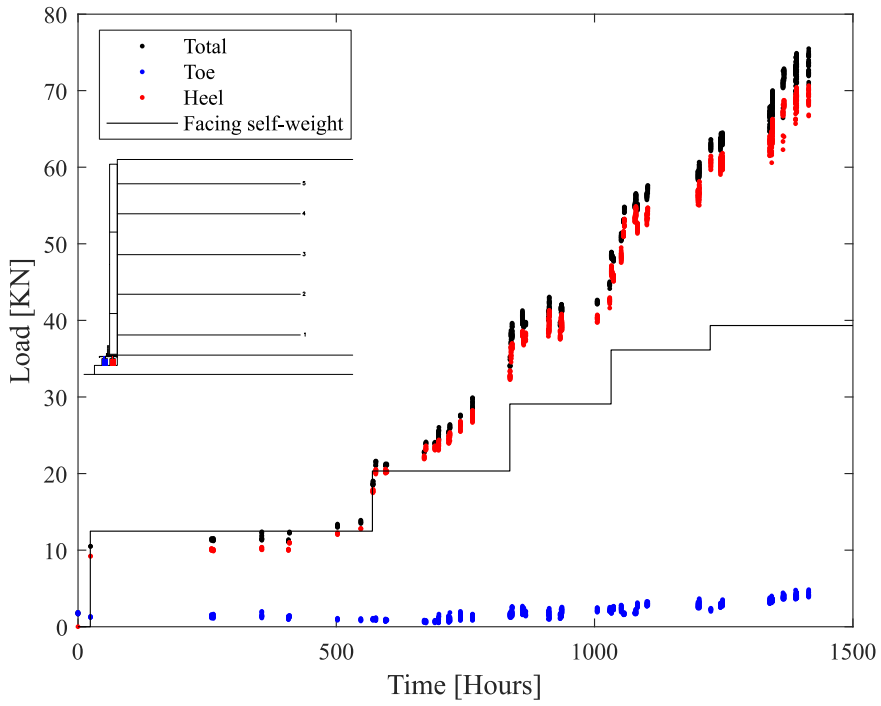

Figure 4-35. Wall #2 – Vertical footing loads vs time during construction.

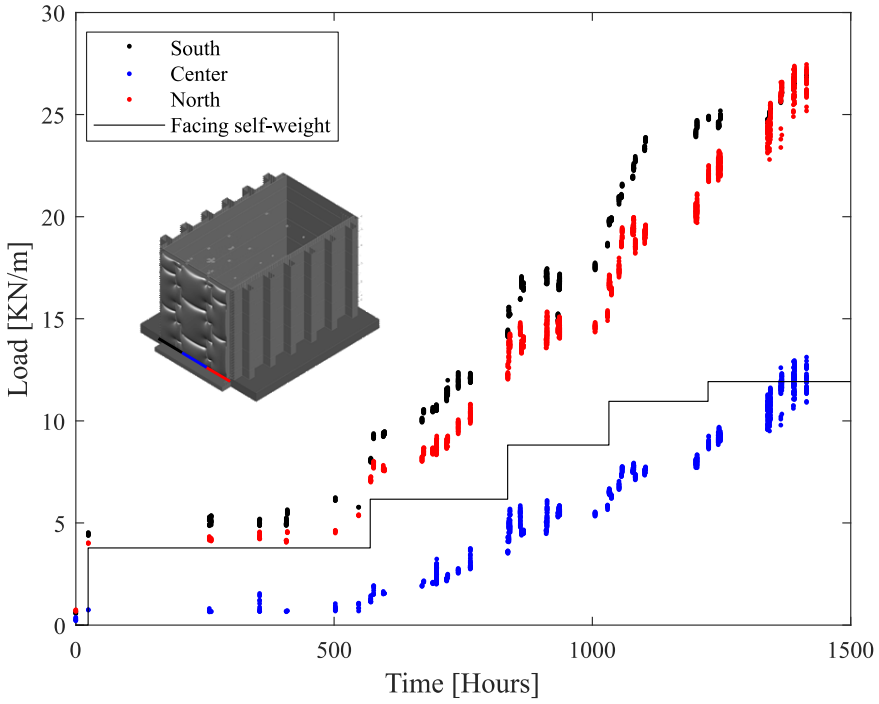

Figure 4-36. Wall #2 – Vertical footing loads per meter length of wall vs time.

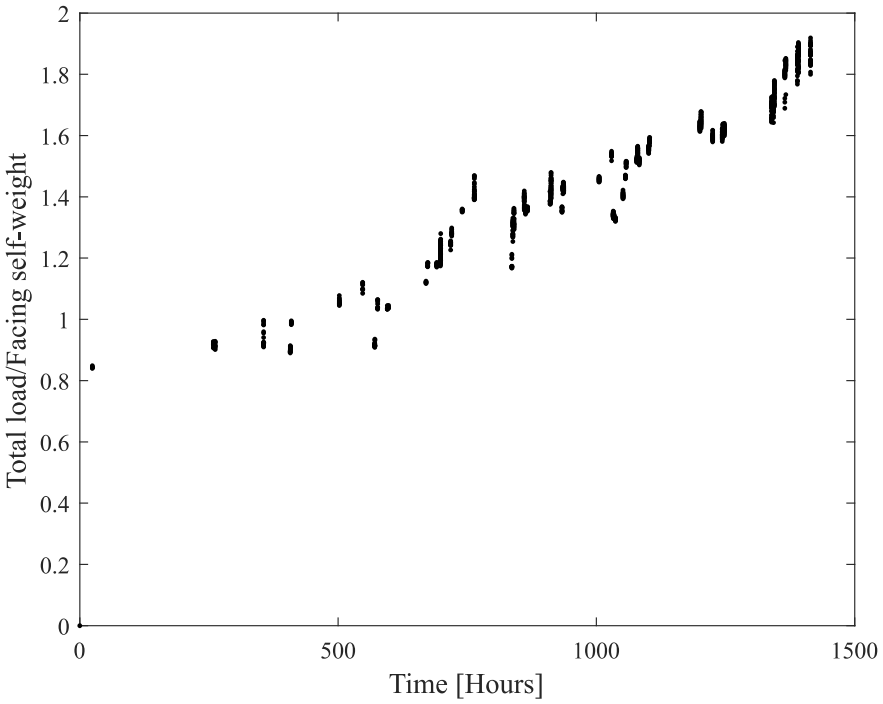

Figure 4-37. Wall #2 – Normalized vertical footing loads.

f) Horizontal Footing Loads

The horizontal footing load sensors were divided in south, north and center. Figure 4.38 shows the measurements for the horizontal footing loads recorded during the construction period. At the end of construction, the maximum recorded load was 1.3 kN/m located at the south side.

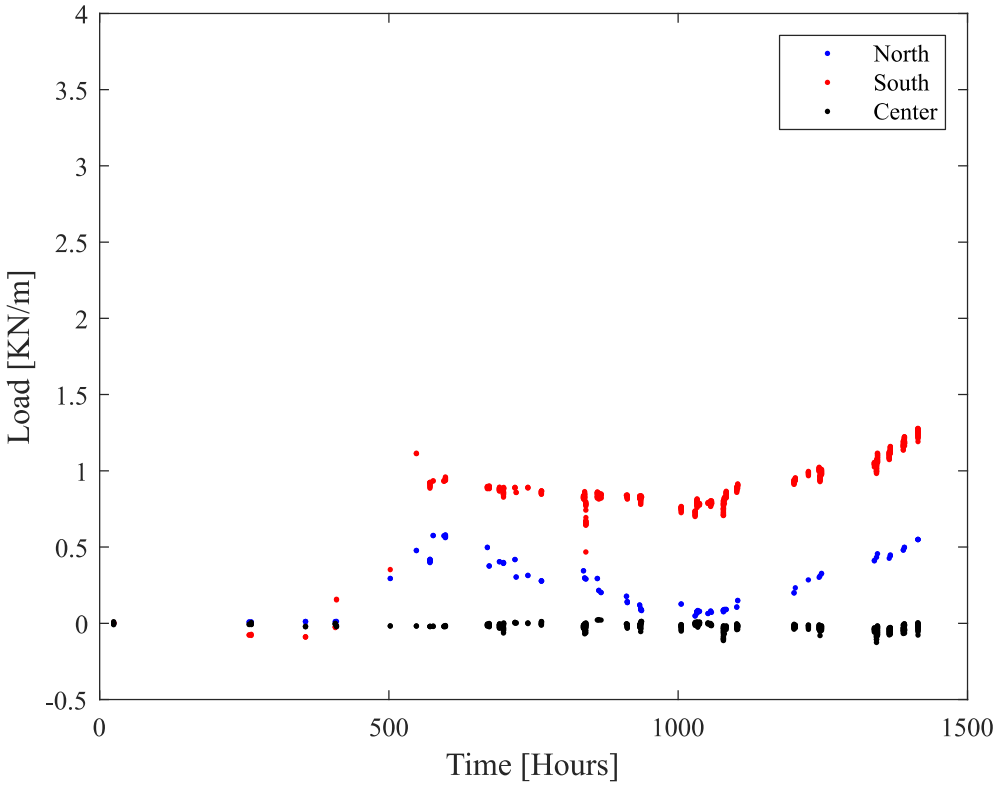

Figure 4-38. Wall #2 – Horizontal footing load per meter length of wall vs time.

Flooding and rapid drawdown test

a) Water level

Figure 4.39 presents the water level for the external tank in front of facing and the two pipes located into the backfill. During the flooding test, the water level reached at 1 meter within 71 minutes. During the filling of the tank, water infiltration into the soil was allowed. For the rapid drawdown test, the external tank took 26 minutes to be emptied.

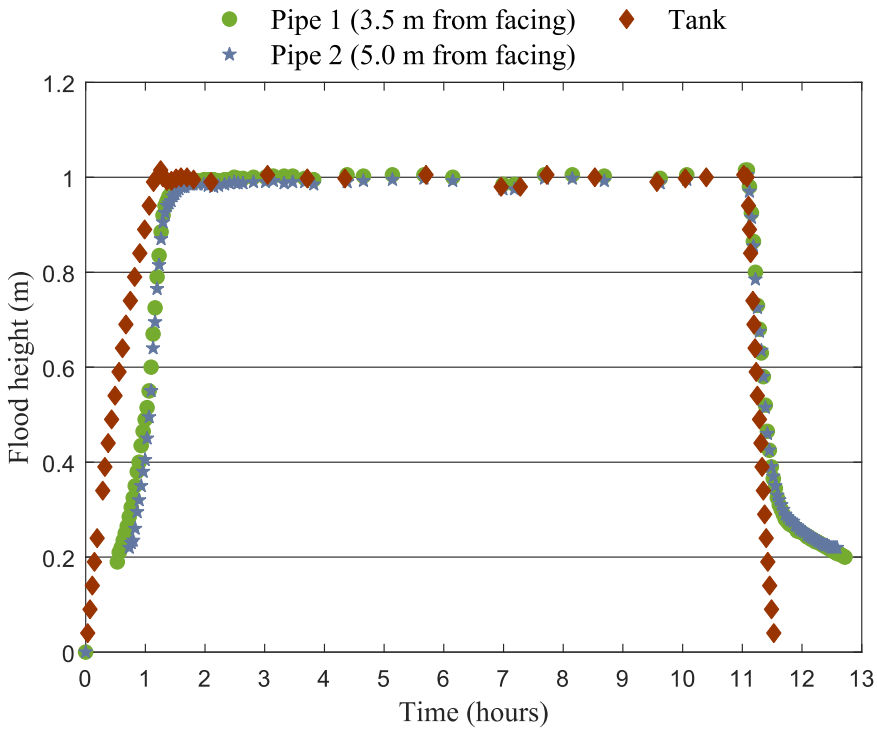

Figure 4-39. Wall #2 – Water level in reservoir and standpipes during a flooding and rapid drawdown event.

b) Volumetric Water Content (VWC)

The position of the VWC reading devices was modified for the second wall. In this way, it was possible to have more observations of the flood/drying front. The first layer of devices was installed at an elevation of 50 cm, the second layer at an elevation of 100 cm (maximum water level) and the third level at 150 cm from the floor.

Figure 4-40 shows the volumetric water content for the three levels during the flood and rapid drawdown test. Some sensors showed erroneous readings of VWC sensors (for example, sensor located at 50cm above the base of the wall and 35cm from the back of the facing). The data is still useful to assess the timing of the wetting front and drying front so it is included in the figures. The curves show the shift from the VWC to layers 1 and 2 over time. The VWC sensor at 150 cm, which is 50 cm above the water level, remains constant throughout the test due to no saturation in the location of the devices.

With the water level curves and VWC it was possible to generate interpretations of the wetting front (Figure 4.41) and the drying front (Figure 4.42). During the flood and rapid drawdown tests, all devices (external and internal) recorded the results and are presented in Appendix A.

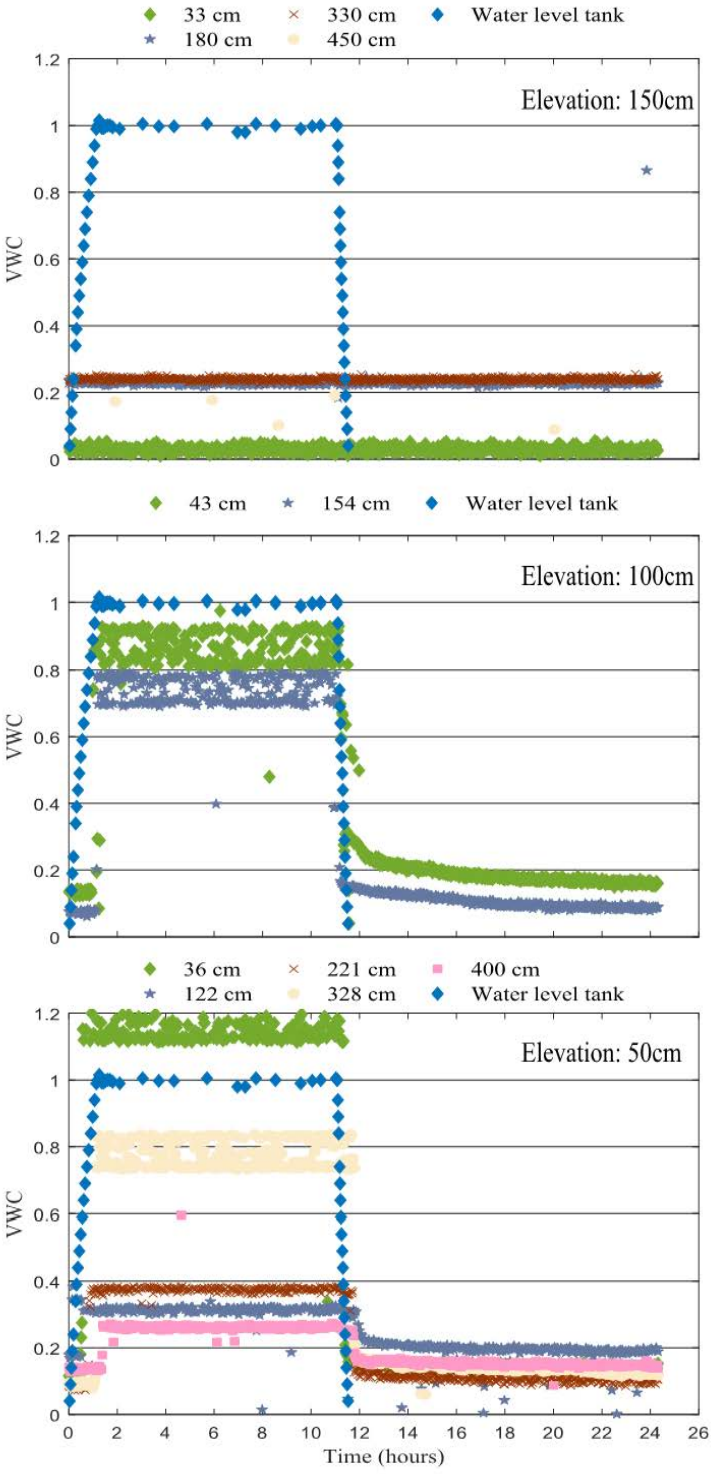

Figure 4-40. Wall #2 – Volumetric Water content (VWC) versus time for the flooding/rapid drawdown test. Note: readings above 0.4 are interpreted to be representative of wetting front / drying front passing location.

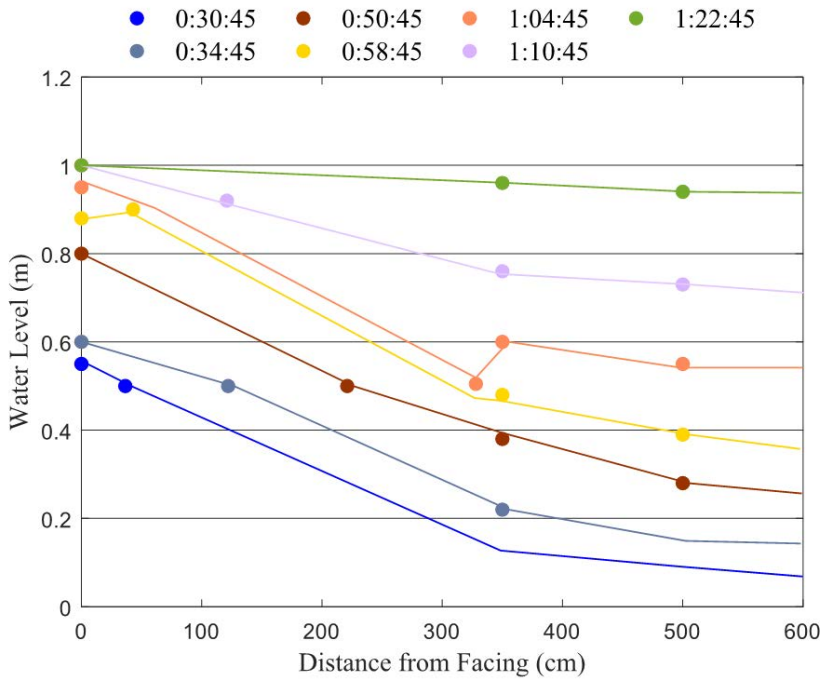

Figure 4-41. Wall #2 – Wetting front at discrete locations during flooding.

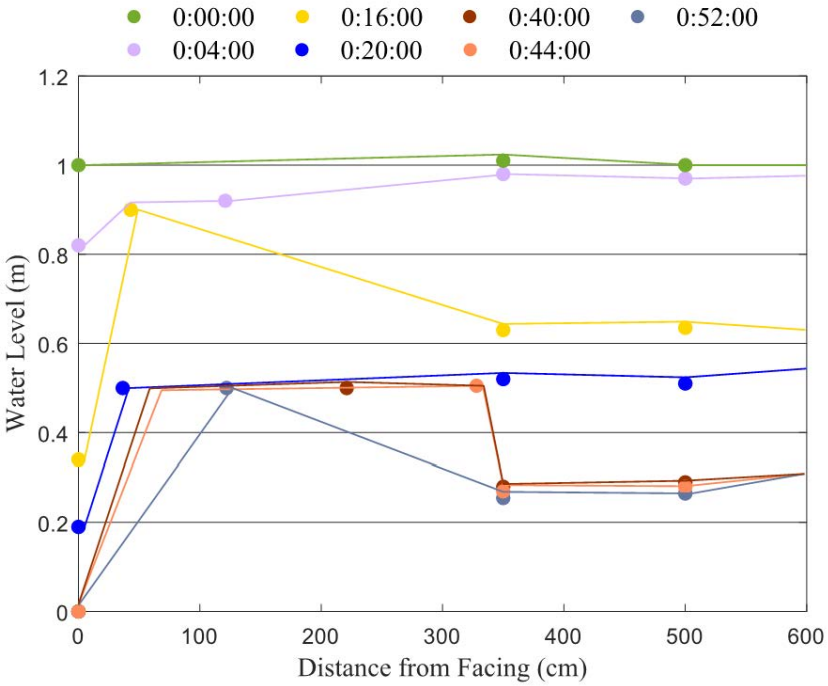

Figure 4-42. Wall #2 – Drying front at discrete locations during rapid drawdown event.

Major Observations and Interpretation of the Performance of Wall 1 and Wall 2

In this chapter, general observations and conclusions regarding Wall 1 and Wall 2 during the construction and flooding/rapid drawdown tests are summarized. Both walls presented the same characteristics including dimensions, facing (degree and material), reinforcement (spacing and material) and boundaries conditions. The only difference between the two walls was the backfill material, the first being sand and the second being coarser granular material (sand with gravel).

Wall 1, with a sand backfill, was constructed in 3900 hours. This large amount of time for the construction occurred due to a problem with the crane that helped in the movement of the backfill soil and the facing. The major observations for wall 1 are summarized below:

1. The out-of-alignment displacement, at the end of construction, was 0.95% of the overall wall height. At the end of flood and rapid drawdown cycle, the facing displacement was approximately 33 mm at the top of panel 3.
2. At the end of construction, the vertical footing load was twice the self-weight of the facing panels. During the flooding and rapid drawdown tests, the load increased 3.1% of the load at the end of construction, however returned for the previous value at the end of rapid drawdown test.
3. The maximum reinforcement strain was 600 με at the end of construction located on the second reinforced layer. Except for the strain gauge located in the first reinforced layer and 15 cm from the facing, the other devices did not show any variation during the flood and rapid drawdown test.
4. The maximum load, at the connection between the panel facing and the reinforcement steel strip, was 4.5 kN at the connection of layer 4 at the end of construction. During the flood and rapid drawdown test, the connection did not show an important load change.
5. The flood test was carried out in approximately 27 hours when all volumetric water sensors located 1 meter from the floor showed saturation, and the piezometers showed the water level at 1 meter.

Wall 2 was sand with gravel backfill and was constructed in 1500 hours. This wall has the same characteristics as the first wall, except for the backfill. The following are the major observations and conclusions based on the construction, flooding and rapid drawdown periods:

1. At the end of construction, out-of-alignment displacement was 23 mm (0.65% of the overall wall height). Similar to Wall 1, Wall 2 showed a facing displacement of less than 1 mm during the flood test, however during the rapid drawdown test, the facing displacement returned to values very similar to those of before the flood test.
2. The vertical footing load was 1.8 times greater than the self-weight of the facing panels at the end of construction. During the flood and rapid drawdown tests, the vertical footing load did not present a significant change in load.
3. At the end of construction, the second reinforced layer presented a maximum of 250 με close to the back of facing. During the flood and rapid drawdown test, the strain gauge located in the first reinforced layer and 15 cm from the facing presented a change of 100 με, however at the end of drawdown test, this device returned to previous values. The other devices did not show any variation during these periods.
4. The maximum load at the connection was 12 kN at the end of construction for the device located at the 4th layer. During the flooding and rapid drawdown test, the connection located at the first reinforced layer varied 2 kN from the beginning of the flood test until the end of rapid drawdown test. It was the only sensor that recorded a change in load.
5. The flooding and rapid drawdown tests were faster for the second wall than the first wall, although the permeability results (constant head) show the greater permeability value for the first wall. The flood test was carried out in approximately 11 hours when the water was 1-meter-high over the entire length of the backfill soil.
6. The time to fill with water (1 m) the tank located in front of the face was 63 minutes for the first wall and 71 minutes for the second wall. It was due to the permeability of the soil of the second wall on the full scale physical model be greater than the first wall, which is also confirmed by the volumetric water content sensors.
7. The water level and the volumetric water content sensors for both walls allowed to account for the transient unsaturated flow processes during flooding and draining cycles, generating the wetting and dry front.

To summarize, the data set summarizes details of construction, flooding/rapid drawdown tests for concrete panel walls with steel strip reinforcement using two different backfills. The two backfill soils used in this study are within the range of particle size distribution specified by AASHTO (2010) and Berg et al (2009). Although both backfills are non-cohesive granular materials, they present different results regarding mechanical and

hydraulic behavior, as can be seen in the results of the large-scale physical model. The construction results display the density of data and indicate the walls are stable over the temporal range of the testing periods. During flooding/rapid drawdown both walls one and two showed minimal impact in relation to the stability. The measurements from these full-scale walls are available for numerical modeling to widen the application for analyzing moisture migration within reinforced and backfill materials to investigate a wider range of conditions.

CHAPTER 5 : NUMERICAL ANALYSIS

Geometry

The model wall is 3.6-m high and 6-m long. This geometry matches the full-scale wall geometry that was built in the Testing Facility at the Royal Military College of Canada (RMC). The boundaries at the bottom and right sides of the wall are treated as impermeable boundaries. The reservoir pressure head is applied at the front of the wall for steady state and transient conditions. Two standpipe piezometers were installed at 3.5 m and 5 m distance from the wall face to monitor water level rise inside the backfill. Various TDR cells were installed at different elevations within the backfill to measure the volumetric water contents during flooding and rapid drawdown scenarios. The water levels at the locations of standpipe piezometers and TDRs from the numerical analyses were compared to those from the measurements for calibration. Figure 5-1 shows a schematic of the instrumented MSE wall that was modeled in full scale in the laboratory. The metal strip reinforcement is assumed to not affect the drainage capacity of the backfill, therefore it is not modeled for the seepage analysis. For stability analysis, metallic reinforcements were placed at vertical spacing of 0.37 m, 0.75 m, 0.73 m, 0.75 m, and 0.55 m beginning from the bottom of the wall, and horizontally extended to 3.3 m inside the backfill. For seepage analysis, SVFlux GT, and for slope stability analysis, SVSlope GT from the software package SVOffice Version 5.0 were used. Figure 5-2 shows the geometries of the MSE walls modeled for seepage and stability analyses. The model wall face is slightly sloped so that it can be run by SVSlope GT.

Figure 5-1. A schematic of the prototype MSE wall.

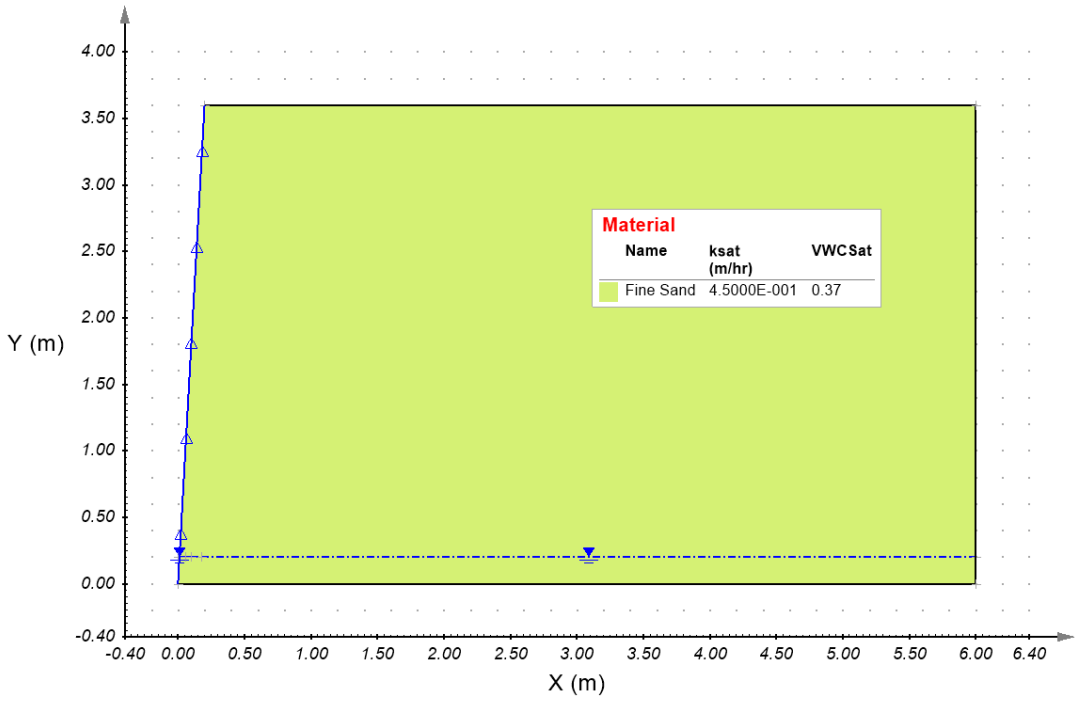

(a)

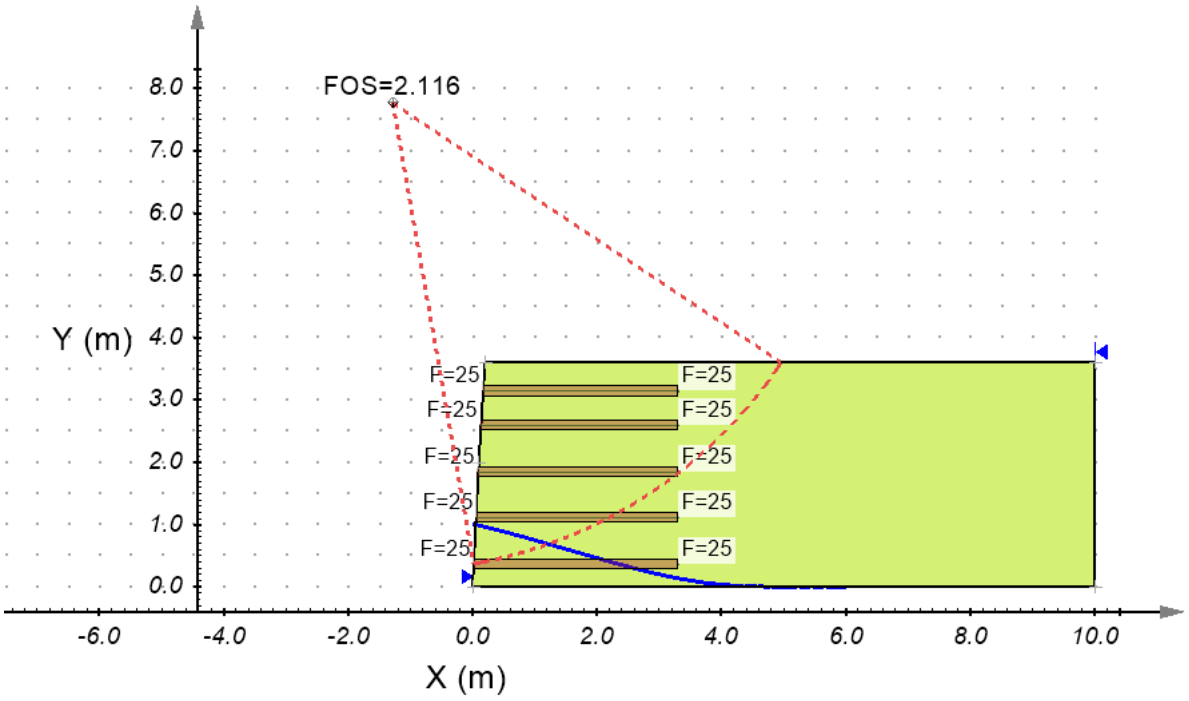

(b)

Figure 5-2. Model MSE wall for (a) seepage and (b) stability analysis.

Initial Conditions

For seepage analysis, the initial conditions include the initial water content, water table, and the initial head in front of the wall. The reservoir water heads of 1 m to 3.6 m were applied in front of the MSE wall for the flooding and rapid drawdown events. For slope stability analysis, the initial condition includes the pore water pressure distribution in the backfill soil obtained from the transient or steady state seepage analysis during flooding or rapid drawdown events. Backfill material properties used for seepage and stability analyses are summarized in Table 3-2 of Chapter 3. The soil friction angle used in the models from the laboratory triaxial tests is 35^{o}.

Seepage Analysis and Model Calibration

The seepage analyses were done for two scenarios: (i) infiltration of the MSE wall backfill from flooding at the face of the wall, and (ii) rapid drawdown. The reservoir water level of 1 m that was applied to the full-scale walls at the RMC facility, was used to simulate the seepage analysis for calibration. The water levels at the wall front and the two standpipe piezometer locations from the seepage model analysis were compared with the measured ones from the full-scale laboratory model test. The backfill hydraulic conductivity was then back-calculated so that the calculated water levels match the measured ones. Wall #1 and Wall #2 were constructed with fine and coarse sands as backfill, respectively. The initial pressure head (water table) for Wall #1 was at 0.2 m and for Wall #2 was at 0 m. The back-calculated hydraulic conductivities from the seepage model calibrations for the fine sand backfill used in Wall #1 is 1.26×10^{-2} cm/s (4.5×10^{-1} m/h) and for the coarse sand backfill used in Wall #2 is 3.3×10^{-1} cm/s (1.2×10^{1} m/h). The higher back-calculated hydraulic conductivity for Wall#2 backfill compared to that of Wall #1 agrees with the fact that the backfill material for Wall #2 is coarser than Wall #1. Although the back-calculated hydraulic conductivities are different from those measured from the lab samples as described in Chapter 3, the back-calculated ones account for soil heterogeneity placed and compacted as backfill and possible various levels of compaction during construction, and therefore are considered more representative of full-scale conditions. Figure 5-3 shows the free water surfaces in the backfills from the seepage analysis and measurements from the full-scale models.

Water infiltration in the backfill for Wall #1 was simulated at different times after flooding. Figure 5-4a shows the evolution of free water surfaces inside the backfill at different times for a water pressure head of 1 m (modeled to develop instantaneously) in front of the wall. Water seeps through the front face of the MSE wall. The rate of evolution of the free

water surface depends on the hydraulic conductivity of the backfill material. For the sand backfill with hydraulic conductivity of $k=1.26\times10^{-2}$ cm/s (4.5×10^{-1} m/h), free water surface in the backfill reaches the elevation of the reservoir water at about 30 hours after flooding and saturates the backfill. On the other hand, Figure 5-4b shows the evolution of free water surfaces in the backfill at different times for a 1-m water rapid drawdown in front of the MSE wall. Similar to the flooding event, water pressure dissipates quickly. Nearly half of the volume of backfill under the reservoir elevation is unsaturated after 10 hours of rapid drawdown. Rapid dissipation of positive pore water pressure immediately behind the wall relative to the regions deeper inside the backfill is due to high hydraulic gradient at the proximity of the wall face.

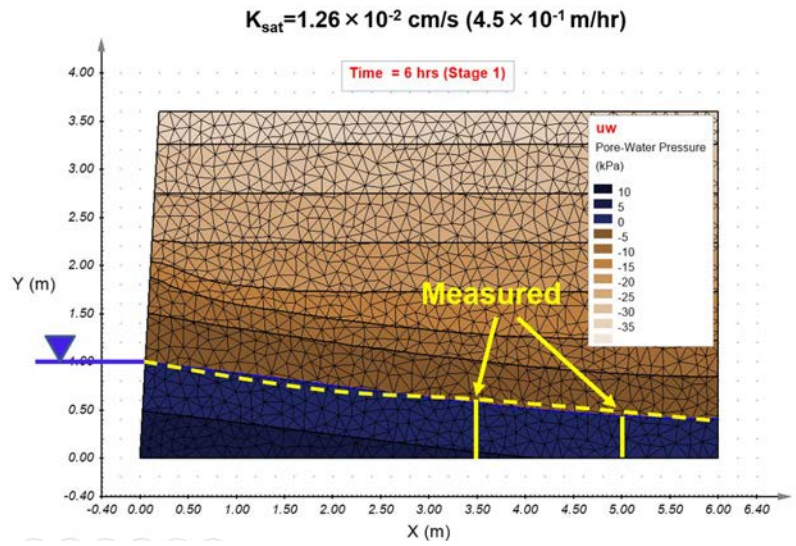

(a)

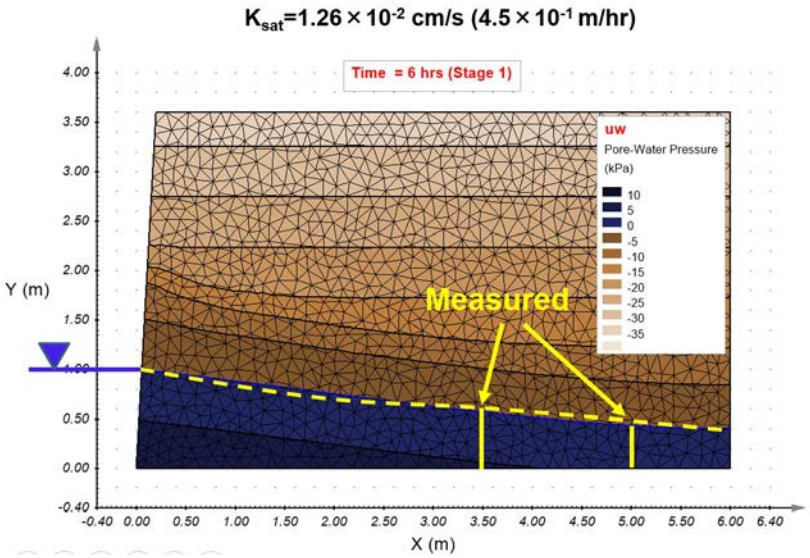

(b)

Figure 5-3. Free water surfaces inside the MSE Wall backfills for (a) Wall #1 and (b) Wall #2.

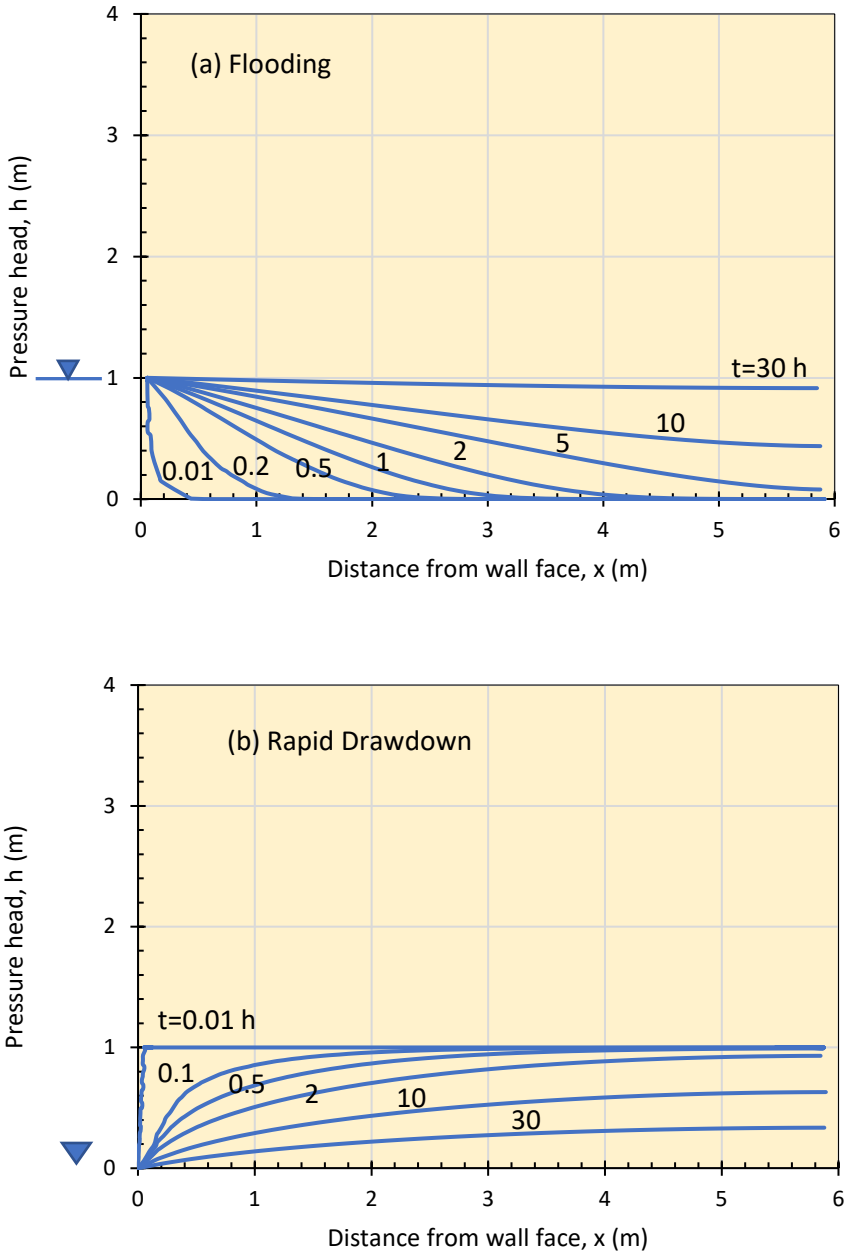

Figure 5-4. Evolution of free water surface inside the backfill (a) after flooding and (b) after rapid drawdown for Wall #1.

Complete backfill desaturation takes longer than backfill saturation because water only dissipates through the front toe of the wall compared to backfill saturation where water seeps through the entire 1-m of the wall. Water infiltration in the backfill for Wall #2 was simulated at different times after flooding. Figure 5-5a shows the evolution of free water surfaces inside the backfill at different times for a water pressure head of 1 m (modeled to develop instantaneously) in front of the wall. For the coarse sand backfill with hydraulic conductivity

of k=3.3×10^{-1} cm/s (1.2×10^{1} m/h), free water surface in the backfill reaches the elevation of the reservoir water at 1.1 hours after flooding and saturates the backfill. This indicates that backfill in Wall #2 with hydraulic conductivity that is about 27 times higher than that of Wall #1, reaches the saturation level about 27 times quicker than Wall #2. On the other hand, Figure 5-5b shows evolution of free water surfaces in the backfill at different times for a 1-m water rapid drawdown in front of the MSE wall. For Wall #2, it takes about an hour to reach the same level of backfill desaturation compared to Wall #1 that would take about 30 h.

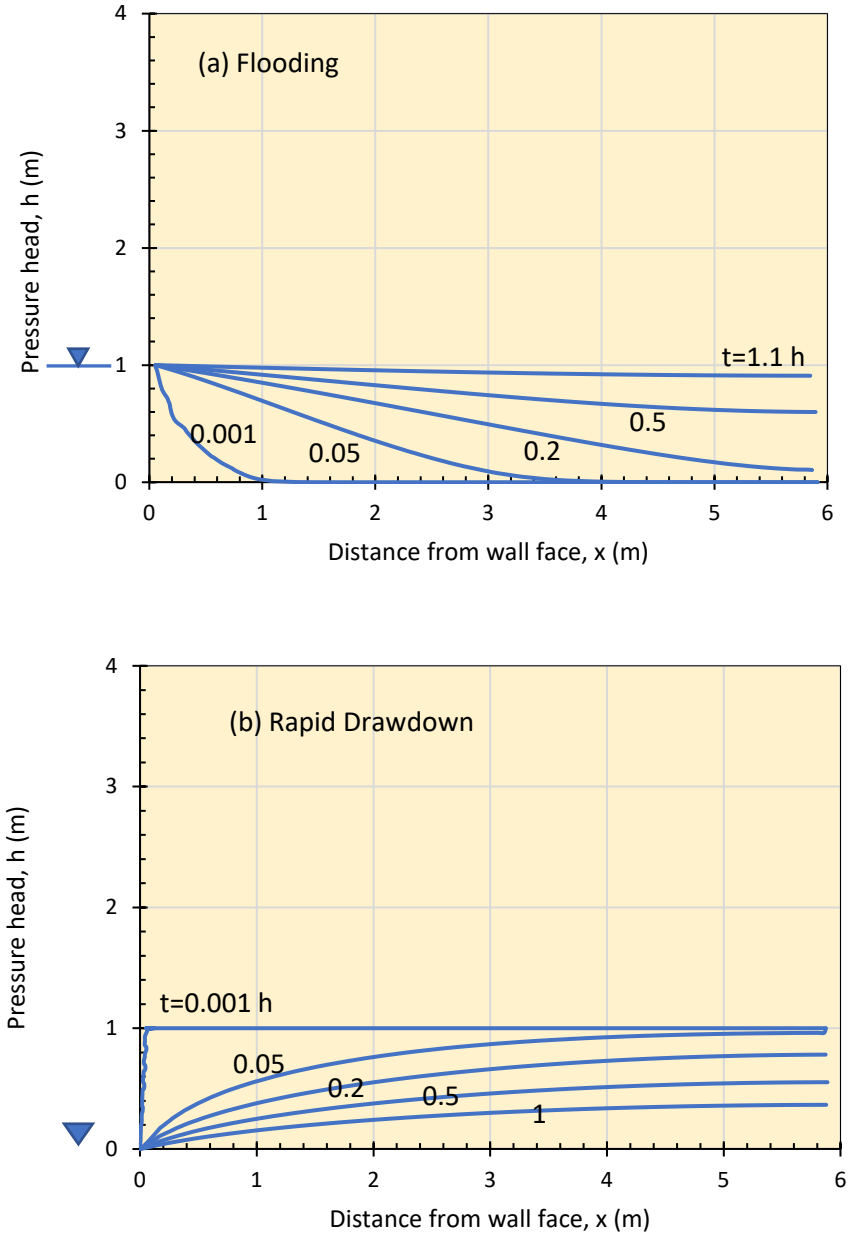

Figure 5-5. Evolution of free water surface inside the backfill (a) after flooding and (b) after rapid drawdown for Wall #2.

Slope Stability Analysis

At each seepage stage, slope stability analysis was conducted to evaluate stability of the MSE wall and calculate the factor of safety (FS) against sliding failure in limit equilibrium condition using GLE (Fredlund) method. Results of the transient seepage analyses were used as initial conditions to include pore water pressure distribution for slope stability analysis. Figure 5-2b shows a failure surface in the MSE wall with a corresponding factor of safety at one hour after flooding. The free water surface from the transient analysis is shown in the figure. Each factor of safety presented herein is the minimum factor of safety computed for many circular failure surfaces at a given loading condition. No erosion of metal strip or adverse scenario for integrity of soil-metal strip during water movement was considered.

For Wall #2, the factors of safety against slope failure at different stages after the flooding and rapid drawdown scenarios were determined and are shown in Figure 5-6. The factor of safety before the flooding event is 2.1. After flooding to 2-m high in front of the wall, the factor of safety increases to 2.6 (an increase of 24%), and gradually decreases to the value before the flooding. The sudden increase in the factor of safety is due to the stabilizing effect of hydrostatic pressure acting towards the wall face. After flooding, water seeps into the backfill and increases the pore water pressure, which results in reduction in the factor of safety. The factor of safety eventually stabilizes to the same value before the flooding. Immediately after the rapid drawdown, the factor of safety drops to 1.8; representing a 14% reduction. Immediately after the rapid drawdown, the water pressure, which acts as a passive pressure in front of the wall, is removed while the positive porewater pressure is still present in the backfill behind the wall. The factor of safety gradually increases as the porewater pressure in the backfill dissipates through the MSE wall face.

Parametric Studies

Backfill hydraulic conductivity, water pressure head (h_w), and length of the backfill (L) affect time to backfill saturation. To develop a graph that the time to complete backfill saturation (T_s) upon flooding can be estimated, several seepage analyses were performed on the model walls with varying K and h_w/L ratio and the times to saturation for wall backfill were calculated. The h_w/L ratio is an indication of hydraulic gradient over the length of the backfill. The higher the h_w/L ratio the lower the T_s. Figure 5-7 shows the variation of T_s versus K at different h_w/L ratios. As expected, the time to saturation decreases with increasing the backfill hydraulic conductivity and h_w/L ratio.

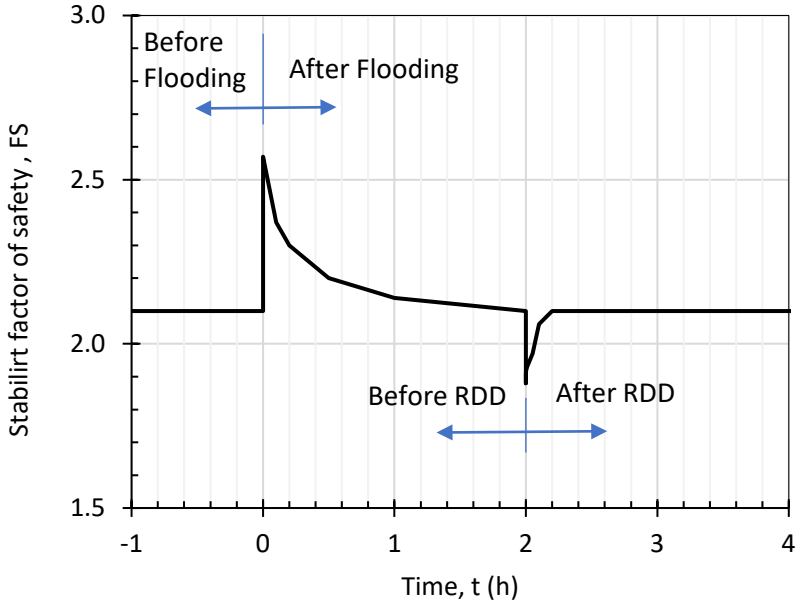

Figure 5-6. Variation of factor of safety against slope failure after flooding and rapid drawdown scenarios.

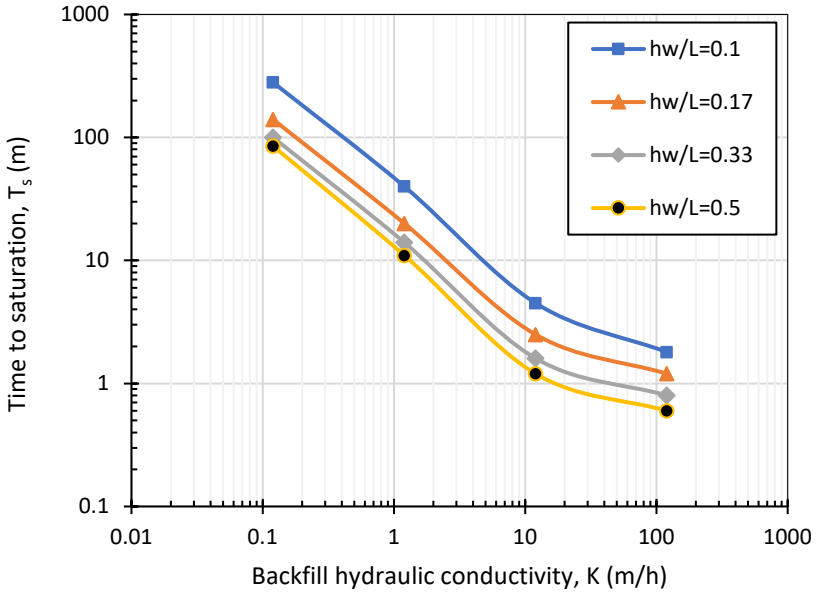

Figure 5-7. Variation of time to saturation with backfill hydraulic conductivity and h_w/L.

To understand the variation of factor of safety with material and geometric properties and loading conditions, a parametric study was conducted to evaluate the factors of safety for different scenarios. Figure 5-8 shows the variation of change in factor of safety (ΔFS) with time for different levels of flooding and drawdown for Wall #2 (with $K=1.2\times10^{1}$ m/h or

3.3×10^{-1} cm/s). The level of flooding and drawdown is defined as the ratio of water pressure head (h_w) in front of the wall to the height of the wall (H). This ratio accommodates the effects of unbalanced hydrostatic pressure relative to the total volume of the sliding mass. The sensitivity of the factor of safety with h_w/H is significant. The factor of safety can increase by up to 105% immediately after flooding and decrease by up to 25% after rapid drawdown when h_w/H ratio increases to 1. It should be mentioned that these percent changes in factor of safety are extreme values assuming sudden rise or drawdown of reservoir. The gradual rise or drawdown that would allow some levels of hydrostatic pressure balance during flooding or pore pressure dissipation during rapid drawdown in the backfill will result in lower changes in the stability factor of safety than those presented herein. The effect of hydraulic conductivity on ΔFS is shown in Figure 5-9. The change of backfill hydraulic conductivity does not change the stability factor of safety immediately after flooding or rapid drawdown but affects the rate of change in ΔFS after flooding or rapid drawdown. The lower the hydraulic conductivity, the slower the change in ΔFS after flooding or rapid drawdown events as indicated in Figure 5-9.

Figure 5-10 shows the effects of reinforcement tensile strength (T) and backfill friction angle on stability factor of safety for flooding and rapid drawdown conditions. The FS increases steadily as T increases from 5 to 15 kN/m beyond which the FS would remain constant. Increasing the backfill friction angle from 30^o to 35^o, increases the factor of safety for both flooding and rapid drawdown by about 20%.

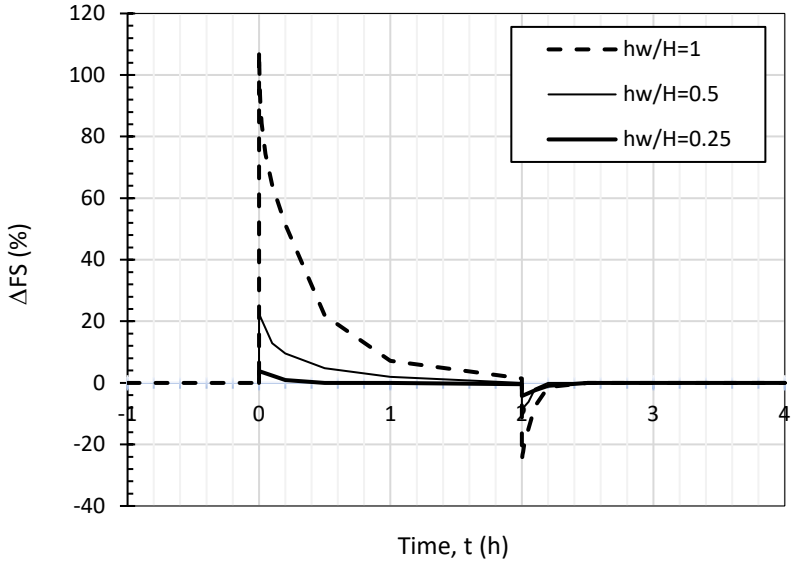

Figure 5-8. Change of stability factor of safety after flooding and rapid drawdown with time at different hw/H (for Wall #2, K=1.2×101 m/h or 3.3×10-1 cm/s).

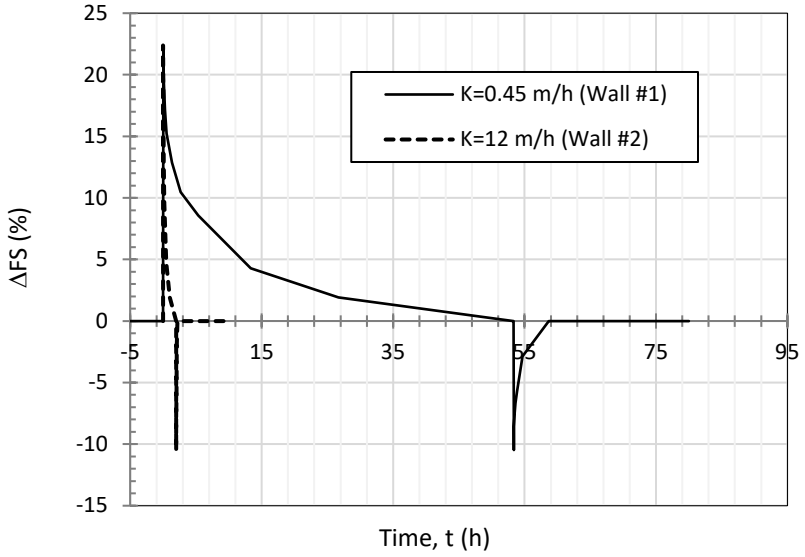

Figure 5-9. Change of stability factor of safety after flooding and rapid drawdown with time at different K (for $h_w/H=0.5$).

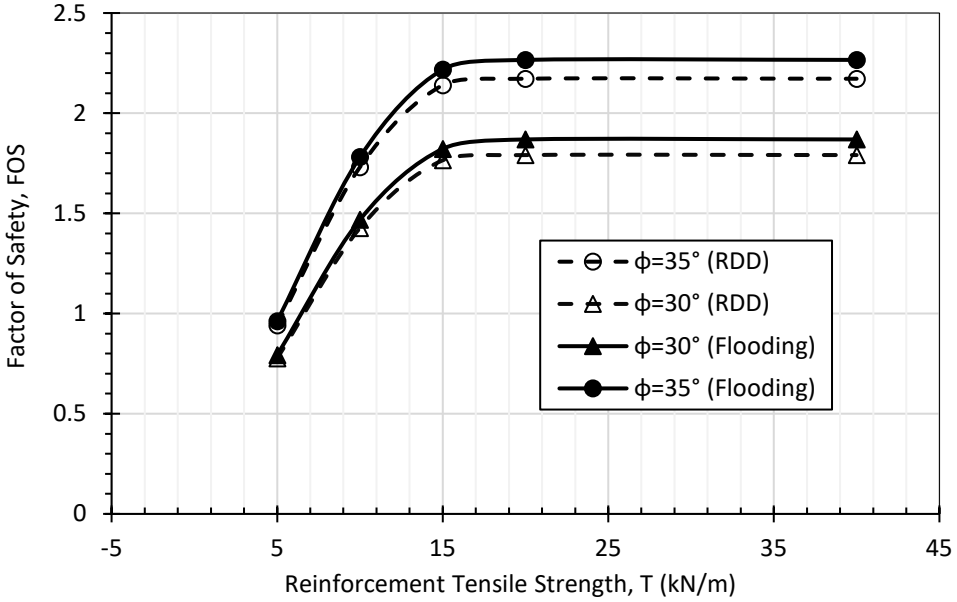

Figure 5-10. Variation of factor of safety with reinforcement tensile strength.

CHAPTER 6 : CONCLUSIONS AND RECOMMENDATIONS

Two MSE walls were constructed with fine and coarse sands that cover the range of typical backfill materials used in MSE walls. Flooding and rapid drawdown events in front of the two MSE walls were simulated using numerical and physical models. The numerical seepage models were calibrated from the direct pore pressure measurements from the full-scale laboratory MSE walls. Evolution of free water surfaces and rate of backfill saturation and desaturation during flooding and rapid drawdown were obtained through transient seepage analyses as well as direct measurements in the laboratory. For the fine and coarse sands that were used as backfill materials, the time for backfill saturation were about 30 h and 1 h; respectively. Evolution of waterfront in the fine and coarse sand backfills and the rate of backfill saturation were determined for different water pressure heads and backfill hydraulic conductivities through a series of parametric studies.

Variation of the stability factor of safety during flooding and rapid drawdown conditions was determined by limit equilibrium slope stability analysis. The stability factor of safety increases immediately after flooding and gradually decreases to the value before flooding as the sand backfill is saturated. On the other hand, the stability factor of safety decreases immediately after rapid drawdown and gradually increases to the value before rapid drawdown as pore water pressure dissipates from the sand backfill. The relative increase and decrease in the stability factor of safety after flooding and rapid drawdown depends on the water pressure head in front of the MSE wall relative to the height of the wall. The higher the pressure head relative to the wall height, the greater the change in the stability factor of safety is anticipated. The factor of safety can increase by up to 105% immediately after flooding and decrease by up to 25% after rapid drawdown when the ratio of the pressure head to wall height increases to 1. The percent rise or drop in the factor of safety presented herein are extreme values assuming sudden rise or drawdown of reservoir. The gradual rise or drawdown that would allow some levels of hydrostatic pressure balance during flooding or pore pressure dissipation during rapid drawdown in the backfill will result in lower changes in the stability factor of safety than those presented in this report. Increasing the reinforcement tensile strength increases the stability factor of safety for both flooding and rapid drawdown conditions by up to a threshold beyond which the factor of safety would remain constant. The increase of backfill friction angle from 30^o to 35^o increases the stability factor of safety by about 20% for both flooding and rapid drawdown conditions.

To estimate the effects of flooding and rapid drawdown on MSE wall stability factors of safety at a given time, t, the following procedure is recommended out of the results of the research:

1. Calculate the stability factor of safety during steady state seepage based on the backfill strength properties, geometry, and reinforcement layout and strength properties.
2. Having the backfill hydraulic conductivity, the applied pressure head ratio (h_w/H), and hydraulic gradient (h_w/L), select the appropriate ΔFS-t graph.
3. In the selected graph, choose or interpolate the change in the factor of safety, ΔFS, at a given time.
4. Compare the new factor of safety with the minimum design factor of safety.

The results and the procedure presented herein are valid for the range of the material properties and wall geometry and reinforcement layout used in this research and are intended to only provide an estimate. For a MSE wall of different reinforcement layout, slope, and backfill material type, the designer should analyze a separate and unique model.

REFERENCES

AASHTO (American Association of State Highway and Transportation) (2010). LRFD Bridge Design Specifications, 5th Edition, American Association of State Highway and Transportation Officials, Washington, DC Officials, Washington, DC.

Anderson, P., Gladstone, R., Sankey, J. (2012). *"State of the Practice of MSE Wall Design for Highway Structures"*. *Geotechnical Engineering* S*tate of the Art and Practice*, 1–21. doi:10.1061/ 9780784412138.0018

ASTM D6913-04. (2004) *"Standard Test Methods for Particle-Size Distribution (Gradation) of Soils Using Sieve Analysis."* ASTM International, West Conshohocken, PA, www.astm.org

ASTM D2487-06. (2006). *"Standard Practice for Classification of Soils for Engineering Purposes (Unified Soil Classification System)."* ASTM International, West Conshohocken, PA, www.astm.org

ASTM D698-12e1. (2012*) "Standard Test Methods for Laboratory Compaction Characteristics of Soil Using Standard Effort (12 400 ft-lbf/ft3 (600 kN-m/m3))."* ASTM International, West Conshohocken, PA, www.astm.org

ASTM D6836-16. (2016). *"Standard Test Methods for Determination of the Soil Water Characteristic Curve for Desorption Using Hanging Column, Pressure Extractor, Chilled Mirror Hygrometer, or Centrifuge."* ASTM International, West Conshohocken, PA, www.astm.org

ASTM D2434-19. (2019). *"Standard Test Method for Permeability of Granular Soils (Constant Head)."* ASTM International, West Conshohocken, PA, www.astm.org

Aubeny, C.P., Biscontin, G., Huang, J., Dantal, V.S., Sadat, R., and Bin-Shafique, S. (2014). *Design Parameters and Methodology for Mechanically Stabilized Earth (MSE) Walls.* Texas A&M Transportation Institute, Rep. No. FHWA/TX-14/0-6716-1.

Basma, A., Tuncer, E. (1992). *"Evaluation and Control of Collapsible Soils". Journal of Geotechnical Engineering*. ASCE 1992.118:1491.-1504.

Bathurst, R. J.; Allen, T. M.; Walters, D. L. (2005). *"Reinforcement loads in geosynthetic walls and the case for a new working stress design method." Geotextiles and Geomembranes*, 23(4), 287–322.

Bathurst, R. J.; Vlachopoulos, N.; Walters, D. L.; Burgess, P. G.; Allen, T. M. (2006). *"The influence of facing stiffness on the performance of two geosynthetic reinforced soil retaining walls." Canadian Geotechnical Journal*, 43(12), 1225–1237

Bathurst, R. J.; Walters, D.; Vlachopoulos, N.; Burgess, P.; Allen, T. M. (2000). *"Full scale testing of geosynthetic reinforced walls."* Invited keynote paper, ASCE Special Publication No. 103, Advances in Transportation and Geoenvironmental Systems Using Geosynthetics, *Proceedings of Geo-Denver 2000*, 201–217.

Bathurst, R. J. (2014). *"Challenges and recent progress in the analysis, design and modelling of geosynthetic reinforced soil walls." 10th International Conference on Geosynthetics*, ICG 2014. Berlin, Germany

Berg, R., Christopher, B., & Samtani, N. (2009). *"Design and Construction of Mechanically Stabilized Earth Walls and Reinforced Soil Slopes–Volume I". Federal Highway Administration (FHWA)*, Report No. FHWA-NHI-10-024.

Bobet, A. (2002). Design of MSE walls for fully saturated conditions, Final Report, FHWA/IN/JTRP-2002/13.

Das, B. (2008). *Principles of Foundation Engineering* (7th edition, pp. 406 – 436). Stamford, CT: Cengage Learning

Elias, V., Christopher, B., & Berg, R. (2001). *"Mechanically Stabilized Earth Walls and Reinforced Soil Slopes Design & Construction Guidelines". Construction*, (132042). doi:FHWA-NHI-10-024 & FHWA-NHI-10-025

Fang, H.-Y.(1990). *Foundation Engineering Handbook* (2nd edition, 923p). Springer US

Holtz, R., Christopher, B., Berg, R. (1998). *"Geosynthetic Design and Construction Guideline"*. Participant notebook. Pdf. Publication no. FHWA HI-95-038. Course no. 13213. National Highway Institute.

Koerner, R.M. and Koerner, G.R. (2012). A Data Base and Analysis of 141 Failed Geosynthetic Reinforced Mechanically Stabilized Earth (MSE) Walls. Geosynthetics Institute, Folsam, PA.

Koerner, R. (2000). *"Emerging and Future Developments of Selected Geosynthetics Applications."* Journal of Geotechnical and Geoenvironmental Engineering, ASCE 126(4), 293-306

Koerner, R. (2005). *Designing with Geosynthetics* (5th edition.). Prentice-Hall. Englewood Cliffs, NJ

Koerner, R. (2005). *Designing with Geosynthetics* (5th edition.). Prentice-Hall. Englewood Cliffs, NJ

Miyata, Y.; Bathurst, R. J. (2007). *"Evaluation of K-stiffness method for vertical geosynthetic reinforced granular soil walls in Japan." Soils and Foundations*, 47(2), 319–335

Nelson, R. (2005). *"Performance of two full-scale reinforced retaining walls – modular block and incremental panel."* MS Thesis, Royal Military College.

Rathje, E., Rauch, A., Trejo, D., Folliard, K., Viyanant, C., Esfellar, M., Jain, A., Ogalla, M. (2006). *Evaluation of Crushed Concrete and Recycled Asphalt Pavement as Backfill for Mechanically Stabilized Earth Walls.* CTR Technical Report *0-4177-3.*

Rinne, N.F. (1985). Evaluation of Interface Friction Between Cohesionless Soil and Common Construction Materials. MS Thesis, University of Waterloo.

SVOFFICE (2018). Soil Vision Office (version 5.4.2), *Soil Vision Systems LTD*, Saskatoon, SK, Canada.

The Reinforced Earth Company (2021) "*Mechanically Stabilized Earth(MSE) Retaining Walls."* accessed 1 April 2021, < reinforcedearth.com/>

Vahedifard, F., Leshchinsky, B.A., Morteza, K., and Lu, N. (2015). "Active earth pressures for unsaturated retaining structures." *J. Geotechnical and Geoenvironmental Engineering*, 141(11).

Walters, D. L.; Allen, T. M.; Nernheim, A.; et al. (2009). *"Influence of reinforcement stiffness and compaction on the performance of four geosynthetic-reinforced soil walls." Geosynthetics International,* 16(1), 43–59

WisDOT (Wisconsin Department of Transportation). (2015). Wisconsin Department of Transportation, Bridge Manual, Chapter 14 – Retaining Walls.

APPENDIX A – Detailed Data from Wall 1 and Wall 2

Response of sensors recorded during the flood test – Wall 1

During the flood/drain tests, all sensors installed during the construction period recorded the behavior of the wall. Below, the behavior of the main sensors was presented.

Figure A-1 shows the behavior of the strain gauges located on the reinforcement bars for the first 4 layers. It is possible to observe that only the sensor located in the first layer and close to the facing showed a difference of 100 με (an axial force of 4kN).

Figure A-2 shows the behavior of the connections between the reinforcement bars and the face panels. The sensor located in the first reinforcement layer failed during construction, however an approximation with the value of the first strain gauge on the reinforced steel strip can be made, thus presenting a variation of 4kN during the flooding/drawdown test The difference between the lateral loads is very subtle during the test, except for the load located in layer 5, which shows a difference of just over 1kN at the end of the test (during the rapid drawdown period). Figure A-8 summarizes the difference in behavior during the flooding test and the rapid drawdown test. Both readings were taken at the end of each test. It is worth mentioning that an important sensor, located in the first reinforcement layer, failed at the start of construction.

Figure A-3 and Figure A-4 show the results of the vertical footing loads. In both graphs, the loads increase, as soon as the flooding test start and decrease with the beginning of the rapid drawdown test. In Figure A-3 the heel curve does not show any difference, this is due to the concrete facing panels being located directly in this position (heel), presenting no space for the accumulation of water and, consequently, the increase in the vertical load.

The earth pressure curves (Figure A-5) show a marginal pressure variation during the flood and rapid drawdown test. This marginal variation is due to the soil being compacted at 95% of the maximum dry compaction, and little space for the water in the voids.

Figure A-6 shows the displacement of the facing during the flood/rapid drawdown test. The position before the start of the test was given as zero, the data showed only the displacement to flooding and rapid drawdown. In the graph, it is clear the movement during the beginning of the flood and rapid drawdown test. Figure A-7 summarizes the displacement after the tests.

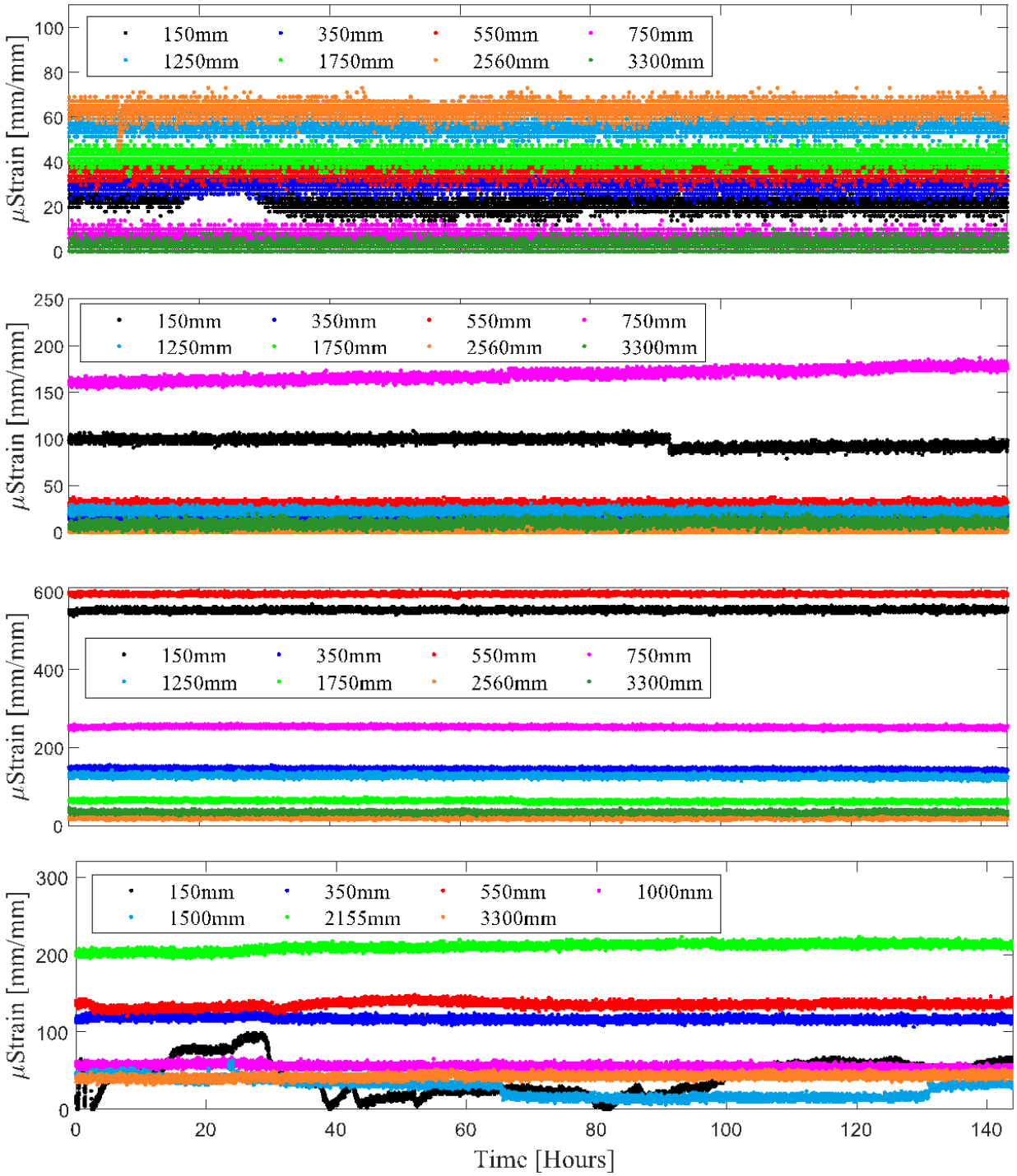

Figure A-1. Flooding test: Reinforcement strain during flood test (Wall 1)

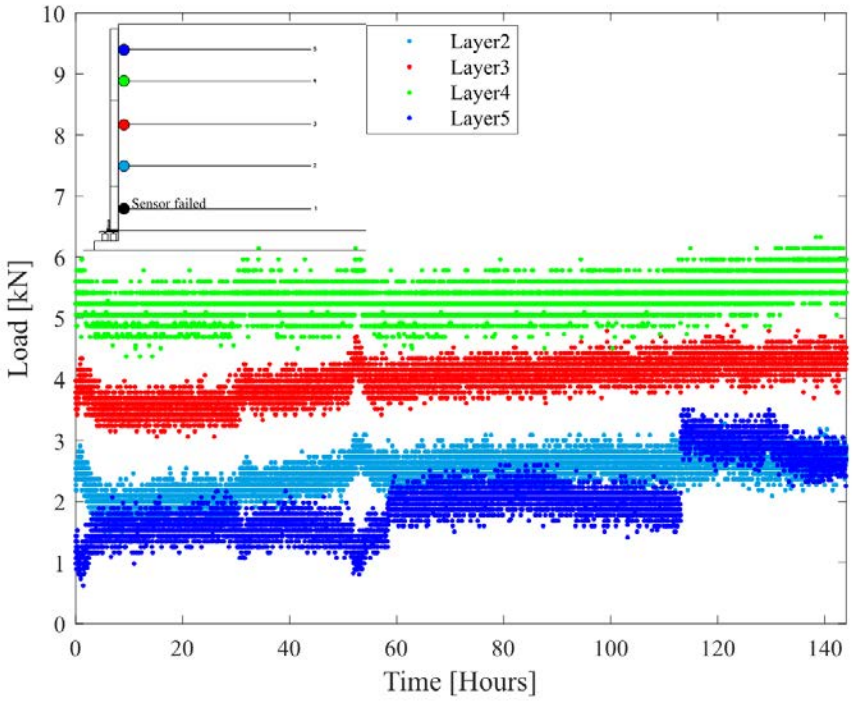

Figure A-2. Flooding test: Connection load vs time (Wall 1)

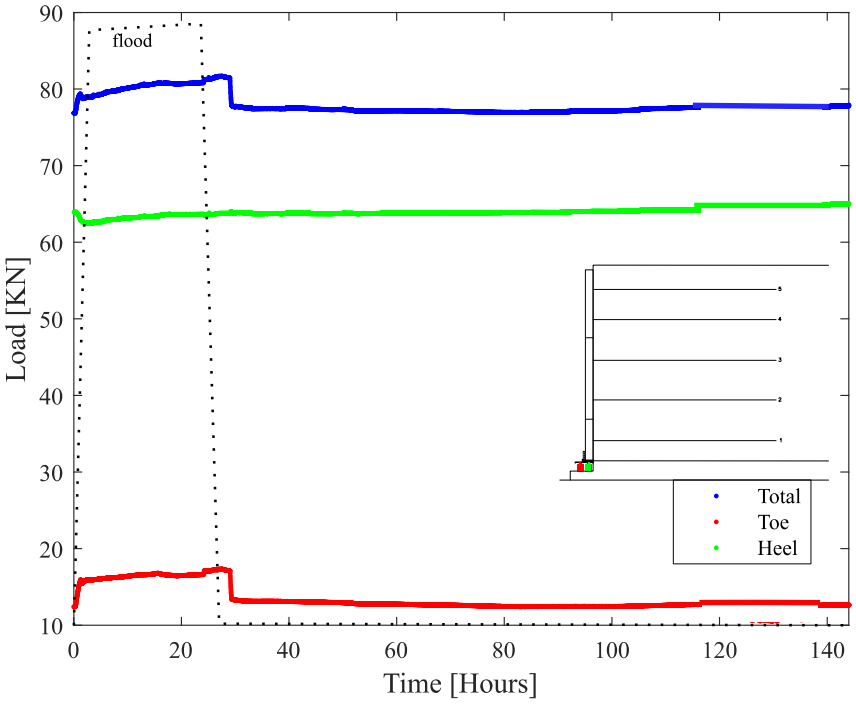

Figure A-3. Flooding test_Vertical footing loads vs time during construction (Wall 1)

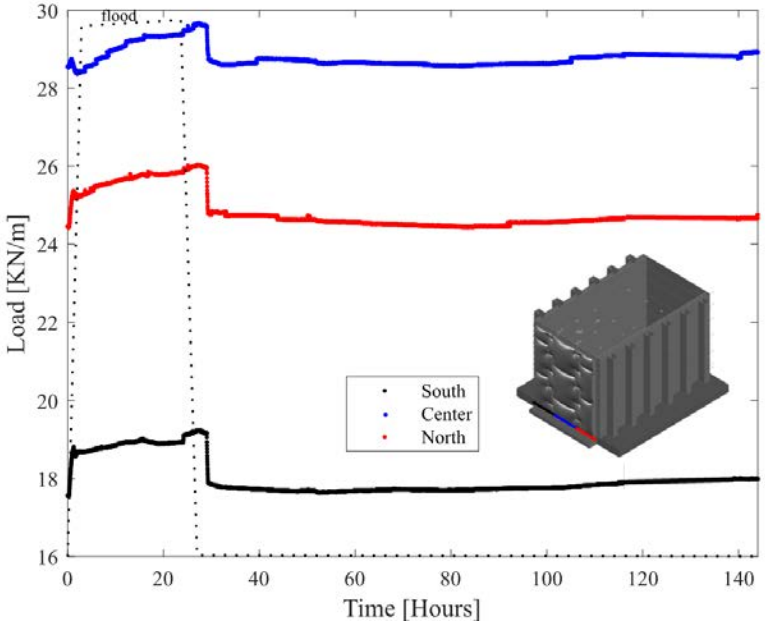

Figure A-4. Flooding test_Vertical footing loads per meter length of wall vs time (Wall 1)

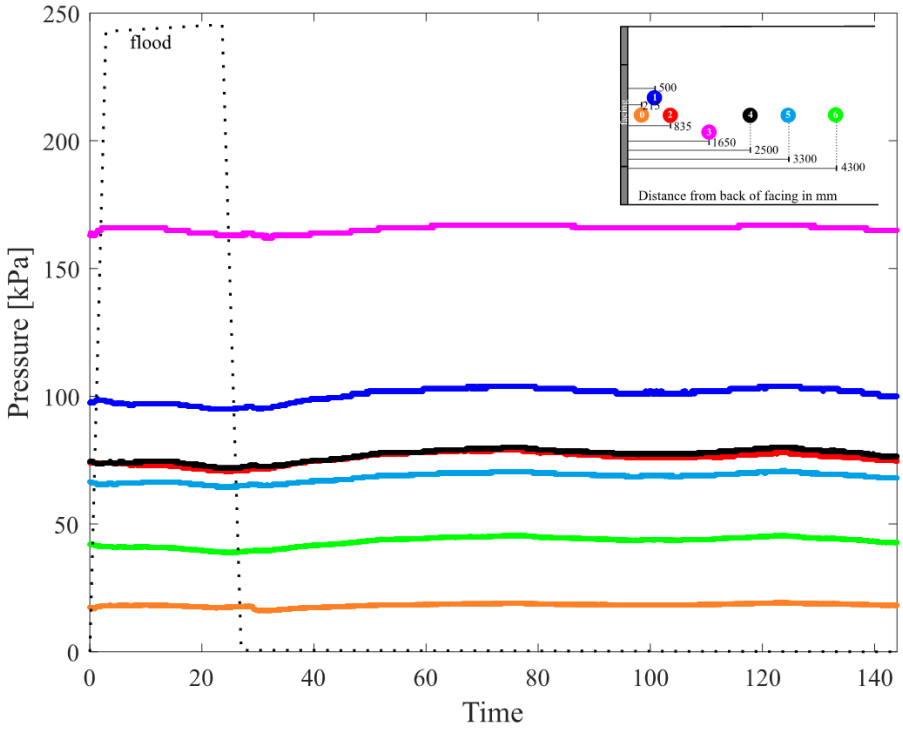

Figure A-5. Flooding test_Vertical Earth pressures recorded at the base of test facility (Wall 1)

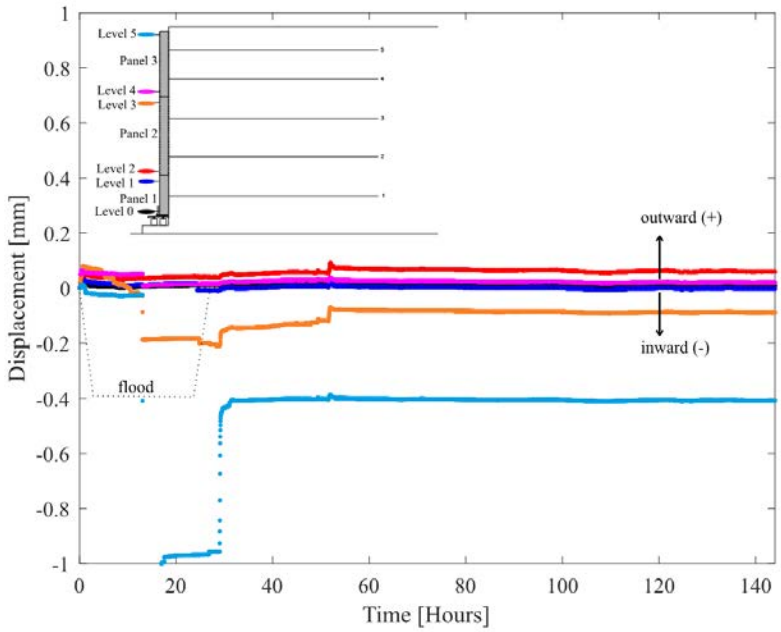

Figure A-6. Flooding test_Wall facing potentiometer measurements (Wall 1)

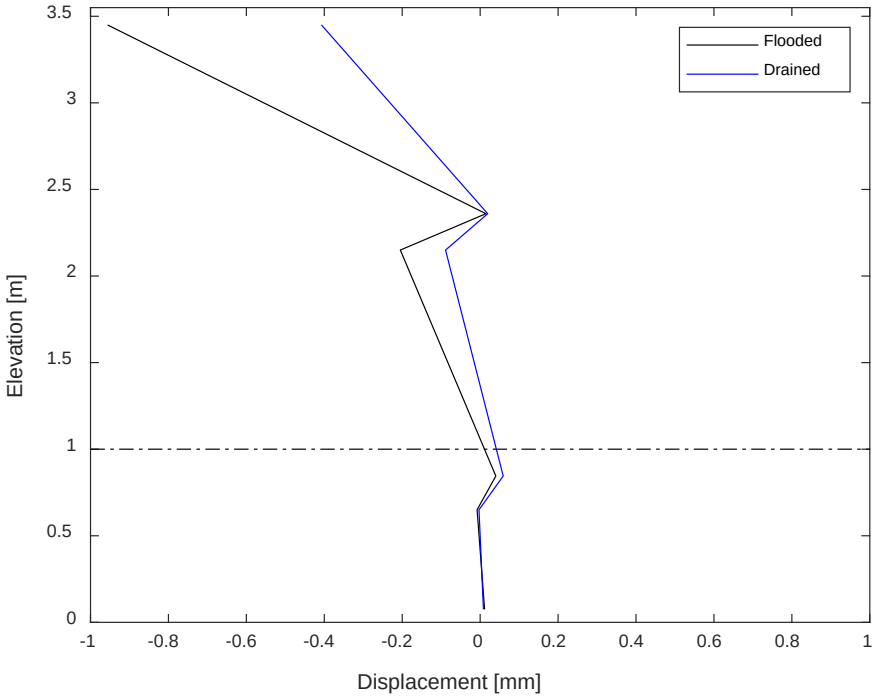

Figure A-7. Flooding test_Facing displacement vs elevation (Wall 1)

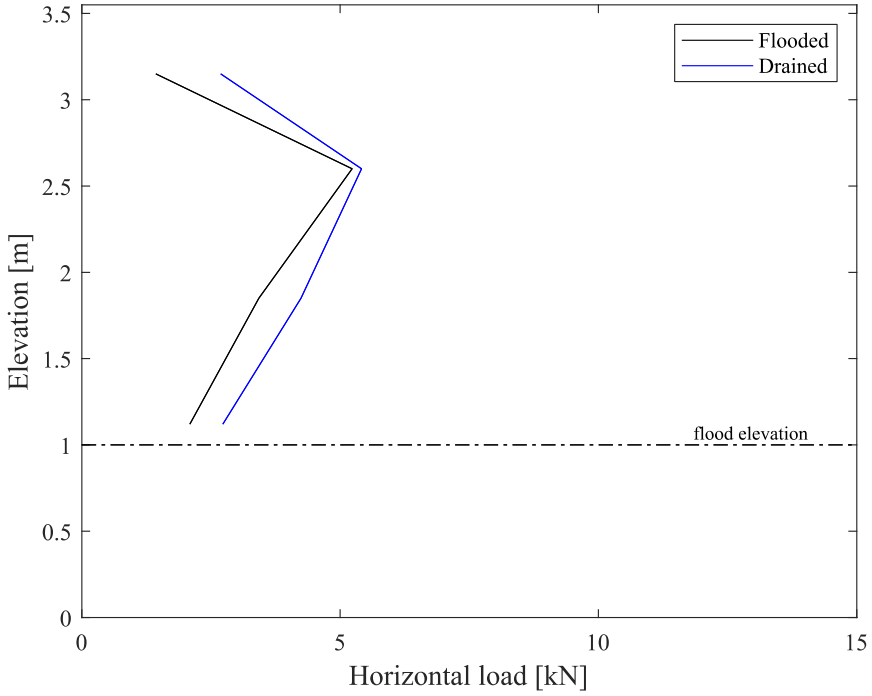

Figure A-8. Flooding test_ Connection load vs elevation (Wall 1)

Response of sensors recorded during the flood test – Wall 2

As with wall 1, sensors of wall 2 recorded the results of the flood and drain test. Figure A-9 presents the results of 5 reinforced layers with the correspondent strain during the flood/ drawdown test. The first layer, similar to wall 1, shows a change in strain during the tests. Only the sensors located at 150 mm from the back of facing presented a change in 100 με (4kN) at the beginning of the flood test and the remaining sensors do not show a relevant change in value.

The connection between the concrete panel facing and the steel strip also was recorded during the tests. Figure A-10 shows the decrease of load from 4 kN to 0.5 kN for the connection located at the first layer. This value is similar to that shown in the sensor located close to the facing and in the first reinforced layer. The summarized difference in behavior during the flood test and the drawdown test is showed in Figure A-17.

Figure A-12 shows the vertical footing load divided into two columns (toe and heel). The toe column presents a small increase in load and the heel a decrease in vertical load. This drop in the heel column is in agreement with the decrease in load on the connection load located at the first reinforced layer, which can mean a decrease in the vertical loads that occur due to the effect of horizontal loads on the back of the facing. Similar results are shown in Figure A-13.

Figure A-14 shows the response to the pressure cells under flood and drawdown conditions. The variation in pressure was marginal, as expected, due to the low volume of voids present in the compacted soil.

Figure A-15 and Figure A-16 summarizes the facing displacement during the flood and drawdown test. Figure A-15 shows the potentiometers measurements, considering zero the moment just before the flooding test start and Figure A-16 shows the results of the facing displacement at the end of the flooding test (black line) and the end of drawdown test (blue line).

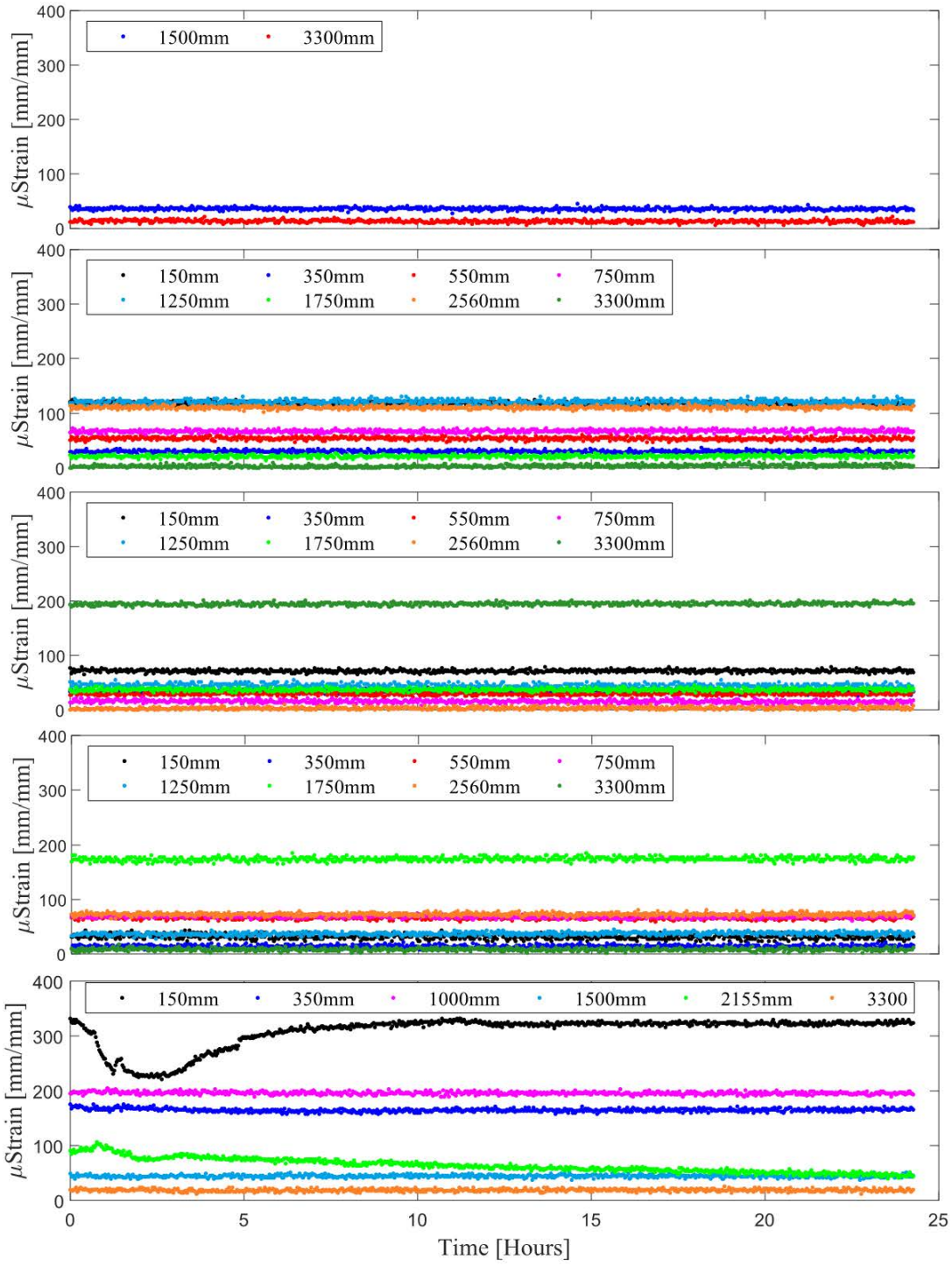

Figure A-9. Flooding test_Reinforcement strain during flood test (Wall 2)

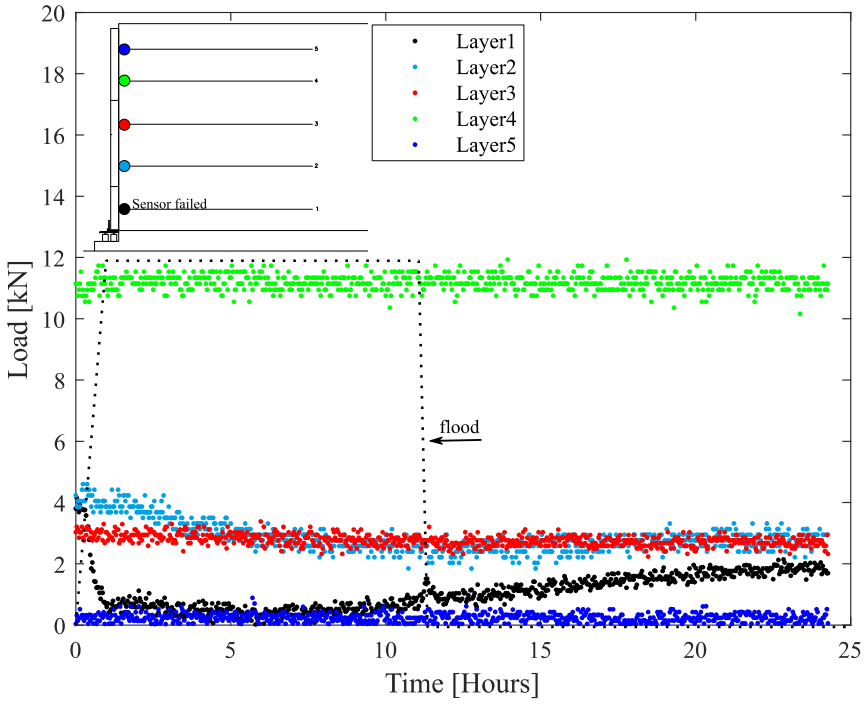

Figure A-10. Flooding test_Connection load vs time (Wall 2)

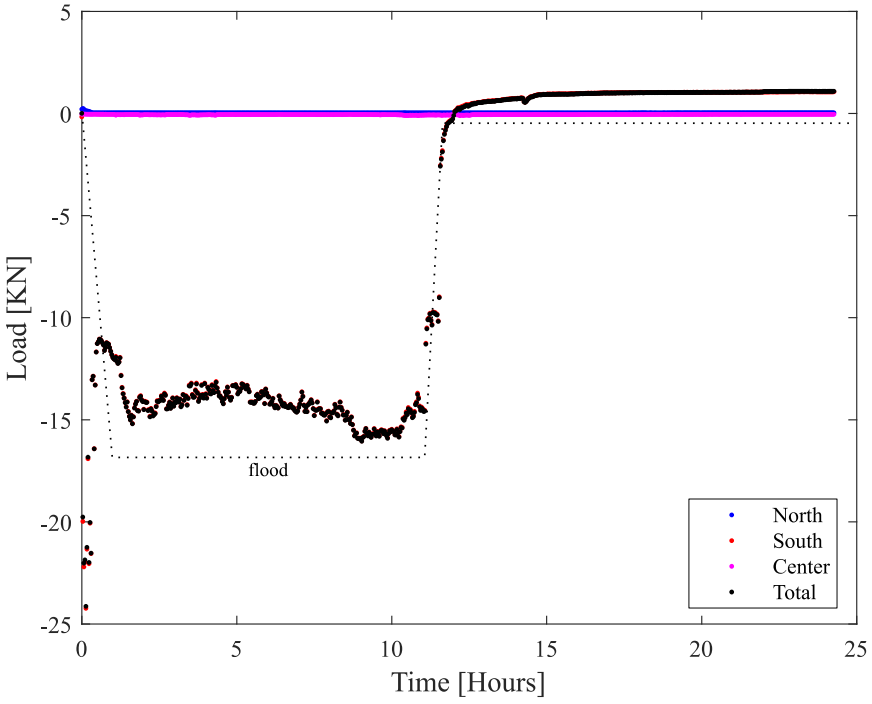

Figure A-11. Flooding test_Horizontal footing load vs time (Wall 2)

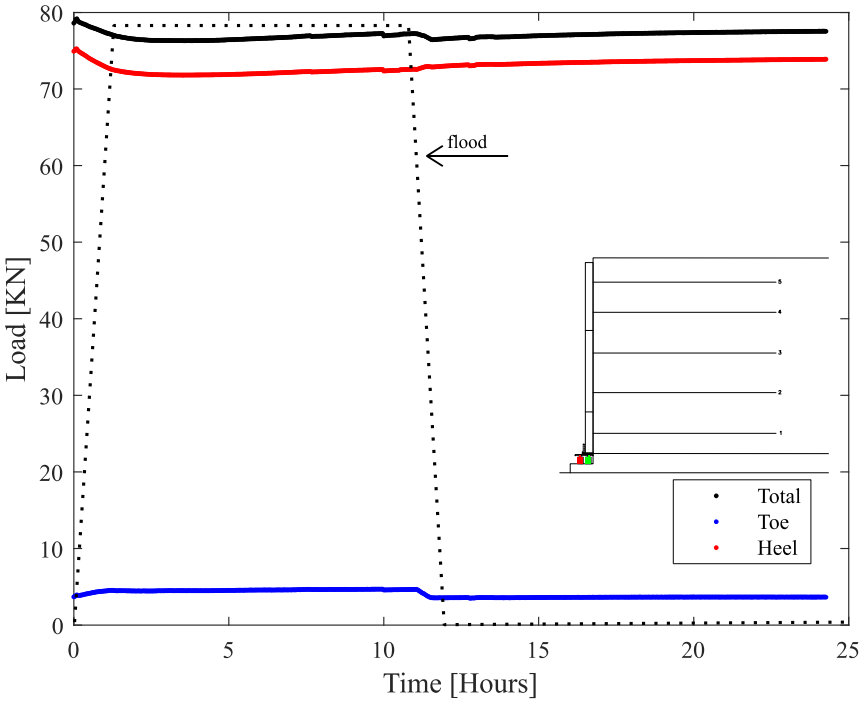

Figure A-12. Flooding test_Vertical footing loads vs time (Wall 2)

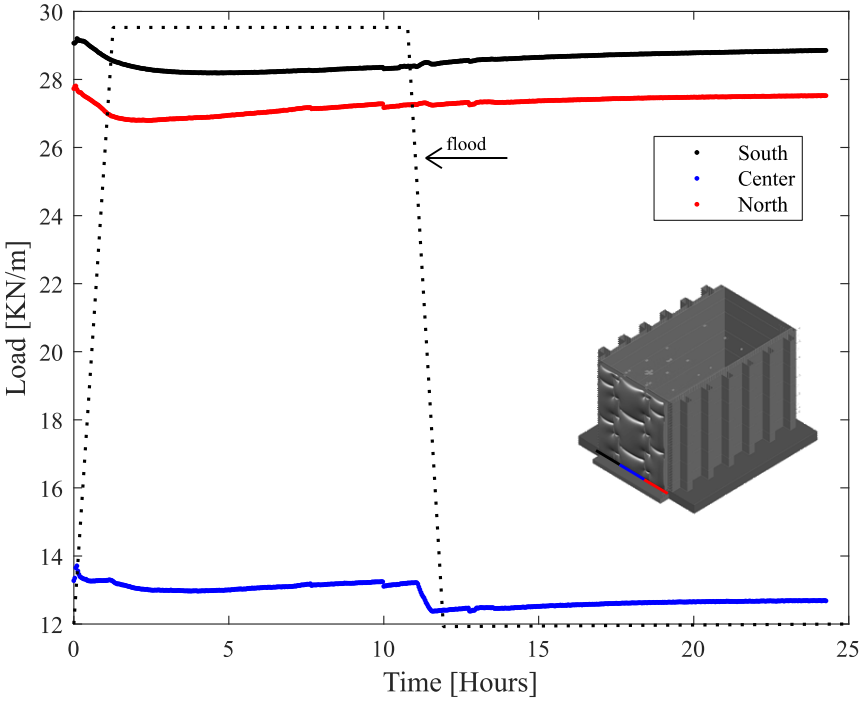

Figure A-13. Flooding test_Vertical footing loads per meter length of wall vs time (Wall 2)

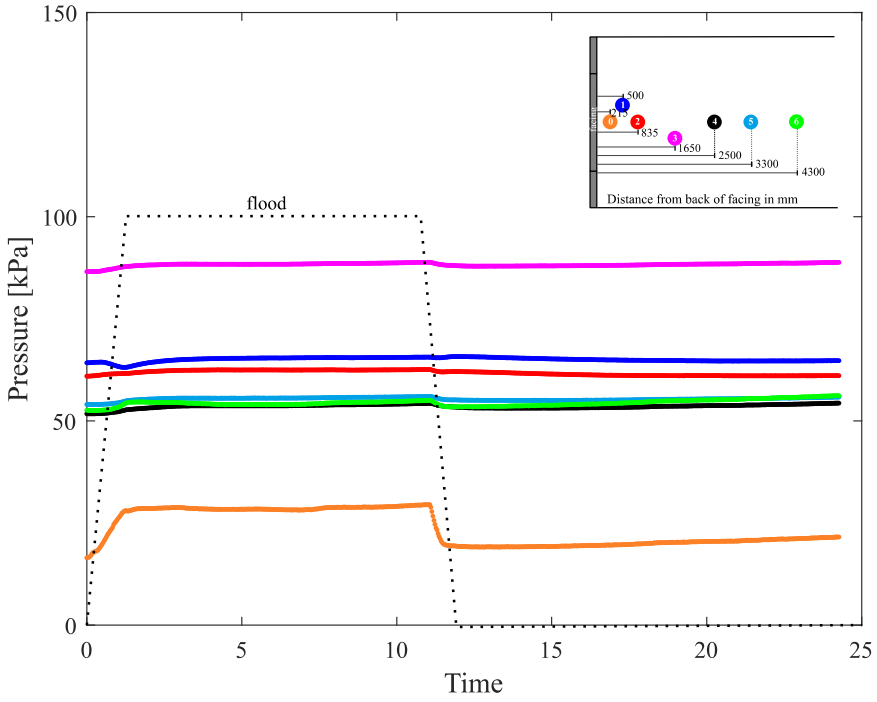

Figure A-14. Flooding test_Vertical Earth pressures recorded at the base of test facility (Wall 2)

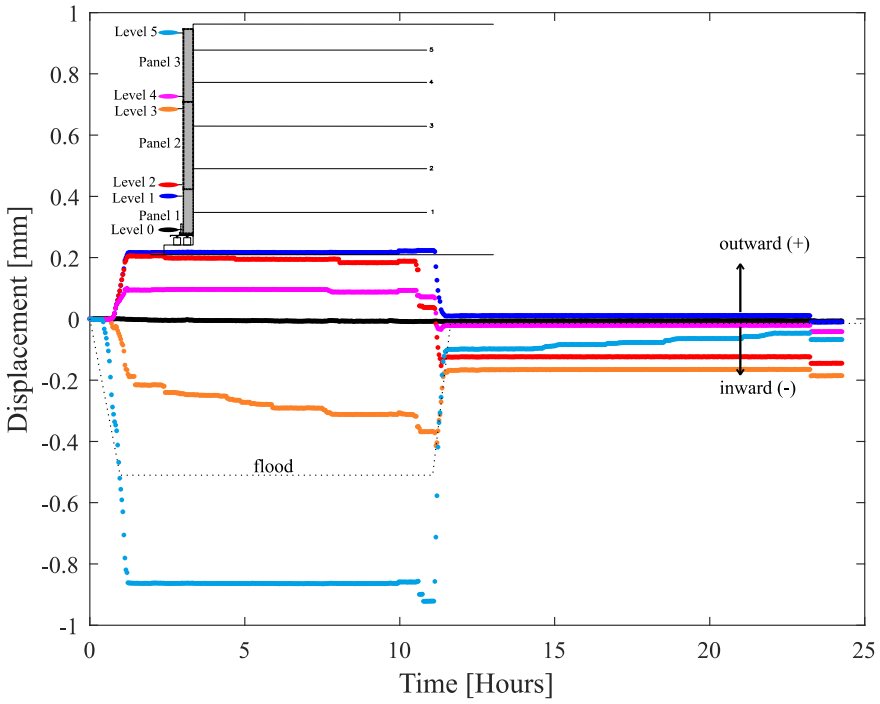

Figure A-15. Flooding test_Wall facing potentiometer measurements (Wall 2)

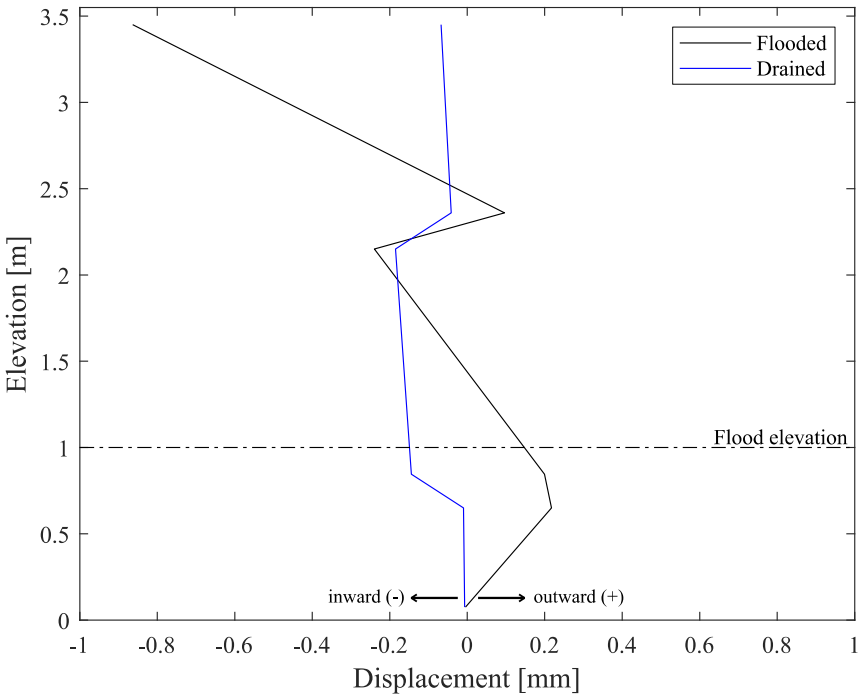

Figure A-16. Flooding test_Facing displacement vs elevation (Wall 2)

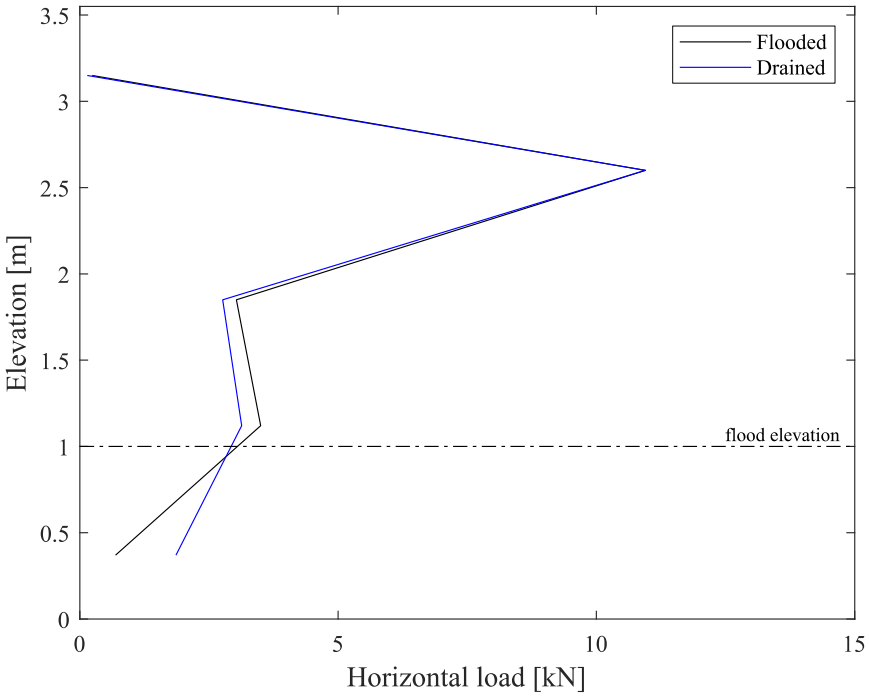

Figure A-17. Flooding test_ Connection load vs elevation (Wall 2)

APPENDIX B – Nuclear Density Gauge (NUC) results

NUC results – Wall 1

Wall 1					
Layer	Moisture content (%)	Dry unit weight (Kg/m3)	Wet unit weight (Kg/m3)	% Compaction	Void ratio
1	6.74	1733.0	1849.80	95.6%	-
2	7.86	1764.9	1903.62	97.3%	-
3	7.94	1814.9	1958.88	100.1%	0.441
4	7.14	1722.2	1845.17	95.0%	0.5682
5	7.77	1794.0	1933.39	99.0%	0.5131
6	7.38	1759.7	1889.49	97.1%	0.535
7	6.94	1744.8	1865.94	96.2%	0.548
8	6.90	1809.4	1934.30	99.8%	0.492
9	7.34	1768.1	1897.97	97.5%	0.527
10	6.66	1805.6	1925.73	99.6%	0.495
11	7.73	1809.0	1948.90	99.8%	0.493
12	5.48	1759.0	1855.35	97.0%	0.535
13	6.46	1805.1	1921.78	99.6%	0.44
14	6.09	1758.9	1865.99	97.0%	0.535
15	6.32	1770.6	1882.49	97.7%	0.525
16	5.86	1775.8	1879.76	97.9%	0.521
17	5.86	1775.8	1879.76	97.9%	0.507
18	6.28	1763.0	1873.68	97.2%	0.528
19	6.45	1767.2	1881.15	97.5%	0.542
20	6.01	1750.1	1855.31	96.5%	0.52
21	7.63	1775.7	1911.21	97.9%	0.519
22	7.69	1777.2	1913.87	98.0%	0.518
23	8.18	1779.0	1924.48	98.1%	0.495
24	7.91	1806.6	1949.47	99.6%	0.511

NUC results – Wall 2

Wall 2					
Layer	Moisture content (%)	Dry unit weight (Kg/m3)	Wet unit weight (Kg/m3)	% Compaction	Void ratio
1	-	-	-	-	-
2	2.79	2112.5	2171.44	94.5%	0.376
3	4.67	2133.1	2232.63	95.4%	0.281
4	4.79	2123.3	2224.93	95.0%	0.286
5	4.14	2125.9	2214.04	95.1%	0.274
6	3.60	2130.0	2206.63	95.3%	0.281
7	5.60	2175.8	2297.62	97.4%	0.243
8	4.34	2123.0	2215.26	95.0%	0.292
9	4.00	2141.1	2226.78	95.8%	0.288
10	4.24	2125.5	2215.70	95.1%	0.275
11	4.78	2159.2	2262.39	96.6%	0.253
12	4.32	2133.9	2226.12	95.5%	0.267
13	5.14	2213.5	2327.42	99.0%	0.209
14	5.93	2234.8	2367.37	100.0%	0.193
15	2.53	2128.7	2182.59	95.2%	0.269
16	3.34	2149.0	2220.87	96.2%	0.259
17	2.39	2123.4	2174.17	95.0%	0.312
18	3.78	2146.6	2227.66	96.0%	0.23
19	4.90	2193.4	2300.85	98.1%	0.233
20	5.20	2214.8	2329.95	99.1%	0.22
21	5.19	2209.3	2323.97	98.9%	0.24
22	5.20	2162.0	2274.42	96.7%	0.291
23	4.89	2141.9	2246.57	95.8%	0.289
24	4.84	2148.8	2252.87	96.1%	0.26